Redox Reactions in Polymeric Systems

by

James R. Black II

A dissertation submitted to the Graduate Faculty of
Auburn University
in partial fulfillment of the
requirements for the Degree of
Doctor of Philosophy

Auburn, Alabama
May 9, 2010

Keywords: Electrochromic, Radicals, Polymers, Polyacrylic Acid, SPEEK, Polyvinyl Alcohol, Silver Nanoparticles

Approved by

German Mills, Chair, Associate Professor of Chemistry and Biochemistry
Rik Blumenthal, Associate Professor of Chemistry and Biochemistry
Vince Cammarata, Associate Professor of Chemistry and Biochemistry
Eduardus Duin, Associate Professor of Chemistry and Biochemistry

Abstract

Reduction-Oxidization (redox) reactions performed in polymeric environments resulted in the reversible formation of stable silver nanoparticle and two reductive radicals. The reversible formation of stable silver nanoparticles in polyvinyl alcohol (PVA) and polyacrylic acid (PAA) crosslinked polymer films containing silver ions was achieved by electrochemical methods for potential applications in electrochromic devices. Cyclic voltammetry and galvanostatic methods were used to reversibly generate silver particles while the particle formation and decay optical absorption spectra were used to evaluate reversibility, relative particle size and minimum cycle speeds. Mechanisms for the formation and decay of particles are discussed with electron microscopy data determining actual size of generated silver particles.

Light activated polymeric radicals produced from sulfonated polyether ether ketone (SPEEK) with PVA or SPEEK with sodium formate solutions were generated using 350 nm photons. The mechanism of radical generation is discussed for potential application for dehalogenating a well known environmental hazard carbon tetrachloride (CCl_4). The reaction of the generated radicals with CCl_4 was followed by ion selective electrode specific for chlorine allowing for the attainment of kinetic data and reaction mechanisms. The degradation of CCl_4 was observed in both SPEEK/PVA and SPEEK/formate solutions but the kinetic data revealed SPEEK/formate to be more efficient.

The success of SPEEK radicals in dechlorinating CCl_4 lead to the investigation of polymeric blends, films and solution of SPEEK and polyamines for the generation of SPEEK

radicals with a higher redox potential. SPEEK/polyamine radicals were generated by exposing polymer blends to 350 nm photons. Optical and electron spin resonance (ESR) spectra confirmed the generation of the anionic radical with a higher reducing potential. Kinetic data was obtained for selected system by following the formation and decay of the optical and ESR signatures. The reactions leading to the generation of highly reductive radicals is discussed.

Acknowledgments

I would like to say thanks to everyone who has helped and dealt with me along this unique and challenging experience. First thanks to my best friends Dr. Roger Birkhead and Dr. Chelesa Ward for sharing their home and non chemistry guidance over the years. To my family, Gloria, Krimson and Nicholas thanks for putting up with me while I have walked this path. My friends and peers, Dr. Neely and Dr. Batteh I am grateful for all the support during the rough times. To Storybook Farm, thanks for a place of refuge from chemistry and the oppertunity to meet some of my greatest friends. The cousins, Josh Westmoreland, Bret Freeman, Brother Scott Moody, Amy Westmoreland and Katie Robison for being the shoulders to lean on and the voices of reason. Dr. Slaten for being a friend, a mentor and allowing me to do chemistry in the Fashion Design building. My committee members, Dr. Blumenthal, Dr. Duin and Dr. Cammarata for spending all the extra time teaching, reviewing and guiding, I really appreciate all that they have done. Dr. Mills for his unique guidance in chemistry and in life with a sense of humor that can make anyone smile.

Table of Contents

List of Tables

List of Figures

List of Abbreviations

Ag^+	Silver Ion
Ag_0	Silver Atom
PVA	Polyvinyl Alcohol
PAA	Polyacrylic Acid
CCl_4	Carbon Tetrachloride
SPEEK	Sulfonated Polyetherether Ketone
PEEK	Polyetherether Ketone
nm	Nanometer
cm	Centimeter
μm	Micrometer
μA	Microamp
OD	Optical Density
λ	wavelength
ITO	Indium Tin Oxide
TEM	Tunneling Electron Microscope
SEM	Scanning Electron Microscope
UV-Vis	Ultraviolet Visible
s	Second
V	Volt

M	Molar (grams/liter or monomer/liter)
BP	Benzophenone
BPK	Benzylphenylketyl
PEI	Polyethyleneimine
EPH	Epichlorohydrin
PVAm	Polyvinylamine
PAAm	Polyally amine
^{0}C	Celsius
K	Kelvin
min	Minute
mL	Milliliter
mil	Mili-inch
DI	Deionized water

I. Polymeric Systems as Key Elements for the Initiation of Reduction Oxidation Reactions

Introduction

The use of polymers is increasingly turning more diverse and widespread, with conventional materials being continuously replaced by new polymeric ones. This trend is a consequence of numerous useful properties exhibited by polymers that are not found in other materials. In the case of non-ionic polymers, blending of macromolecular materials enables further tuning of their properties. Blending of non-ionic with ionic polymers seems a feasible way to achieve interesting materials that may enable the realization of chemical reactions not easily achievable in the absence of the macromolecules. Presented in this dissertation is evidence that the behavior of certain reduction-oxidation (redox) reactions can be altered to some degree by blends of ionic and non-ionic polymers, enabling the formation of desired products. The polymeric materials that form the basis for the present investigations will be presented and discussed in the subsequent sections.

1.1 Polyvinyl Alcohol

This polymer, popularly known as PVA, is a macromolecular material that has found use in many applications ranging from food packaging to flexible displays.[1,2] PVA is predominantly used in the formation of polyvinyl butyral, which is the primary component of safety coatings for glass.[3] Not surprisingly, PVA has such a wide range of markets because this polymer can be produced inexpensively and has properties that make it easy to use. Herman and Haehnel originally developed the production of PVA in 1924 by polymerization

of vinyl acetate into polyvinyl acetate, followed by hydrolysis of the acetate group with a strong base, a method that is still in use today.[4,5]

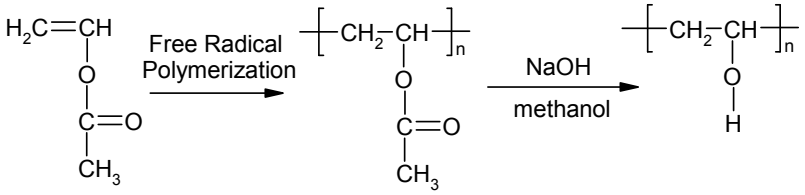

[1]

Reaction 1 depicts the sequence of transformations that produce PVA. The properties of PVA vary depending on polymer chain length and percent hydrolyzed but the main physical property sought after is optical clarity. PVA is transparent to visible light and partially transparent in the ultraviolet region of the spectrum. Macromolecules of low molecular weights, and lower percent of hydrolysis, are very flexible and dissolve easier in H_2O. Polymer samples of high molecular weights, or higher percent of hydrolysis, are less flexible and harder to dissolve in H_2O but exhibit a higher tensile strength. They are less sensitive to the presence of water or other solvents, and their solutions are highly viscous.[6] PVA is primarily an amorphous, odorless and non-toxic material, with a melting point of 200 ^{0}C at which temperature the polymer rapidly decomposes.

The degree of crystallinity is dependent on the percent of hydrolysis, molecular weight and water content. Polyol samples of low molecular weight, or those hydrolyzed to a low percent, contain higher amounts of water, which increases gas permeability and lowers the polymer strength. The electrical conductivity of fully hydrolyzed PVA is on the order of 10^{-7} S m^{-1}; this value is also dependant on the amount of water and ions present in the solid polymer. Increasing amounts of water or ions increases the conductivity by several orders of magnitude.[5,7,8,9] PVA exhibits a glass transition (TG) point at 80 ^{0}C; once the TG point is reached the segmental

motion of the polymer chains have enough rotational energy to become more flexible allowing for the polymer to reside in a semi fluid state.[8,10] Because of these properties, PVA is well-suited to serve as a matrix for redox reactions involving low mobility processes, such as the photochemical formation of metal particles. PVA matrices are well suited for such photoreactions because of the low absorption of light by the polyol allows the use of conventional detection methods such as Ultraviolet-Visible spectrometry. The water solubility of PVA can be controlled via formation of solid films using crosslinking agents such as dialdehydes, cyano compounds and epichlorhydrin.[11-15]

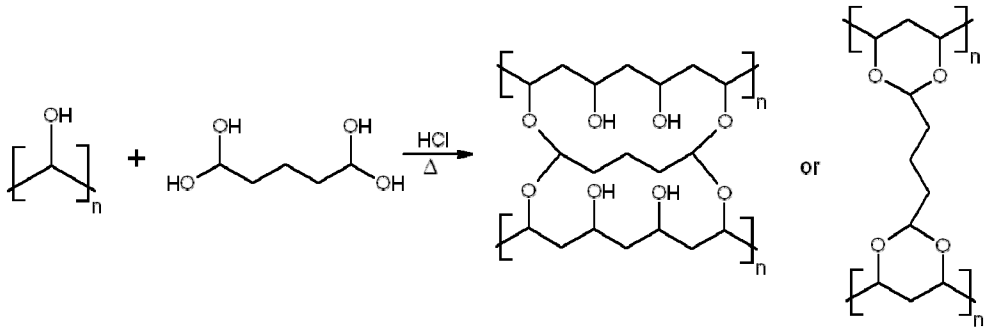

[2]

Dialdehydes are preferred because of their lower toxicity; the degree of crosslinking can be manipulated by controlling the amount of crosslinker and the thermal conditions employed.[12] Reaction 2 summarizes the process believed to occur when glutaraldehyde is used as a crosslinking agent. Increasing the crosslinker concentration, reaction time and/or temperature yields higher degrees of crosslinking. The degree of crosslinking also affects the flexibility, solubility in different solvents and tensile strength; a higher degree of crosslinking results in less flexible films with a higher resistance to water/solvents and higher tensile strength.[6,7,11] Crosslinked films exhibit optical properties similar to those of PVA solutions permitting substantial light transmission in the UV/Vis range but the transmittance decreases with increasing thickness. The sensitivity of PVA to humidity and to solvents can be utilized for the

removal of residual chemicals present in the solid matrices, or to dope them with ionic materials.[15,16] Increasing the concentration of ionic dopants increases the conductivity of PVA films until a maximum is reached at 30% doping. No further conductivity increases result at higher doping levels due to ion pairing.[8,10] Included in Table 1 are several important physical properties of PVA films.

PVA films have been used as barrier layers in food packages that aim at inhibiting permeation of O_2.[17] Such strategy has been successful because the solubility of gases in PVA films is proportional to the water content in the solid matrices. A consequence of this behavior is that O_2 diffusion through the solid polymers is severely hindered when the films are kept dry.

Table 1

Transmission between 400 – 1200 nm	85%
Melting Point (PVA degrades before it melts)	150 ^{0}C
Conductivity	~10^{-7} S m^{-1}
Tensile Strength	44 – 64 MN/m^2
% Elongation at breaking point	150 - 400 %
Tear Strength	147 – 834 N/mm
Glass transition Point	85 ^{0}C
Amorphous Density	1.26 g/cm^3

1.2 Nanoparticle Formation in PVA Matrices

Recently PVA matrices have been utilized for the photochemical generation of metal nanoparticles.[18-22] The reduction of silver ions requires a reducing agent that can be easily stimulated to donate an electron to an Ag^+ ion producing a silver atom. Formation of Ag particles is commonly achieved by using sodium borohydride and a silver salt.[23] The produced silver atoms are highly mobile since they are uncharged particles and their fast formation inevitably generates large concentration gradients. Aggregation occurs upon contact between an Ag atom with another metal atom, or with silver particles and even with Ag^+ ions. Binding of Ag

atoms with Ag^+ forms metal clusters that may contain several metal atoms and ions. Such processes decrease the mobility of the Ag atoms. The flux of particles and ions follow the general form of the Nernst-Plank equation for particles with no interaction of the medium,

$$J_j = -D_j \nabla C_j - \frac{z_j F}{RT} D_j C_j \nabla \phi + C_j \nu \qquad (2)$$

where the flux, J, is dependent upon three factors, diffusion, migration and convection.[23] Diffusion is primarily dependent on the concentration gradient ∇C_j and the diffusion coefficient D_j. Migration is dependent on the charge of the species z_j, cross sectional area of the species, applied electric field, temperature, diffusion coefficient and concentration. The contribution of convection to the overall flux is dependent on concentration and solution viscosity, η.[24] If the system is a solid polymer then the convection contribution is zero but the viscosity will affect the diffusion cofficeient.

As the nanoparticles grow they become less mobile but the resulting crystallites possess an increasing number of valence electrons that can easily polarize, forming short-lived surface dipoles and/or quadruples. Polarization of this electron cloud by light induces an optical transition called plasmon resonance. Once nanoparticles of metals such as Cu, Ag and Au are formed their plasmon resonance depends on particle size, shape and dielectric medium according to the Mie theory.[22,25] If small metal crystallites are not stabilized by the medium or matrix, they will diffuse and combine to ultimately produce larger particles having properties of bulk metal that inevitably precipitate out of solution.

In previous studies on light-induced formation of metal crystallites PVA served as a matrix that can stabilize particles against precipitation, and also as an electron donor that aided the photoreduction of metal ions.[18-22] The stabilizing effect of PVA is believed to involve strong interactions of the polar groups of the macromolecules with the particles. Such interactions lead

to partial coating of the crystallite surface with polymer chains, which, in turn, inhibits collisions between particles that induce particle growth. Recent data have provided evidence that PVA acts as a donor of H-atoms during the photoreduction of Ag^+ ions by SPEEK radicals.[21] Abstraction of H-atoms from PVA chains yields α-hydroxy radicals of the polyol that are reducing species.[26] Thus, PVA can aid the formation of metal particles by acting as a reductant that first donates H-atoms, followed by the contribution of the reducing α-hydroxy radicals that result from atom abstraction process.

1.3 Polyacrylic Acid Stabilized Nanoparticles

Ag particles can be stabilized by salts and polymers such as tetrabutylammonium halides and polyacrylic acid, PAA (Figure 1-1), the structure of which is shown below.[24,27] The negatively charged carboxylate group of PAA can interact with charged particles or clusters allowing for the charge to be stablized.[25,28] Alterations in the dielectric constant of the medium will occur in the presence of PAA due to changes in electronic interactions, which will influence the plasmon resonance. The photochemical generation of silver particles in PVA/PAA films was initiated by excitation of the silver ions with UV light.[19,22] PVA/PAA films swell in aqueous or methanolic solutions, which enabled diffusion of metal ions into the swollen polymer matrices. Ion exchange between protons from the PAA carboxylate groups and Ag^+ induced binding of the metal ions to the polymer matrix. Thus, the presence of PAA in the polymer films enabled reproducible incorporation of Ag^+ ions in the films. Reduction of metal ions electrochemically produces metal atoms; diffusion and grow of such species into particles in the presence of a polymer stabilizer can also accomplish the production of metal nanoparticles.[25,29] Results from

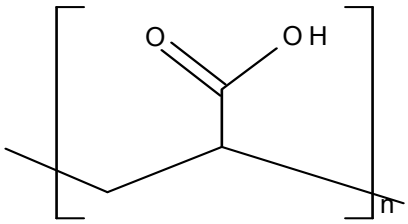

Figure 1-1 – The chemical structure of PAA.

an investigation presented later show that swollen PVA/PAA films can function as suitable matrices for the electrochemical generation of small Ag crystallites.

1.4 Benzophenyl Ketyl Radicals as Reducing Agents

The use of benzophenone (BP) as a chromophore that aids the initiation of photochemical redox reactions is well documented.[30] BP undergoes excitation of the carbonyl group upon exposure to 350 nm photons from ground state to the first singlet excited state. Fast intersystem crossing yields an excited triplet state that can abstract a hydrogen atom from alcohol molecules. The result is the formation of an α-hydroxy (or benzophenyl ketyl, BPK) radical of BP together with an α-hydroxy radical of the alcohol molecule.[31,32,34] Reaction 4 depicts the formation of the two α-hydroxy radicals resulting from photolysis of the well studied solution system consisting of BP in the presence of 2-propanol. The BPK radical has strong absorptions centered at 340 and 545 nm, a lifetime of about 10^{-8} seconds,[31,32] and behaves as a reductant capable of reducing Ag^{+} ions.[33]

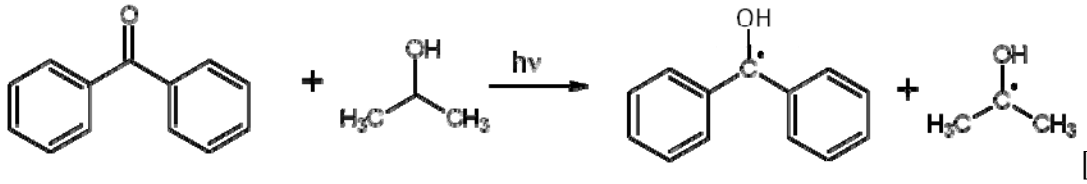

[4]

The benzophenone/isopropanol system can be envisioned as a model for the design of systems containing only macromolecular reagents able to photogenerate reducing polymeric BPK radicals under illumination. Such systems require the use of a polymeric benzophenone and macromolecular alcohol. Poly(ether etherketone), PEEK, is a commercially available macromolecular material containing BP functions that is frequently used in ion exchange membranes.[35] However, PEEK is insoluble in almost all liquids at room temperature, whereas polymeric alcohols dissolve only in polar solvents such as water and DMSO. Thus, preparation

of films containing polymeric alcohols as the solvents and PEEK as the solute is not possible by simple solution procedures. A strategy that solved this problem consisted of reacting PEEK with H_2SO_4 to produce sulfonated poly(ether etherketone), SPEEK, which is soluble in several polar solvents.[35-37] The transformation of PEEK into SPEEK is shown in reaction 5:

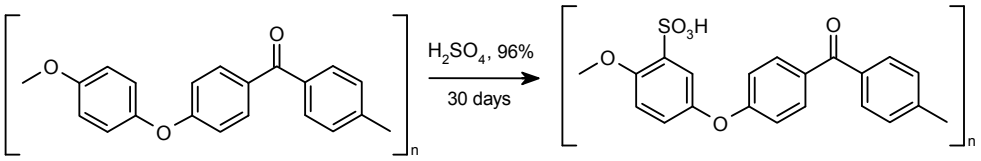

[5]

The degree of sulfonation affects the properties of final product, such as solubility and conductivity; fully sulfonated PEEK samples are water-soluble.[35,37] PVA was chosen as the polymeric alcohol given the favorable physical properties (optical transparency and ability to form flexible films) of this material. In addition, given the structural similarities between 2-propanol and the PVA monomeric units, this polyol was anticipated to be an effective hydrogen atom donor. The optical spectrum of SPEEK is similar to that of BP and absorption of 350 nm photons by the polymer (extinction coefficient (ε) = 900 M^{-1} cm^{-1}) yields an α-hydroxy radical which can be detected by UV/Vis spectrometry at 565 nm having an extinction coefficient of about 3.5 x 10^3.[20] ESR determinations confirmed that the species with a wavelength of maximum absorption (λ_{max}) at 565 nm is a BPK radical derived from SPEEK (from now on referred to as •SPEEK).[21] α-hydroxy radicals from PVA were not detected by ESR, presumably because these reactive species attack BP groups of SPEEK fast, forming another BPK radical of the polyketone. The SPEEK radical was determined to have a relatively long lifetime of several minutes in air-free solutions and up to 40 minutes in films consisting of blends prepared from SPEEK and PVA.[21]

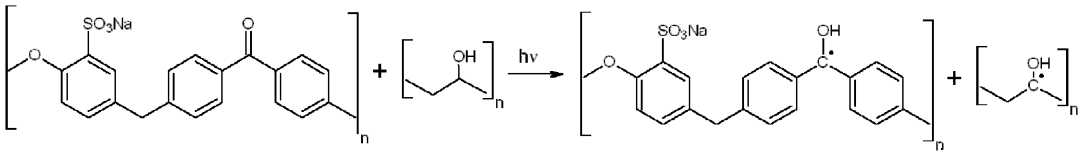

[6]

Upon exposing air-free aqueous solutions of the two polymers containing several metal ions to 350 nm photons the radicals generated metallic particles. Interruption of the light exposure stopped the generation of BPK radicals, terminating the formation of metal crystallites. PVA and presumably the sulfonic groups of SPEEK stabilized the produced metal particles against growth and coagulation for periods of time of several weeks. The polymeric BPK radicals produced in this system were strong enough reductants to reduce Ag(I) amd Au(III) to the metal state but Cu(II) ions were reduced only to Cu(I) species, not to metallic copper.[20] The reduction potential of •SPEEK radical was estimated to be about -1.3 V in aqueous solution. Preparation of films from SPEEK/PVA blends was achieved by use of the crosslinking agent, gluteraldehyde, which covalently linked the PVA chains immobilizing the SPEEK polymer. Illumination of crosslinked - SPEEK/PVA blend films that were ion-exchanged with silver ions also yielded stable Ag particles even in the presence of air.[17,21] These results suggest that the radical photogenerated in SPEEK/PVA films exhibits a reducing strength similar to the polymeric BPK radical produced in solution. Since the SPEEK radicals react fast with O_2 in solution, the fact that they were detected optically after exposing films of the blends to 350 nm photons under air confirms that the solubility of oxygen is very low in solid PVA. Hence, because of the low [O_2] present in the films, the concentration of oxygen was probably reduced quickly by •SPEEK and exerted negligible interference in the reduction of Ag^+. As discussed below, •SPEEK was utilized in conjunction with carboxyl radical anion ($\bullet CO_2^-$) to initiate efficient dechlorination of CCl_4.

1.5 Sodium Formate as a Source of Reducing Carboxyl Radical Anions

The large positive oxidation potential of the SPEEK radical suggests possible applications for this species as a reductant capable of inducing transformations of harmful chemicals and environmental hazards.[24,38] Earlier studies have shown that reducing radicals, such as $(CH_3)_2C\bullet OH$ or $\bullet CO_2^-$, formed via illumination of titania particles suspended in water transform halogenated organic compounds including chlorofluorocarbons (CFCs) through reductive dechlorinations.[39,41,42] An interesting feature is that efficient chain dehalogenations resulted when $\bullet CO_2^-$ radicals were photogenerated by titania suspensions. The enhanced dehalogenation efficiency obtained with the formyl radical anion is related to the higher reducing power of this radical, $E^0(\bullet CO_2^-/CO_2) = -1.8$ V than that of α-hydroxy radicals, for example, $E^0((CH_3)_2C\bullet OH/((CH_3)_2C=O, H^+) = -1.4$ V.[43] Interestingly, the BP triplet excited state is known to abstract a H-atom from HCO_2^- yielding a BPK radical and $\bullet CO_2^-$.[44] A similar reaction between the triplet excited state of BP groups from SPEEK, ^{3}(SPEEK)*, and HCO_2^- ions seemed possible, which was expected to yield •SPEEK and $\bullet CO_2^-$. As in the case of the α-hydroxy radical from PVA, $\bullet CO_2^-$ can reduce a carbonyl group of SPEEK forming a second polyketone BPK radical. Alternatively, the formyl radical anion may react with solutes present in the solution. However, the solutes must exist in solution at concentrations high enough to compete with the reduction of C=O groups from SPEEK by $\bullet CO_2^-$. Given the known ability of $\bullet CO_2^-$ to induce efficient reductions of halogenated organic compounds,[40,41,42] chain dehalogenations seemed feasible at high concentrations of such compounds. In contrast, •SPEEK was expected to be the main reducing agent in solutions with low concentrations of halogenated organics, or in SPEEK/PVA systems (where $\bullet CO_2^-$ is not photogenerated). Under such conditions the reductive dehalogenations were anticipated to occur with lower efficiencies.

Thus, a straightforward test seemed possible to confirm that photolysis of aqueous solutions of SPEEK and formate ions indeed photogenerated $\bullet CO_2^-$. The anticipated result of such a test consisted of a more efficient chlorocarbon reduction when HCO_2^- was used as a H-atom donor instead of PVA. Another potential consequence of substituting PVA by HCO_2^- was an increase in the yield of reducing radicals generated via photolysis of SPEEK. Formate ions are smaller and, therefore, more mobile in water than PVA chains, allowing for a higher number of energetic collisions between ^{3}(SPEEK)* and HCO_2^- that produce radicals. In addition, the high [PVA] (0.36 M) needed to ensure efficient H-atom abstraction results in a viscosity of the SPEEK/PVA solutions that is about 4 times that of H_2O.[20] Replacement of PVA by HCO_2^- was anticipated to lower the solution viscosity, increasing the mobility of the reactants as well as accelerating the formation of radicals and of the redox processes.

One of the aims of the present studies was to investigate the ability of radicals formed via illumination of SPEEK systems to induce reductive degradation of toxic chemicals including chemical warfare agents, CWA's. The ultimate goal was to identify combinations of SPEEK with electron donors that upon incorporation in protective clothing could serve as light-activated (self-cleaning) barriers able to degrade toxic chemicals. Obviously, studies using CWA are not possible due to safety concerns, but simulants that mimic some of their properties are frequently employed. The choice of simulant was restricted to chemicals with moderate toxicity that are water-soluble and exhibit some properties similar to those of undesirable halogenated organic compounds or chemical warfare agents. Carbon tetrachloride was chosen because this is a moderately toxic, commercially available chlorocarbon that dissolves significantly in water and is optically transparent above 300 nm. In addition, CCl_4 exhibits several chemical and physical properties similar to those of halogenated toxins and CWA's.[38,45,46,47] Experiments were

performed in aqueous solutions of SPEEK and H-atom donors since preliminary attempts to photoreduce gaseous CCl_4 on SPEEK/PVA films designed to mimic self cleansing textiles yielded erratic results. The reason for such outcome is related to the low permeability of the films toward CCl_4.

1.6 Benzophenone Anion Radical

α-hydroxy radicals from simple alcohols are known to deprotonate in basic solutions forming radical anions.[43] The BPK radical of benzophenone also behaves as a weak acid ($pK_a = 9.2$) forming in basic solution a radical anion with an absorption maximum at about 620 nm.[32,45] Considering the chemical similarities between the BPK radical of BP and that of SPEEK, ionization of •SPEEK was anticipated to occur in alkaline solution forming a polymeric radical anion. While the redox potential of the BPK radical ion of benzophenone in H_2O is not known, reversible electrochemical reduction of BP in DMF occurs at -1.7 V.[48] Deprotonation of α-hydroxy radicals increases their reduction potential in water by about -0.7 V, meaning that the reduction potential of the SPEEK radical anion should be close to -2 V. Accordingly, the radical anion of SPEEK was predicted to behave chemically in a way similar to $\bullet CO_2^-$, and be able to induce highly efficient reductions of halogenated organic compounds. Another way to generate radical anions of BP in organic solvents consists of exposing benzophenone to UV light in the presence of metals such as Na and K.[49] The resulting radical anion is a very strong reducing agent able to reduce poly(tetrafluoro ethylene), an extremely inert polymer.[50] Formation of the BP radical anion has also been achieved by UV irradiation of benzophenone in the presence of amines which act as electron donors.[51,52] Reaction 7 illustrates the photoreduction of BP by trimethyl amine,

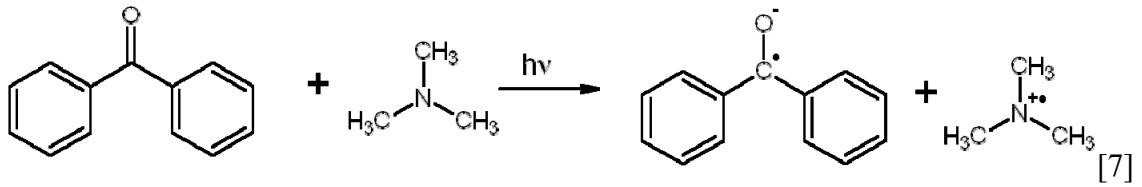

[7]

The BP/amine system served as a model to develop strategies for producing the SPEEK anionic radical using mainly combinations of macromolecular materials. As was demonstrated in the SPEEK/PVA system, the use of soluble macromolecules to photogenerate reactive radicals is advantageous since the polymer blends are photoactive in solution and also when present as films. Systems comprising SPEEK and water-soluble polyamines were considered ideal, as they would enable preparation of thin polymer films employing simple casting methods from aqueous solutions. Ion-exchange polyamine membranes have been used extensively in fuel cells and may offer higher gas permeabilities than that of PVA, enabling gases to diffuse into films and react with photogenerated radicals. Exposure of ketones to amines yields imines, but this reaction is reversible in H_2O and occurs mainly in the case of primary amines.[53] Preliminary experiments showed that in water the photoactivity of SPEEK was not significantly altered by the presence of some polymeric materials containing primary amine groups. However, imine formation was predominant when water was vaporized during film preparation, yielding solid matrices that were photoinactive. Thus, the ideal polyamine needed to possess less reactive secondary and tertiary amines groups in the polymer chains that would still be capable of donating an electron. The polymer of choice was polyethyleneimine, PEI, which contains a large number of primary, secondary and tertiary amine functions. PEI has been used in a number of polymeric systems, including as a solid electrolyte and as a cation exchange material in membranes.[54,55] In addition, the ability of PEI to act as a reducing agent has been recently demonstrated.[56] This polyamine also exhibits several properties that are necessary in order for this polymer to be a good

replacement of PVA, such as its solubility in water and high transparency above 300 nm. Other favorable properties are a significant high gas permeability and the ability to crosslink via a thermally induced ring-opening reaction of epichlorohydrin resulting in flexible films that are insoluble in water.[57,58] Similar to the PVA case, the degree of PEI crosslinking is a function of heating time and temperature. Because the crosslinking process involves mainly the primary amine groups of PEI, enough secondary and tertiary amine functions should remain available in the resulting films to react with ^{3}(SPEEK)* and generate anionic BPK radicals. Reaction 8 depicts the anticipated phototransformation,

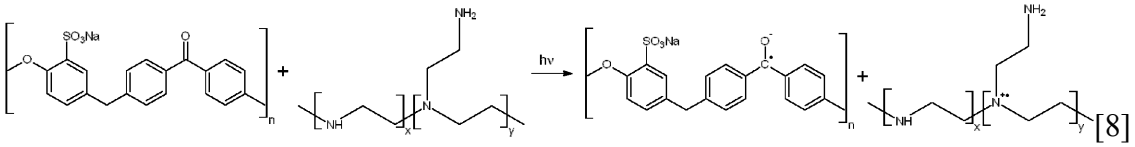

[8]

As will be shown below, illumination of SPEEK/PEI blends produced a new absorption that persists for several minutes. The newly generated radical exhibits an absorption maximum located at 600 nm, close to that of the anionic BPK radical of benzophenone.[44]

References

(1) Saito, R.; Hosoya, T. *Polymer* **2008**, *49*, 4546-4551.

(2) Chim, H.; Inoguchi, Y.; Loechner U. *Chemical Economics Handbook Marketing Research Report Polyvinyl Alcohol*; SRI Consulting, 2002.

(3) Chim, H.; Inoguchi, Y.; Loechner U. *Chemical Economics Handbook Marketing Research Report Polyvinyl Butryl*; SRI Consulting, 2007.

(4) Roff, W.J.; Scott, J.R.; Pacitti, J. *Handbook of Common Polymers*; CRC Press, Cleveland; 1971, p. 72.

(5) Yang, C. C.; Lin, J. L.; Wu, G. M. *Mater. Chem. Phys.* **2005**, *92*, 251-255.

(6) Hodgkinson, N.; Taylor, M. *Mater. World* **2000**, *8*, 24-25.

(7) Vargas, R. A.; Zapata, V. H.; Delgado, M. I.; Palacios I. *Solid State Ionics* **2004**, 175, 729-732.

(8) Hirankumar, G.; Selvasekarapandian, S.; Bhuvaneswari, M. S.; Baskaran, R.; Vijayakumar M. *J. Solid State Electrochem* **2006**, 10, 193-197.

(9) Yang, C. C.; Lin, S. J. *Mater. Letters* **2002**, 57, 873-881.

(10) Jeong, S. K.; Jo, Y. K.; Jo, N. J. *Electrochimica Acta* **2006**, 52, 1549-1555.

(11) Yeom, C. K.; Lee, K. H. *J. Membr. Sci.* **1996**, 109, 257-265.

(12) Shu. P.; Schmitt, K. D. *Colloids and Surfaces A. Physiochem. Eng. Aspects* **1996**, 110, 273-285.

(13) Wang, Z.; Luo, J.; Zhu, X. X.; Jin, S.; Tomaszewski, J. *J. Comb. Chem.* **2004**, 6, 961-966.

(14) Davis, T. L.; Farnum, J. M. *J. Am. Chem. Soc.* **1934**, 56, 883-885.

(15) Philipp, W. H.; Hsu, L. C. *Three Methods for In Situ Cross-Linking of Polyvinyl Alcohol Films for Application as Ion-Conducting Membranes in Potassium Hydroxide Electrolyte;* NASA Technical Paper 1407, Cleveland, OH, 1979.

(16) El-Rehim, H. A.; Hegazy, E. A.; Ali, A. M. *J. App. Poly. Sci.* **2000**, 76, 125-132.

(17) Rooney, M. L. *Innovations in Food Packaging*; Han, J. H., Ed; Elsevier: Amsterdam, 2005; p. 123.

(18) Korchev, A. K.; Bozack, M. J.; Slaten, B. L.; Mills, G. *J. Am. Chem. Soc.* **2004**, *126*, 10-11.

(19) Gaddy, G. A.; Korchev, A. S.; McLain, J. L.; Slaten, B. L.; Steigerwalt, E. S.; Mills, G. *J. Phys. Chem. B* **2004**, 108, 14850-14857.

(20) Korchev, A. S.; Shulyak, T. S.; Slaten, B. L.; Gale, W. F.; Mills, G. *J. Phys Chem. B* **2005**, 109, 7733-7745.

(21) Korchev, A. S.; Konovalova, T.; Cammarata, V.; Kispert, L.; Slaten, L.; Mills, G. *Langmuir* **2006**, 22, 375-384.

(22) Gaddy, G. A.; McLain, J. L.; Steigerwalt, E. S.; Broughton, R.; Slaten B. L.; Mills G. *J. Cluster Sci.* **2001**, *12*, 457-471.

(23) Chaki, N. K.; Sharma, J.; Mandle, A. B.; Mulla, I. S.; Pasricha, R.; Vijayamohanan, K. *Phys. Chem. Chem. Phys.* **2004**, 6, 1304-1310.

(24) Bard, A. J.; Faulkner, L. R. *Electrochemical Methods, Fundamentals and Applications*, Wiley 2004.

(25) Mulvaney, P. *Langmuir* **1996**, 12, 788-800.

(26) Von Sonntag, C.; Bothe, E.; Ulanski, P.; Adhikary, A. *Radiat. Phys. Chem.* **1999**, *55*, 599-603.

(27) Rodriguez-Sanchez, L; Blanco, M. C.; Lopez-Quintela, M. A. *J. Phys. Chem. B* **2000**, 104, 9683-9688.

(28) Dasenbrock, C. O.; Ridgway, T. H.; Seliskar, C. J.; Heineman, W. R. *Electrochemica Acta* **1998**, 43, 3497-3502.

(29) Wang, Z.; Chumanov, G. *Adv. Mater* **2003**, 15, 1285-1289.

(30) Gilbert, A.; Baggott, J. *Essentials of Molecular Photochemistry*; CRC Press: Boca Raton, FL., 1991; Chapter 7.

(31) Porter, G.; Wilkinson, F. *J. Chem Soc. Faraday Trans.* **1961**, 57, 1686-1691.

(32) Wilkinson, F. *J. Phys. Chem.* **1962**, 66, 2569-2574.

(33) Kometani, N.; Doi, H.; Asami, K.; Yonezawa, Y. *Phys. Chem. Chem. Phys*. **2002**, *4*, 5142-5147.

(34) Beckett, A.; Porter, G. *J. Chem. Soc. Faraday Trans.* **1963**, 59, 2038-2050.

(35) Mikhailenko, S. D.; Zaidi, S. M. J.; Kaliaguine, S. *Catalysis Today* **2001**, 67, 225-236.

(36) Jin, X.; Bishop, M. T.; Ellis, T. S.; Karasz. E. *Brit. Poly. J.* **1985**, 17, 4.

(37) Devaux, J.; Delimoy, D.; Daoust, D.; Legras, R.; Mercier, J. P.; Strazielle, C.; Nield, E. *Polymer* **1985**, 26, 1994-2000.

(38) Prasad, M. A.; Sangaranarayanan, M. V. *J. Electroanal. Chem.* **2004**, 569, 127-135.

(39) Calhoun; R. L.; Winkelmann, K.; Mills, G. *J. Phys. Chem. B* **2001**, *105*, 9739-9746.

(40) Winkelmann, K.; Calhoun, R. L.; Mills, G. *J. Phys. Chem. A* **2006**, 110, 13827-13835.

(41) Weaver, S.; Mills, G. *J. Phys. Chem. B.* **1997**, 101, 3769-3775.

(42) Choi, W.; Hoffmann, M. R. *Environ. Sci. Technol*. **1997**, *31*, 89-95.

(43) Schwarz, H. A.; Dobson, R. W. *J. Phys. Chem*. **1989**, *93*, 409-414.

(44) Ledger, M. B.; Porter, G. *J. Chem. Soc. Faraday Trans.* **1971**, 68, 539-553.

(45) Pischel, U.; Nau, W. M. *Photochem. Photobiol. Sci*. **2002**, 1, 141-147.

(46) Radlowski, C.; Sherman, W. V. *J. Phys. Chem.* **1970**, 16, 3043-3047.

(47) McDowall, L. *Australia Defense Science and Technology Organization* 2005.

(48) Jensen, B. S.; Parker, V. D. *J. C. S. Chem. Comm.* **1974**, 367-368.

(49) Minegishi, T.; Hiratsuka, H.; Tanizaki, Y.; Mori, Y. *Bull. Chem. Soc. Jpn.* **1984**, 57, 162-165.

(50) Sakurai, H.; Kubo, Y.; Shiotani, M.; Yahiro, H.; Okuda, Y. *J. Appl. Polym. Sci.* **1999**, *74*, 286-289.

(51) Bartholomew, R. F.; Davidson, R. S.; Howell, M. J. *J. Chem. Soc.* **1971**, 2804-2806.

(52) Okada, K.; Yamaji, M.; Shizuka, H. *J. Chem. Soc. Faraday Trans.* **1998**, 94, 861-866.

(53) Carey, F. A.; Sundberg, R. J. *Advanced Organic Chemistry, Part A: Structure and Mechanisms*; 3rd Ed., Plenum Press: New York, 1993; p. 448.

(54) Hu, H.; Ortiz-Aguilar, B. E.; Hechavarria, L. *Opt. Mater.* **2007**, 29, 579-584.

(55) Wang, J.; Yao, Y.; Yue, Z.; Economy J. *J. Membrane Sci.* **2009**, 337, 200-207.

(56) Kim, K.; Lee, H. B.; Lee, J. W.; Park, H. K.; Shin, K. S. *Langmuir* **2008**, *24*, 7178-7183.

(57) Ergozhin, E. E.; Mukhitdinova, B. A.; Chalov, T. K.; Iskakova, R. A. *Rus. J. App. Chem.* **2005**, *78*, 1716-1726.

(58) Kioussis D. R.; Smith, D. F.; Kofinas, P. *J. App. Polym. Sci*. **2001**, *80*, 2073.

II. Reversible Optical Switching of Silver Nanoparticles in PVA/PAA Swollen Polymers

Introduction

The reversible changes in optical absorption under electrochemical reactions define electrochromism.[1] Materials that exhibit electrochromism (ECM) have a variety of uses, from displays,[1,2] to electric mirrors,[1-3] electrochromic windows,[3] smart windows,[1,3] optical storage,[2] active camoflauge,[2] and sensors.[4,5]

Numerous strategies have been employed in attempts to realize electrochromic systems that are stable and efficient.[6] However, electrochromic devices (ECDs) that are able to operate effectively in the presence of air and H_2O based on robust, yet flexible, polymeric matrices have not been achieved. Such devices are highly likely to find numerous applications and are therefore relevant to the Army's Flexible Display Initiative.

Traditional ECDs are constructed of two transparent conductors sandwiching an electrochromic material. Thin films of metallic conductors, indium tin-oxide (ITO), and gold or carbon nano-tubes, are deposited on glass or polymeric substrates to create the working electrodes.[3] Each substrate has its own advantages and disadvantages: ITO is expensive because of the lack of availability of indium; thin films of gold are not 100% transparent; and carbon nanotubes have size-production limitations. But, all three have been studied for flexible substrates by applying a thin layer to a flexible polymer. However, problems arise when the electrode is bent beyond the limits of the metal bonding, causing a short in the service. The merits by which ECDs are judged are: 1) response time, 2) cycle life, and 3) coloration

efficiency.[1,7] The response time is often directly related to the size of the coloration area; larger areas require longer times. Yet, fast switching speeds are not necessary for all devices. Some optical glasses require several minutes to change. Cycle lifetime is determined by the number of redox cycles the device can handle without losing more than 10% of the original coloration. Coloration efficiency is defined by the change in absorbance (ΔA_λ) per unit charge (q) as shown in equation 1.[4]

$$CE = \Delta A_\lambda / q \qquad [1]$$

Most ECDs can be classified two ways, first, by dividing into four categories, or secondly, by the basic types. The four categories are: 1) metal oxides, for example, tungsten oxide (WO_3); 2) Inorganic coordination complexes, such as prussian blue; 3) organic redox compounds like viologens; and 4) electron conducting polymers like polyaniline.[7] The second classification, the three basic types, are Type 1) where the reduced and oxidized form are soluble in a given electrolyte, ex. viologens,[4] Type 2) the material is soluble in one redox state and solid in the other, ex. heptyl viologens,[2] and Type 3) where both redox states are solid, conductive polymers such as polyaniline.[7]

Metal oxides such as tungsten oxide were the first electrochromic materials discovered starting the electrochromic era.[3] WO_3 devices are Type 3; where both redox states are solid, the device utilizes tungsten's ability to change oxidization states by the addition or removal of electrons via charged ions (M = H^+, Na^+ K^+, etc.), equation 2, where WO_3 is transparent and M_xWO_3 exhibits a deep blue coloration.

$$WO_3 + xM + xe^- \rightarrow MxWO_3 \qquad [2]$$

Inorganic compounds, like prussian blue (also Type 3), are based on one electron transfer of an iron centered around ferricyanide molecules shown in equation 3,[3] where the iron (II) complex is transparent and the iron (III) is a blue color.[5]

$$M_4Fe^{II}(Fe^{II}(CN)_6)_3 \rightarrow Fe^{III}(Fe(CN)_6) + 4M^+ + 4e^- \quad [3]$$

Organic compounds like viologens, which can be Type 1 or Type 2 based upon the terminating molecular linkage, change colors through the formation of stable radical cations by delocalizing the electron though the π-framework of the molecule, (as in equation 4[2]). Pyr represents pyridinum moieties, with the radical or charged state being centered on the nitrogen. The ability to generate multiple radicals also allows viologens to exhibit several colors, causing it to become a polyelectrochromic material.[2]

$$R\text{-}^+Pyr\text{-}Pyr^+\text{-}R \rightarrow R\text{-}^+Pyr\text{-}Pyr^*\text{-}R \rightarrow R\text{-}Pyr\text{-}Pyr\text{-}R \quad [4]$$

Conductive polymers such as polyaniline are Type 3 materials that change colors by both electron transfer and proton doping as shown in equation 5. Benzenoid units (B) are converted into a quinoid units (Q), resulting in a yellow to blue color change.[3]

$$(\text{-B-N(H)-B-N(H)-})_x \rightarrow (\text{-B-N=Q=N-})_{1-x} \quad [5]$$

Oxidized conductive polymers are doped with counter ions which delocalize the π-electron band structure by reduction of the polymer. The counter ions diffuse out of the polymer leaving the polymer undoped.[2,7] The optical properties of the conductive polymer are inherently based on the gap between the highest occupied π-electron band when the polymer is doped (valence band), and the lowest unoccupied band (conduction band), when the polymer is undoped.[2,7] Conductive polymers have been the most interesting and promising for flexible ECDs, due to the elimination of a metal oxide conductive substrate. Several prototypes have been made using conductive polymers.

Each device has its own drawbacks and limitations. Some of these include, but are not, limited to: sensitivity to water and oxygen, short life cycles, poor CE, frailty, and for some applications, long switching speeds.

Table 2 - 1

ECM	Type	CE (cm^2/C)	Life Time (cycles)	Switching speed (s)
Metal Oxides				
WO_3 [3]	3	37-50	$10^4 – 10^6$	2-60
NiO [3]	3	25-100	10^3 - 10^4	2-200
Nb_2O_5 [3]	3	12-27	10^3 - 10^4	120-160
Inorganic Compounds				
Prussian Blue[3,8,9]	1	73-100	10^3 - 10^5	23 - 300
$Lu(Pc)_2$ [7]	1	-	10^6	~2
Organic Compounds				
Methyl Viologen[4]	1	<100	10^5 - 10^6	<1
Heptyl Viologen[4]	2	100-150	10^5 - 10^6	<1
Conductive Polymers				
Polyaniline[10,11]	3	~150	10^6	2-300
PEDOT[10]	3	~150	10^4	3-13

There are currently commercially available devices based on metal oxides with applications in electrochromic glasses used in windows and sunglasses, having lifetimes up to 10^6 cycles and switching speeds of minutes.[3] Several ECDs are hybrids of systems such as suspended ECM particles using conductive polmers.[3,4]

Most research has been done to improve the current qualities of existing devices, with recent advances producing devices such as electrophoretic ink,[3] conductive polymers,[12] and incorporation of nanoparticles.[1,4,13] Current properties of ECM and ECDs are summarized in Table 2-1. Recent advances in ECDs includes the preparation of poly(imide-benzidine) films

electropolymerized onto indium-tin oxide electrochromic windows and conductive polymers based on PEDOT that function as reversible, high coloration displays.[12,14,15] Reversible electrochemical coloration of these materials are insensitive over 10^5 cycles in air and in moderate amounts of water.

The incorporation of metal nanoparticles has been widely used from modifying TiO_2 which allows for a higher coloration efficiency of viologen[4] to color tuning by exploitation of nanoparticles properties, in systems classified as Type 3.[13] A special class of nanoparticles comprising of Au, Cu, and Ag exhibit surface plasmon resonance in the visible spectrum.[16] When the frequency of incoming light is in resonance with an active particle, the light can be absorbed or scattered. The absorption band is dependent on the size, shape and dielectric constant of the environment.[16] The Ag nanoparticle plasmon resonance exhibits a very strong absorbance in the visible region. Attempts have been made to use the size-dependent optical properties of silver nanoparticles for ECDs. Metallic ions have no visible optical absorption and as these ions are electrochemically reduced into metallic atoms an optical absorption occurs, being an inorganic Type 2 system. The atoms can combine in numerous ways, from interactions with ions to interactions with other atoms building nanoparticles. The growth of nanoparticles can occur with only a few metallic atoms having a fast diffusion rate in solution resulting in growth into large irreversible particles which without stabilizers precipitate out of solution.[17,18] These large particles are not easily oxidized due to surface area limitations. This results in long switching times (minutes), poor reversibility, and unstable systems. The production of metallic nanoparticles has also been accomplished by photochemical methods where metallic ions were exposed to strong light intensities.

Presented here are results from a study aimed at the reversible formation of Ag particles with nanometer dimensions within thin, optically transparent polymer films employing electrochemical methods. Silver particles of such dimensions are known to exhibit optical properties that vary to some extent with size.[19] In addition, some Ag clusters generated as intermediates during the particle formation process are also colored. Recent studies have shown that Ag nanoparticles can be generated by photoreduction of Ag^+ ions present within optically transparent crosslinked films consisting of poly(vinyl alcohol), PVA, and poly(acrylic acid), PAA.[20-22] Given that stable Ag particles form in the presence of air and water, and that metal generation is induced only at high photon intensities, but not under ambient light, such polymer systems appear to be interesting materials for ECDs.

Experimental

Poly(vinyl alcohol), PVA, (MW = 8.9-9.8 x 10^4 g/mol) and poly(acrylic acid) PAA, (MW = 2 x 10^3 g/mol), were purchased from Sigma Aldrich. Anhydrous silver perchlorate and sodium perchlorate were purchased from Alfa. Methanol, gluteraldehyde (GA, crosslinking agent), and HCl (crosslinking catalyst), were purchased from Fisher. All chemicals were used without further purification. Solutions containing PVA, PAA, GA, and HCl that served as precursors for the polymer films were prepared as described previously.[20] The solution was cast into a well made of glass microscope slides stacked 2 mm high and taped to a larger piece of glass. Placed inside the well were optically transparent quartz substrates with an indium tin oxide coating (25mm x 75mm x 1 mm ITO coating Delta Technologies, 15 ohm resistance). Cross-linking of PVA by GA was carried out in an oven at 58^0C for 3.5 - 4 h, followed by separating the polymer-coated ITO substrates from the well and immersing them overnight in methanol. This last step removed any residual acid catalyst, quenching the cross-linking reaction. The carboxylate groups of PAA were ion-exchanged in a methanolic solution containing 1 x 10^{-2} M $AgClO_4$ for 24 hr. The final concentration of Ag^+ inside the films was determined using a Radiometer phm220 conductivity meter with an Orion internal reference silver ion selective electrode.

Experiments with the polymer-coated ITO plates used a custom-built spectroelectrochemical cell (Figure 2-1), with a Lexan outer housing and Teflon inner cell. The cell comprised of an ITO substrate coated with a PVA/PAA film and a glass slide, which were compressed on both sides of the hollow inner cell using Teflon seals (Figure 2-2). The outer housing placed the necessary pressure to seal the cell and allow for the attachment of the optics

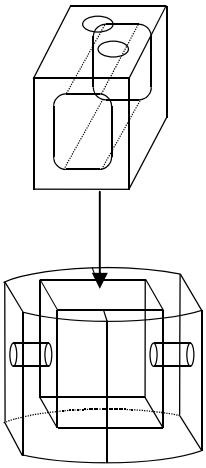

Figure 2-1 – A schematic drawing of the Teflon inner cell (top), and the Lexan outer cell (bottom). The outer cell is held together by four screws.

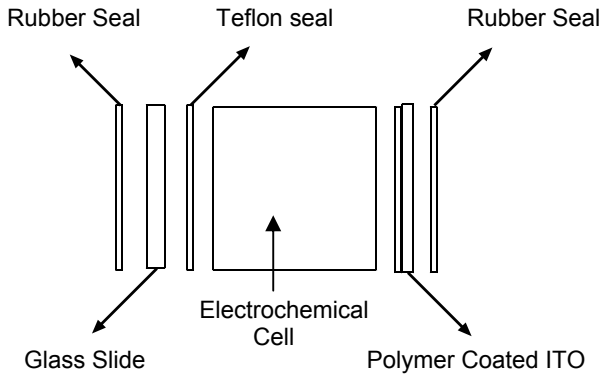

Figure 2-2 – The assembly of the cell. In the center was the Teflon inner cell surrounded by a glass slide and the polymer coated ITO then rubber seals. All this was placed into the outer cell from Figure 2-1.

(Ocean Optics ADC500 UV-Vis with a LS-1 source), perpendicular to the ITO substrate. Electrodes and electrolyte (0.1 M $NaClO_4$ in methanol) were introduced from the top of the cell.

Assembly of the cell followed the schematic in Figure 2-2. Once the cell was assembled the electrolyte was added until the cell was full. Care was taken that no air bubbles were trapped at the top. The counter (Pt wire mesh) and reference electrodes ($Hg/HgSO_4$, Princeton Applied Research) were placed into the solution through the top of the cell. A PINE Instruments AFRDE5 BiPotentiostat was used as a voltage/current source. A custom built interface connected the potentiostat to a computer containing a National Instruments Digital Acquisition Board. Also connected to the computer were the optical fibers from the spectroelectrochemical cell. In Galvanostat mode the alternating current was controlled by an EG&G Parc (Model 175) pulse generator connected to the potentiostat. The resulting data was processed using Origin Lab 7.0 software.

Electron microscopy was used to image the produced particles. Embedded particle films were microtomed and imaged on a Zeiss EM 10C 10CR Transmission Electron Microscope. Any particles found on the ITO surface were imaged using a Zeiss EVO 50 Variable Pressure Scanning Electron Microscope with Digital Imaging and EDS.

Results and Discussion

2.1 - Cyclic Voltammetry (Potentiostatic Cycling)

Initial attempts to reversibly generate Ag particles employed cyclic voltammertic (CV) techniques. Illustrated in Figure 2-3 is current/voltage data obtained from a film produced, as described earlier, and exposed to a linear sweep from -0.6 V to 0.6 V. This method allows for the construction of conventional current vs. potential graphs (Figure 2-3). The cathodic peaks (-.43 V), and the aniodic peaks (.375 V), are attributed to the formation of silver particles and oxidization. These peaks correspond with the accepted literature values for the oxidation and reduction of silver in solution.[23] Similar results have been obtained by prior researchers and other authors for systems using water.[17,18, 23] With each subsequent cycle, the peak maximum decreased, showing that each scan is not 100% efficient in recycling the Ag^+ ions.

During potentiostatic cycling the UV-Vis spectral changes were recorded. As the applied potential changes, oxidization and reduction of silver occurs while the optical density changed accordingly. This is evident in Figure 2-3, which follows five cycles with the associated optical spectrums being presented in Figure 2-4. Changes in particle formation can be tracked by following the plasmon resonance band peak for silver. In this particular system the optical absorption peak was centered at 450 nm during reduction of silver ions for each sweep. This maximum peak location is red shifted from similar results of 400 nm for ~100 nm particles, implying that the resulting particle size is large.[17] After the removal of the polymer from the ITO, the polymer was embedded, cross-sectioned by microtoming, and analyzed via TEM. The resulting particles were black in color, found on both the surface of the polymer and ITO surface. It appeared that, due to the large particle size, reoxidization was not completely reversible. Large black particles that were incapable of reoxdizing within the desired time scale were

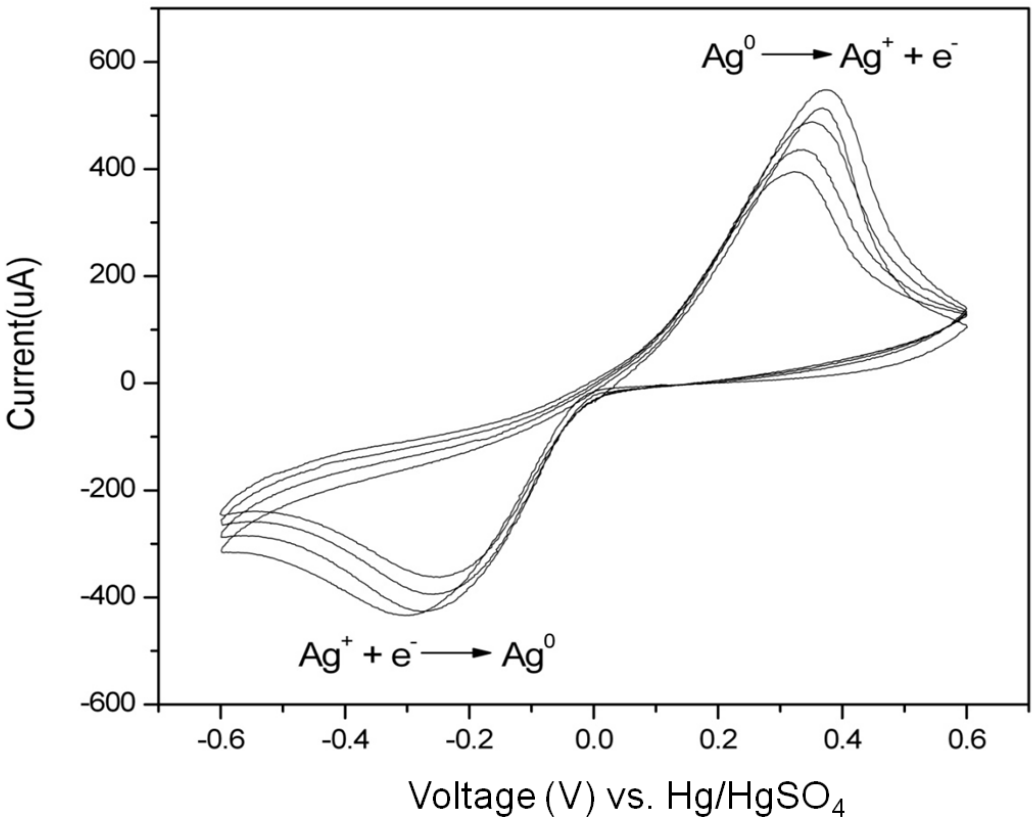

Figure 2-3 – CV of a ~60μm polymer film ion exchanged with 1 x 10^{-2} M Ag^{+} exposed to 5 potentiostatic cycles at a scan rate of 50 mV/s. The methanolic electrolyte solution contained water and air.

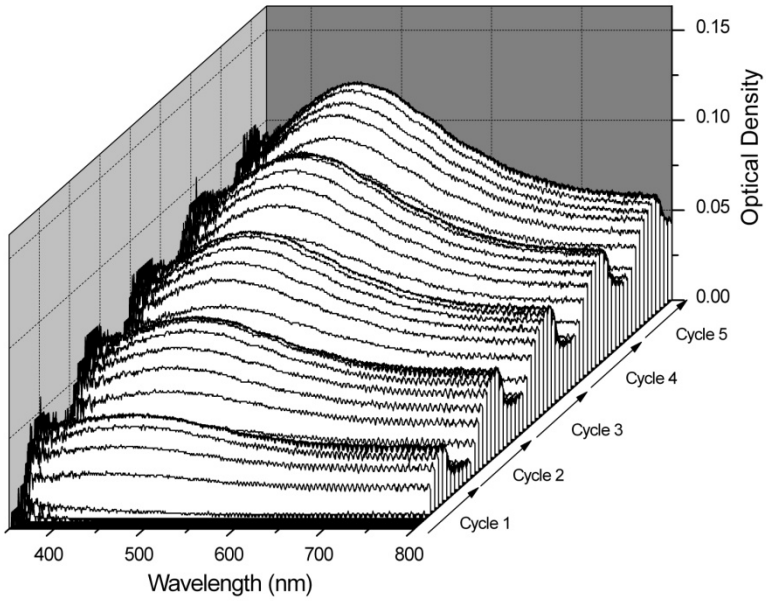

Figure 2-4 –UV-Vis spectra of the polymer film in Figure 2-3 obtained during the 5 potentiostatic cycles.

confirmed via TEM (Figure 2-5), and SEM (Figure 2-6). Large, non-uniform, distribution of particles in the TEM can only be found less than a 100 nm into the film from the ITO/Polymer interface. Large particles would be very immobile and were likely produced on the ITO surface. This was confirmed in the SEM image in Figure 2-6, where most of the particle formation was discovered. Large aggregates and particles were observed ranging from 100 nm to several microns. The observation of large particles confirmed our UV-Vis spectral observation to red-shifted longer wavelengths.

2.2 – Applied Current Density of 155 $\mu A/cm^2$

In order to overcome the production of large irreversible particles the CV method had to be abandoned. Galvanostatic switching was employed in place of the CV method, and with this method, previous researchers had been able to obtain reversibility in open circuit experiments.[24] Here current is applied in an alternating square wave while the voltage responds freely. Under galvanostatic switching a series of different current densities were used and the resulting voltage and optical spectra were recorded. The first set of experiments started by application of alternating square waves of 155 $\mu A/cm^2$ current densities. The change in OD was small and almost indistinguishable with the OD_{max} versus time shown in Figure 2-7. The optical spectrum recorded was similar to what is seen in Figure 2-4 with the OD_{max} located at 462 nm, inferring that the particles produced are large and semi irreversible as seen in Figure 2-7. In this experiment we switched first in 1 second pulses, then changed to 3 second pulses in attempts to optimize the switching speed. The attempts to switch faster than 3 seconds produced no identifiable optical response. From ohms law, V = iR, current and voltage are directly dependent on the polymeric films giving a constant resistance. This is seen in Figure 2-8 with the recorded voltage output as a function of time, where the application of 155 $\mu A/cm^2$ results in less

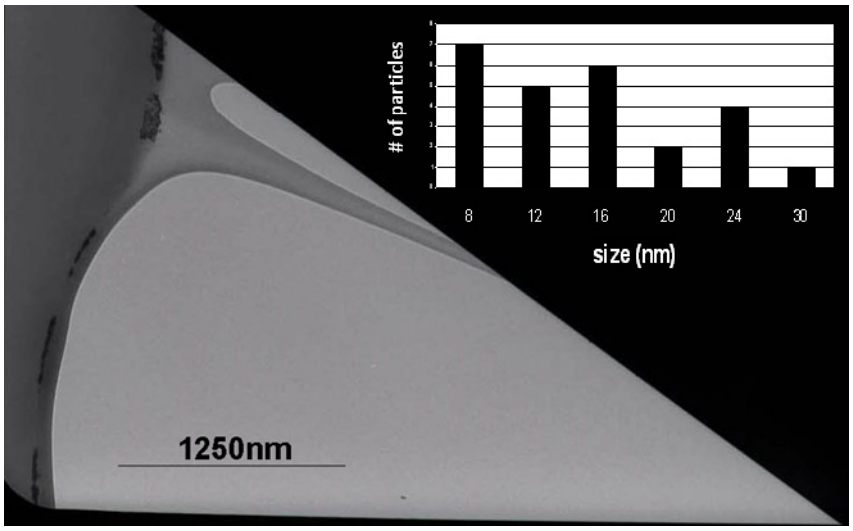

Figure 2-5 – A cross sectional TEM image of the polymer film from Figure 2-3, following removal from the ITO, embedding, and microtoming. The inset shows a size histogram for the Ag particles embedded in the PVA/PAA matrix found near the ITO polymer interface.

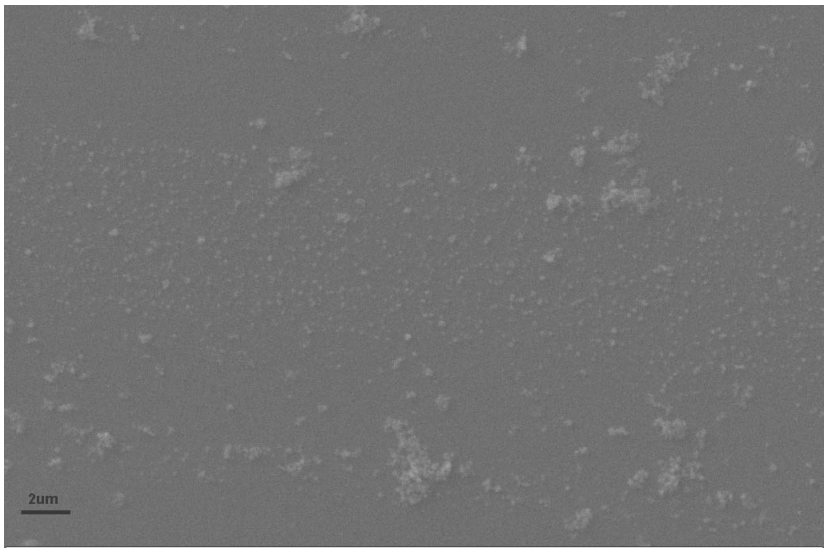

Figure 2-6 – SEM image of the ITO surface following the removal of the PVA/PAA polymer from the film described in Figure 2-3.

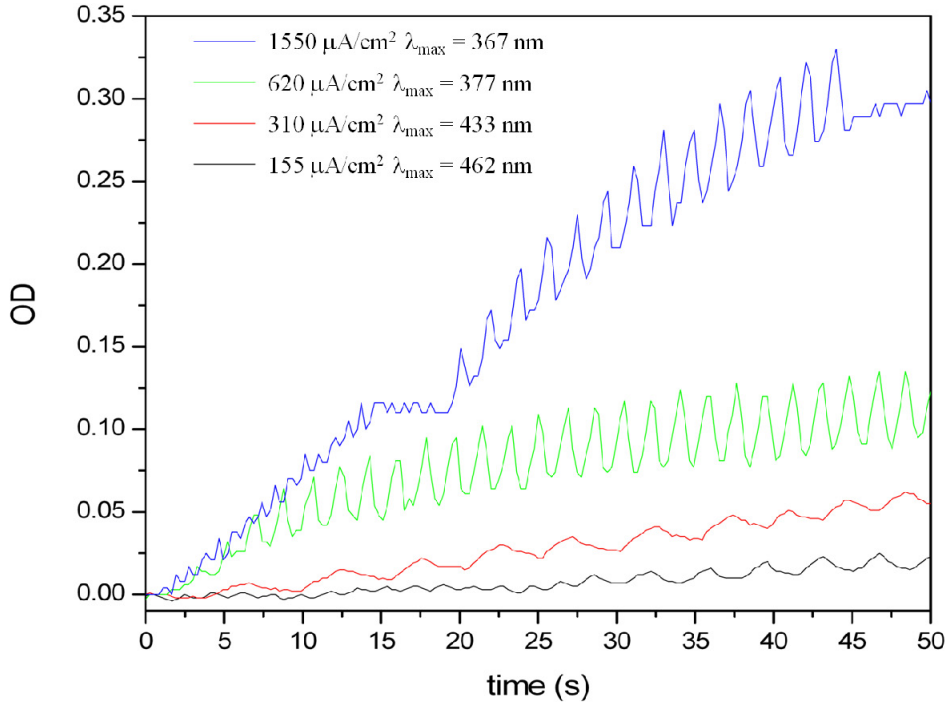

Figure 2-7 – UV-Vis spectra observed from ~60μm thick films ion exchanged with 1.0 x 10^{-2} M Ag^{+} during exposure to alternating current densities ranging from 155 to 1550 μA/cm^2 and varying cycle rates from 0.5 to 3 seconds. Spectra were reported at the observed maximum optical density for each current density.

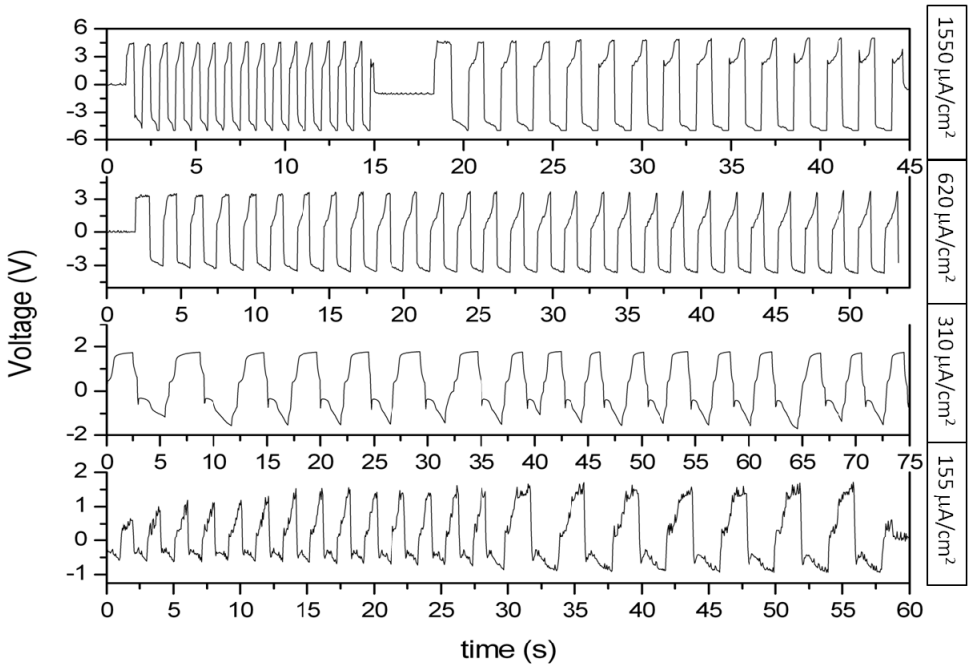

Figure 2-8 Measured voltage at the ITO electrode ITO/PVA/PAA interface as a function of time during the application of a controlled alternating square wave current for ~60 μm polymer films exposed to 1.0 x 10^{-2} M Ag^{+}. The supporting electrolyte solution contained 0.1 M $NaClO_4$ in methanol and was exposed to ambient room conditions.

than a 2 volts response for particle oxidization and less than 1 volt for particle formation. Confirmation of large particles can be seen from the TEM image shown in Figure 2-9, which shows an average particle size corresponding to 30 nm. Particles were only found near the ITO/PVA/PAA interface and extend less than a 100 nm into the film. Unlike the CV method, particles were only discovered in the PVA/PAA polymer and not on the ITO surface. Lack of particles on the ITO surface suggests that particles began to develop well into the polymer.

2.3 – Applied Current Density of 310 $\mu A/cm^2$

The next sequential current step in the process was 310 $\mu A/cm^2$ galvanostatic cycles. The same procedure was followed as with the 155 $\mu A/cm^2$ method, starting with 3 second cycles. Similar spectra to the 155 $\mu A/cm^2$ were recorded but with a blue shifted λ_{max} to 433 nm as seen in Figures 2-7 and 2-10. Large particle (50 nm) formation is predicted at this wavelength, though the particles are predicted smaller than those from the 155 $\mu A/cm^2$ case, but as shown in Figure 2-7, the produced particles have a more intense absorption and distinguishable spectra than the experiment at 155 $\mu A/cm^2$. Unlike the previous case, a new phenomenon was found: switching faster than 3 seconds produced similar OD changes. The switching time limit was only 2 seconds; faster attempts produced the same response as the 155 $\mu A/cm^2$ case. Being able to switch faster could be due to a voltage increase seen in Figure 2-10, where the voltage consistently stayed about 2 volts for particle oxidization and greater than -1 volt for ion reduction. Higher voltages result in shorter charging time leaving more electrons for the redox reaction equaling shorter time to switch redox states. TEM imaging was not performed on these samples due to the similarities seen from the CV method and 155 $\mu A/cm^2$ case.

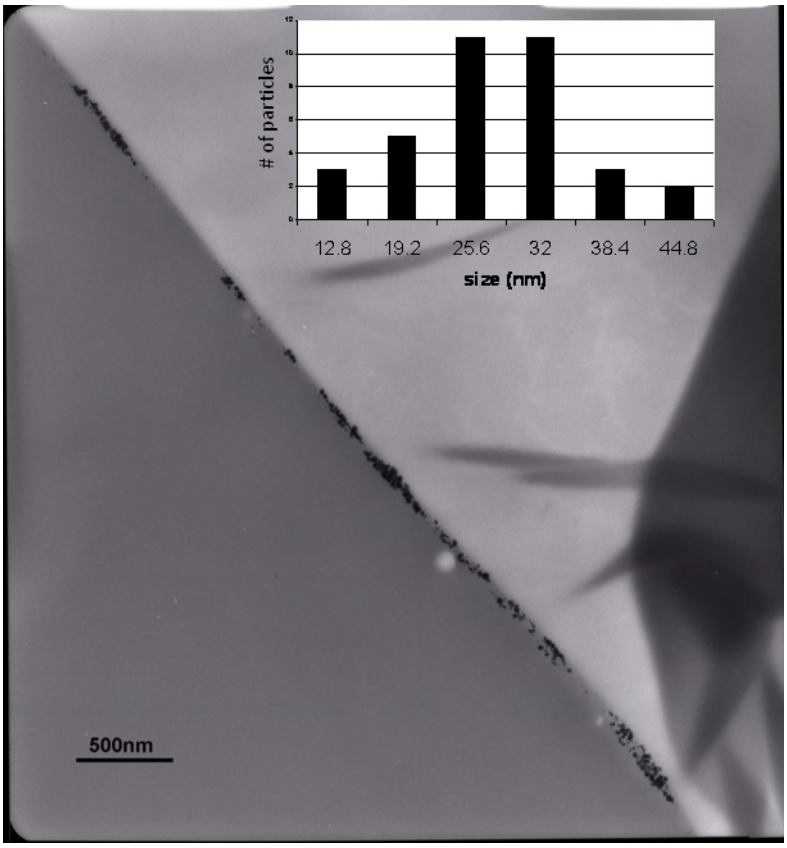

Figure 2-9 – A cross-sectional TEM image of a ~60um polymer film ion exchanged with 1.0 x 10^{-2} M Ag^{+} exposed to alternating 155 μA/cm^2 current densities, following removal from the ITO, embedding, and microtoming. The inset shows a size histogram for the Ag particles embedded in the PVA/PAA matrix found near the ITO polymer interface. No other particles were located deeper into the film.

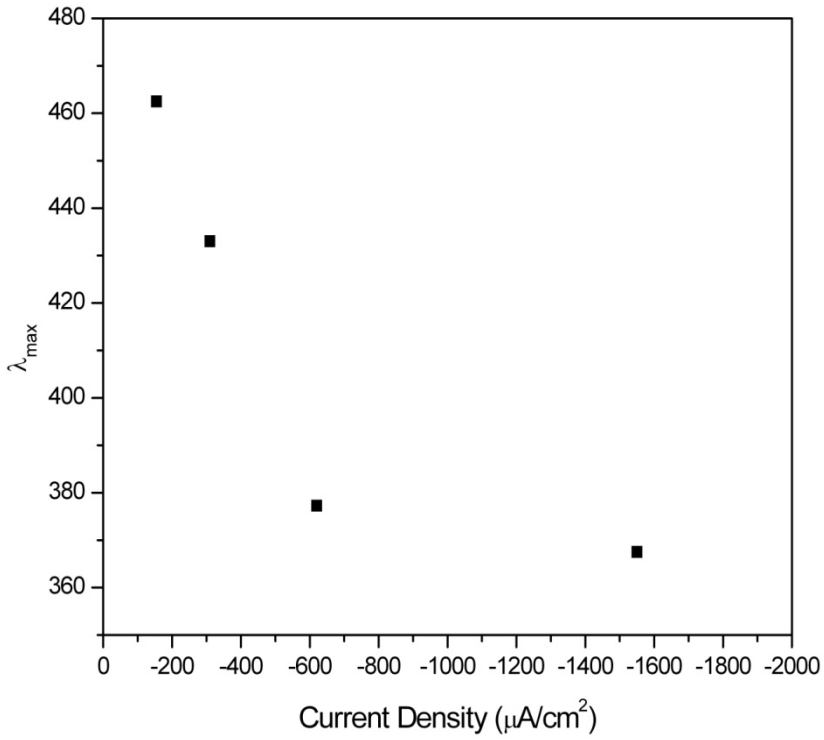

Figure 2-10 – A plot of applied current density versus observed wavelength absorption maximum for polymer films in Figure 2-7.

2.4 – Applied Current Density of 620 μA/cm^2

Following the emerging trend of larger current densities producing smaller particles, the next experiment was conducted at 620 μA/cm^2. Following previous experiments, 3 second cycles were performed while measuring the resulting spectra and voltage. The initial spectra and voltages showed a continuation of the previous trends, with the resulting spectra shown in Figure 2-11, where the absorption maximum is centered at 380 nm, producing a yellow colored polymer film predicted to contain small nanoparticles. As before, faster switching speeds were conducted in attempts to speed the optical density changes, with the optimized system shown in Figure 2-7, where switching rates of 1 s cycles for over 20 cycles were obtained. The switching was very reversible; with each oxidation the peak maximum returned to near constant value (Figure 2-7). The change in optical density is more pronounced than in the 155 or 310 μA/cm^2 system showing a system with better reversibility. Following the expected increasing voltage trend, the measured voltage in Figure 2-8 is larger with the oxidization peak being near 3 V while the reduction peak is near -3 V. We speculate that the voltage increases are the reason for the particle size decreasing from large to small. The small sized particles were confirmed by TEM in Figure 2-12, where an average particle size of ~4 nm can be seen with a uniform distribution 2.8 μm into the film. Larger particles of ~8 nm can be found near the electrode polymer interface.

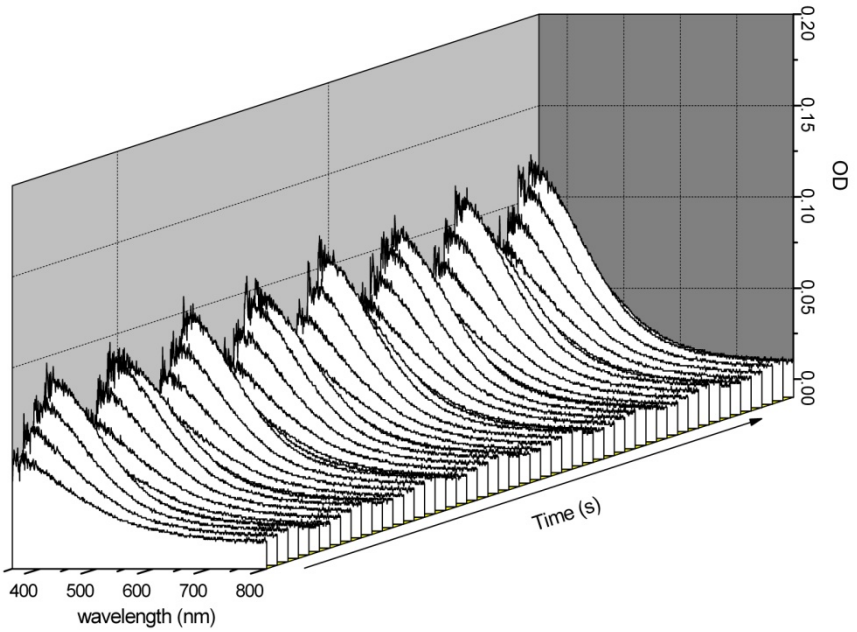

Figure 2-11 – UV-Vis spectra was observed during ~30 alternating 620 μA/cm^2 square wave current cycles for 1 second; the ~60μm PVA/PAA polymer was exposed to 1.0 x 10^{-2} M Ag^+.

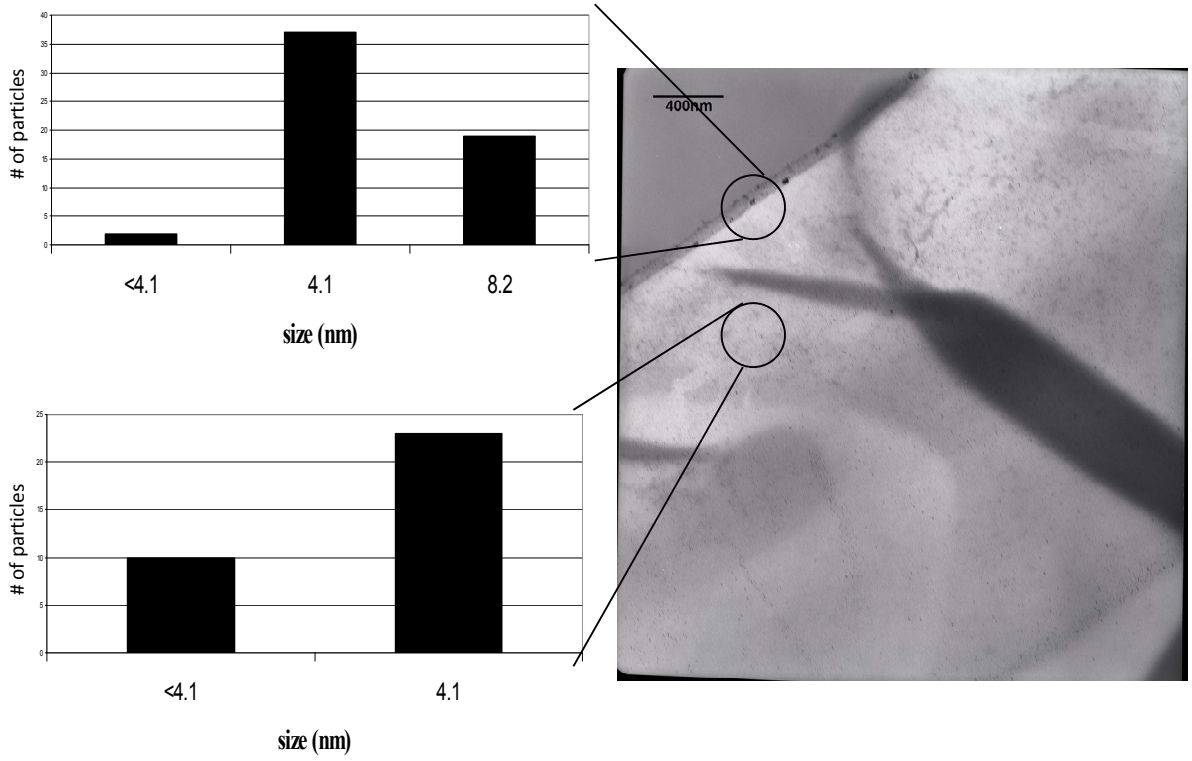

Figure 2-12 – A cross sectional TEM image of a ~60 μm polymer film, ion exchanged with 1.0 x 10^{-2} M Ag^{+} and exposed to alternating 620 μA/cm^2 current densities for ~30 cycles, following removal from the ITO, embedding, and microtoming. Size histograms show the particle sizes for the Ag particles embedded in the PVA/PAA matrix found near the ITO polymer interface and for particles that found up to 3000nm into the film; no other particles were located deeper into the film.

2.5 – Applied Current Density of 1550 $\mu A/cm^2$

In attempts to achieve a faster switching time than 1 second, the system was run at 1550 $\mu A/cm^2$ cycles. From Figure 2-7 the system is reversible at 1 second pulses, and the resulting measured voltage came very close to the 5 V maximum; in this region degradation of the ITO was observed upon polymer removal. The maximum optical density was more intense than any of the previous systems, but a general baseline drift also occurred. Once the switching time was changed to 0.5 seconds shown in the first 15 seconds of figure 2-13, the voltage dropped and the response from the optical spectrum was very minimal. The TEM image in Figure 2-14 shows a cross sectional overview of the particle formation in the polymer, with particles being present up to about 200 nm into the film. The inset expands on the region of the film showing a particle size of ~3 nm particles being present deeper into the film, with larger particles of 8 -12 nm being present near the ITO/PVA/PAA interface.

2.6 Baseline Drift

In every optical spectrum there is a baseline drift; some are more dramatic than others. The baseline drift could be from numerous things: leakage of the solvent, delamination of the film from ITO surface, formation of irreversible particles, or diffusion/migration of particles away from the oxidization/reduction zone are just a few. From experience with the system, most of the large baseline shift is due to delamination of the film from the ITO, resulting in optical scattering and inefficient contact with the electrode surface. Observations of other shifts can be seen in Figure 2-13; when the applied current stops the baseline shift also ceases. The baseline drift observed in Figure 2-13 could be due to reduction of the ITO surface as the voltage extends above -4.5 V. The true nature of the baseline drift is unknown.

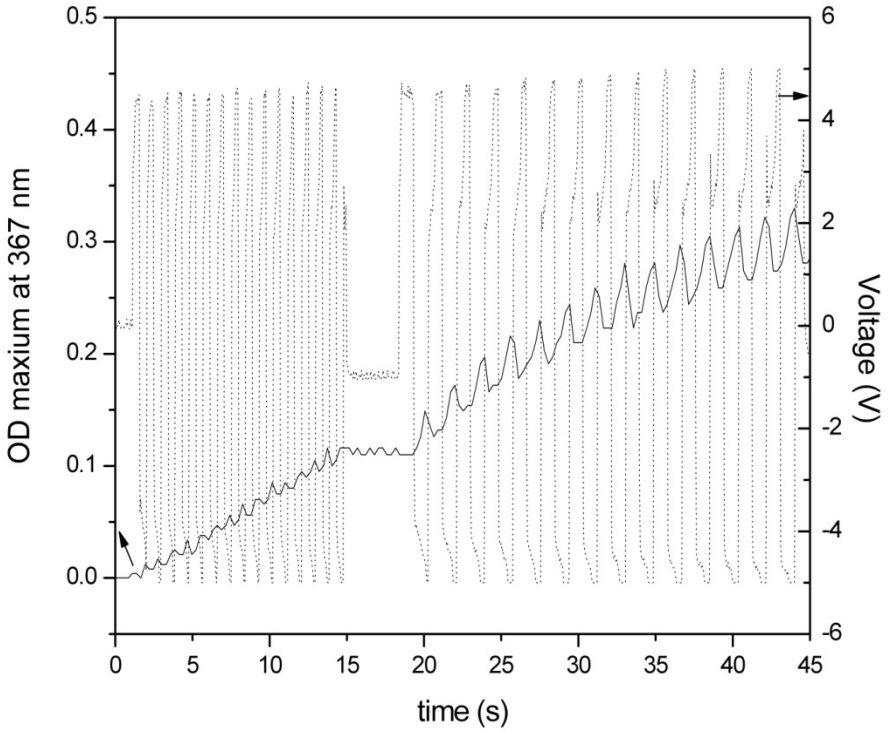

Figure 2-13 – Observed UV-Vis and measured voltage changes versus time for a PVA/PAA polymer ion exchanged with 1.0 x 10^{-2} M Ag^{+} and exposed to alternating 1550 μA/cm^2 square wave cycles for 0.5 and 1 second. Dotted line represents measured voltage, while the solid line is the observed optical spectra at the maximum optical absorbance.

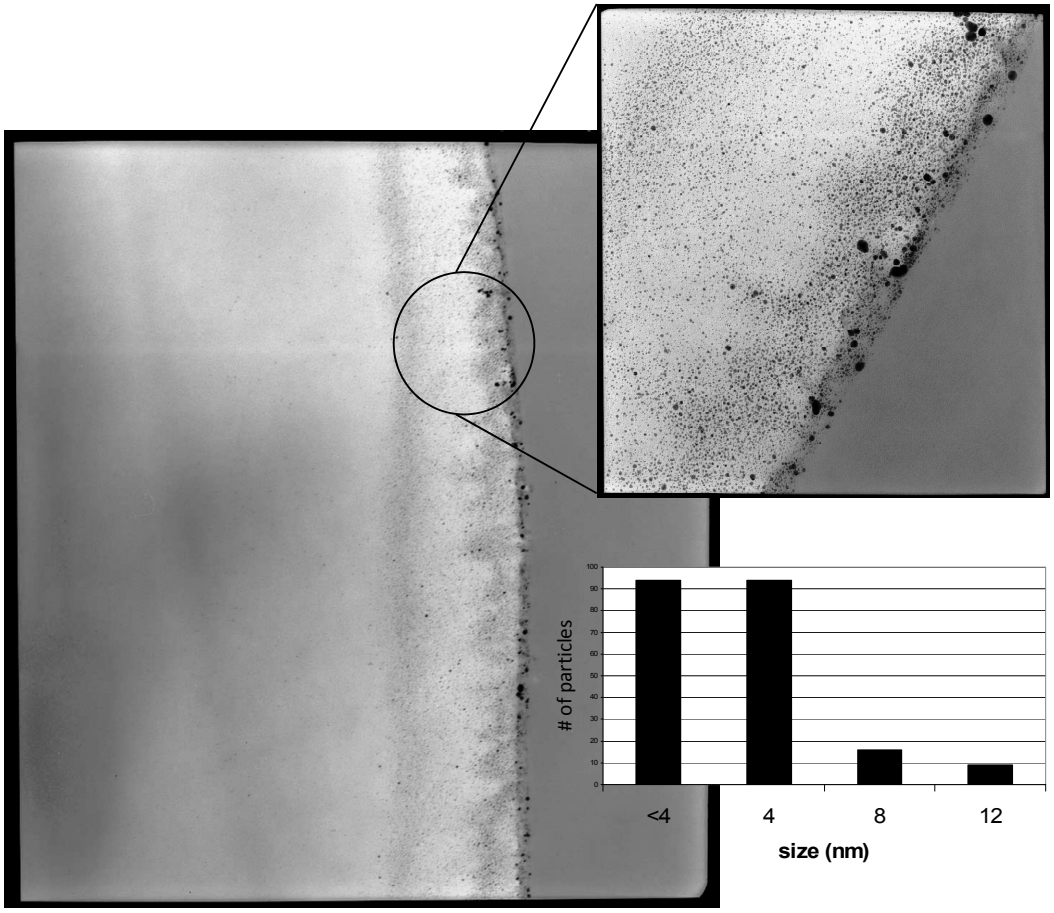

Figure 2-14 – A cross sectional TEM image of a ~60um polymer film, ion exchanged with 1.0 x 10^{-2} M Ag^{+} and exposed to alternating 1550 μA/cm^2 current densities for ~30 cycles, following removal from the ITO, embedding, and microtoming. The top inset shows an enlarged view of the Polymer/ITO interface. A Size histogram inset show the particle sizes for the Ag particles embedded in the PVA/PAA matrix found near the ITO polymer interface and for particles found ~200 nm into the film.

2.7 - Discussion

The electrochemical production of nanoparticles has been accomplished in many ways. The major problem occurs when trying to turn particles back into ions. This has been accomplished electrochemically by Mulvaney in a polymer matrix.[25] The particles were produced using cyclic voltammetry and the oxidation of the particles required a period of time on the order of a magnitude greater than the times necessary for a fast switching electrochromic device. These results were confirmed by the production of large particles by the CV method. The oxidation of large particles takes longer than the reduction of ions based on size. The kinetics involved is size dependent; a large particle is unable to move quickly in a polymeric system, and in order to be oxidized the outer layer must oxidize exposing unoxidized atoms. The mobility of ions and particles is size dependent, according to the Stokes-Einstein (equation 6), where D is the diffusion rate, κ is Boltzmann's constant, T is temperature, r is the particles radius, and η is the viscosity of the medium.

$$D = \frac{\kappa T}{6\pi r \eta} \qquad [6]$$

Because the polymer is concentrated with ions, the reduction of ions is faster than the oxidation of particles. The diffusion of species is also dependent on the concentration according to Nernst-Plank equation in equation 7.

$$J_x = -D_x \frac{d}{dx} C_x x - \frac{Z_x F}{RT} D_x C_x \frac{d}{dx} \phi \qquad [7]$$

Because the ions in the polymer are smaller than particles, and have a greater concentration gradient, this results in faster diffusion or large flux. Diffusion of ions begins when the reduction of silver ions occurs at the electrode surface in accordance with Equation 8.

$$Ag^+ + e^- \leftrightarrow Ag^0 \qquad [8]$$

The rate of reduction and atom formation occurs in accordance with Equation 9, which is directly dependent on the number of electrons and silver ions available.

$$\frac{d[Ag^0]}{dt} = k[e^-][Ag^+] \quad [9]$$

Once silver atoms have been generated they can react in multiple pathways, resulting in the generation of particles.

$$xAg^0 + yAg^+ \rightarrow Ag_{x+y}^{y+} \quad [10]$$

$$nAg^0 + mAg^0 \rightarrow Ag_{n+m} \quad [11]$$

As particles grow in size their concentration decreases, resulting in slower diffusion rates and increased difficulty to oxidize due to less electrode interaction. The rate in which the ions diffuse can be measured by exhaustive electrolysis, which results in a Cottrell plot where $t^{1/2}$ is plotted against current. The resulting diffusion constant for the ions is 2.0 x 10^{-8} cm^2/s, which is in agreement with other observed values of silver ions in other polymers.[21] The determination of diffusion constant of particles is more difficult due to the non-uniformity in size and low relative concentration. The reaction pathway for oxidization is limited to the free surface area of the particle because surface atoms need to be oxidized and removed before the subsurface atoms are available for oxidization, particle oxidization follows the Equation 12.

$$Ag_n \rightarrow Ag_{n-m} + me^- + mAg^+ \quad [12]$$

Because smaller particles diffuse faster and have a less total number of silver atoms, they are easier to oxidize back into ions. Larger particles were observed in the smaller current densities of 155 and 310 $\mu A/cm^2$. This is due to a lower concentration of silver atoms generated near the electrode surface giving a slower diffusion rate. Though silver atoms are small enough to diffuse readily into the polymer, their diffusion speed is slow because of a low concentration gradient allowing for the form particles near the electrode surface. With the continued generation of

atoms, the particles continue to grow, ultimately producing particles too large for oxidization in the desired time frame. At larger current densities, 620 and 1550 μA/cm^2, an order of magnitude higher of electrons are available for silver reduction. The higher concentrations of silver atoms being generated results in a faster diffusion away from the electrode. The diffusion layer starts to extend deeper into the polymer as the concentration increases. When the atoms begin to nucleate in the polymer more ions are available for interaction, slowing the speed of particle growth and producing smaller particles, but larger numbers of them. With the generation of smaller particles the switching speed of the device also decreased. The location of nucleation for particles is not well understood, atom-polymer interactions may play a key role in the diffusion and nucleation. PAA is terminated in carboxylic acid groups, which may be able to stabilize charged clusters as shown in Equation 13.

$$C - COO^- Ag^+ + Ag^0 \rightarrow C - COO^- Ag_2^+ \quad [13]$$

Because the polymer is not homogenous, areas of high and low charge may exist, allowing for nucleation to occur. The polymer, though swollen with electrolyte solution, may have varying density due to lack of cross-linking in certain areas, producing regions where charge can accumulate.

Voltage also plays a role in the particle generation; for the lower current densities, reduction potentials of less than a -0.5 were observed during the charging period. Charging occurred at the beginning of each current change and in the lower current densities reduction was dominated by charging. The generation of particles requiring a voltage in excess of -0.3V and destruction requiring greater than 0.3 V as observed in the CV shows that the production of particles by the lower current densities was near the minimum necessary voltage. When the

current density was increased in the 620 and 1550 $\mu A/cm^2$ cases, the responding voltage far exceeded the minimum required voltage of -0.3V and they were not dominated by charging.

The UV-Vis results are also in agreement with the Mie Theory based on plasmon resonance. As silver particles are produced they share electrons, eventually producing a dipole of electrons (plasmon) on the surface of the particle resulting in an optical absorption.[13] This plasmon interacts with light, producing minor shifts in the λ_{max}. With the increasing particle size, the more red shifted the spectrum becomes, as seen with lower current densities, and blue shifted with the higher current densities.

Conclusion

The production of a reversible electrochromic system was achieved by using silver as the chromic material and PVA/PAA as the supporting matrix. The developed system employs metal particles which are insoluble and become entrapped in the supporting matrix. With the silver particle size dictating the reversibility and generated color, this system would be classified as Type 2 inorganic compounds. Reversibility was achieved by using alternating current densities greater than 310 $\mu A/cm^2$ and obtained cycle rates faster than 3 seconds. The most unique part of this research was not the production of reversible particles, but that the system operated with nominal amounts of air and water. This achievement should help in the production of more robust ECD, allowing systems that require flexibility where air and moisture can penetrate.

References

(1) Nah, Y.; Kim, S.; Park, J.; Park, H.; Jo, J.; Kim, D. *Electrochem. Commun.*, **2007**, 9, 1542-1546.

(2) Mortimer, R. J. *Electrochimica Acta*, **1999**, 44, 2971-2981.

(3) Baetens, R.; Jelle, B. P.; Gustavsen, A. *Solar Energy Materials and Solar Cells*, **2010**, 94, 87-105.

(4) Vlachopouls, V.; Nissfolk, J.; Moller, M.; Briancon, A.; Corr, D.; Grave, C.; Leyland, N.; Mesmer, R.; Pichot, F.; Ryan, M.; Boschloo, G.; Hagfeldt, A.; *Electrochimica Acta*, **2008**, 53, 4065-4071.

(5) Karyankin, A. A. *Electroanalysis*, **2001**, 13, 813-819.

(6) Monk, P. M. S.; Mortimer, R. J.; Rosseinsky, D. R. In *Electrochromism: Principles and Applications*; Wiley-VCH: Weinheim, 1995.

(7) Mortimer, R. J.; Dyer, A. L.; Reynolds, J. R. *Displays*, **2006**, 27, 2-18.

(8) Chen, L.; Huang, Y.; Ho. K. *J. Solid State Electrochem.* **2002**, 7, 6-10.

(9) Ho, K.; *Electrochimica Acta*, **1999**, 44, 3227-3235.

(10) Huang, L.; Chen, C.; Wen, T. *Electrochimica Acta*, **2006**, 51. 5858-5891.

(11) Yoo, S. J.; Cho, J.; Lim, J. W.; Park, S. H.; Jang, J.; Sung, Y. *Electrochem. Commun.,* **2010**, 12, 164-167.

(12) Zang, C.; Hua, C.;Wang, G.; Ouyang, M.; Chunan, M. *J. Electroanal. Chem.*, **2010**, 645, 50-57.

(13) Pang, Y.; Chen, Q.; Shen, X.; Qian, H.; *Thin Solid Films*, **2010**, 518, 1920-1924.

(14) Cammarata, V.; Zhu, W.; Liang, J. *Polymer Preprints*, **2005**, *46*, 537.

(15) Cammarata, V.; Zhu, W.; Liang, J. *Polym. Mater. Sci. Eng*. **2004**, *91*, 975.

(16) Mulvaney, P.; *Langmuir* **1996**, 12, 788-800.

(17) Rodriguez-Sanchez, L.; Blanco, M. C.; Lopez-Quintela, M. A. *J. Phys. Chem. B* **2000**, 104, 9683-9688.

(18) Chapman, R.; Mulvaney, P. *Chem.l Phys. Lett.*, **2001**, 349, 358-362.

(19) Kreibig, U.; Vollmer M. *Optical Properties of Metal Clusters*; Springer Verlag: Berlin, 1995.

(20) Gaddy, G. A.; McLain, J. L.; Steigerwalt, E. S.; Broughton, R.; Slaten, B. L.; Mills, G. *J. Cluster Sci*. **2001**, *12*, 457-471.

(21) Gaddy, G. A.; McLain, J. L.; Korchev, A. S.; Slaten, B. L.; Mills, G.; *J. Phys. Chem. B*. **2004**, *108*, 14858-148565.

(22) Gaddy, G. A.; Korchev, A. S.; McLain, J. L.; Slaten, B. L.; Steigerwalt, E. S.; Mills, G. *J. Phys. Chem. B.* **2004**, *108*, 14850-14857.

(23) Chaki, N. M.; Sharma, J.; Mandle, A. B.; Mulla, I. S.; Pasricha, R.; Vijayamohanan, K. *Phys. Chem. Chem. Phys*. **2004**, 6, 1304-1309.

(24) Saez, V.; Mason, T. *Molecules* **2009**, 14, 4284-4299.

(25) Cammarata, V., Talham, D.R., Crook, R.M. and M.S. Wrighton, *J. Phys. Chem.* **1990**, 94, p. 2680-2684.

III. Radical Chain Reduction of CCl_4 Initiated by Illumination of SPEEK Solutions

Introduction

Light-initiated reductions of undesired organic compounds are interesting processes driven by reactive intermediates that form when photons are used as the energy source. Reductions can provide a direct and efficient pathway for dehalogenations, particularly in the case of halogenated compounds that are resistant to oxidative attack. Earlier studies have identified strongly reducing radicals, including $\bullet CO_2^-$ and α-hydroxy radicals of simple alcohols (such as $(CH_3)_2C\bullet OH$), as suitable reactive intermediates that can induce chain dehalogenations of organic compounds.[1-10] Participation of these radicals as carriers of long chain reactions has resulted in highly efficient reductions of a variety of halogenated chemicals. Several molecular sensitizers can photogenerate the reducing radicals, enabling efficient dechlorinations to take place in homogeneous solutions.[11-15] llumination of titania particles suspended in water also produces reducing radicals that have been used to initiate dehalogenations;[16-17] optimization of the reaction conditions led to selective and efficient reductions in the case of chlorofluorocarbons.[18-20]

Recent studies have shown that blends of sulfonated poly(ether-etherketone), SPEEK, and poly(vinyl alcohol), PVA, are capable of photogenerating α-hydroxy radicals (from now on denoted as SPEEK•) of the polymeric ketone.[21-24] SPEEK/PVA blends mimic the well known solution system composed of benzophenone (BP) and isopropanol that generates α-hydroxy (known as benzophenyl ketyl, BPK) radicals of BP upon illumination.[25] In polymeric blends

SPEEK functions as a sensitizer like BP, whereas PVA acts as the H-atom donor in a fashion analogous to $(CH_3)_2CHOH$. The fact that both polymers are soluble in H_2O enables the photochemical process to occur in solution and also in optically transparent films of the blends produced by crosslinking the macromolecules.[21-24] SPEEK• radicals exhibit long lifetimes (tens of min) when photogenerated in oxygen-free water and upon photolysis of blend films in the presence of air. Because of the long lifetime of SPEEK•, this radical is able to reduce oxidizers (for instance Ag^+) which are unable to react efficiently with α-hydroxy radicals that decay fast via diffusion-controlled processes.[21] The standard reduction potential of BPK radicals from BP has been estimated to be around -1.3 V and a similar value is anticipated for SPEEK•.[22,26] Therefore, SPEEK• is expected to be a reductant nearly as strong as $(CH_3)_2C•OH$, $E°[(CH_3)_2C•OH/(CH_3)_2C=O, H^+] = -1.4$ V.[27] According to this analysis, reductions of halocarbons by SPEEK• in a way analogous to the dehalogenations induced by $(CH_3)_2C•OH$ seem feasible.

SPEEK• was found to exhibit similar reactivities when photogenerated in water and within thin polymer films.[21-24] Based on such results, the SPEEK/PVA sensitizing systems appear, in principle, capable of inducing dehalogenations upon illumination of the solid matrices. The potential ability of SPEEK/PVA films to induce reductive degradation of chemicals at the solid-liquid or solid-gas interfaces would enable them to function as light-activated barriers against toxins. Reactive barriers are currently of interest given their possible utilization as "self-cleaning" surfaces for protective fabrics.[28,29] However, solution photoreactions are simpler to study than transformations involving polymer films and can provide information useful to understand processes occurring on the latter systems.[30] Reported here are results from a kinetic investigation on the reduction of CCl_4 by photogenerated SPEEK• radicals in air-free aqueous

medium. One of the aims of this study was to test the effectiveness of the polymer radicals to induce dehalogenations. Selection of CCl_4 as a model chlorocarbon stems from the fact that this pollutant is quite toxic,[31] mimics carbon based chorine containing chemical warfare agent, and is a standard for testing sorptive materials present in protective fabrics.[32] Furthermore, CCl_4 is impervious to oxidative attack but undergoes reduction induced by free radicals, $E^0(CCl_4/\bullet CCl_3,Cl^-) = -0.23$ V,[33] and has been extensively used in prior photodechlorination studies that employed homogeneous and heterogenous sensitizers.[11-14,16-17]

Another goal of the present investigation was to identify experimental conditions leading to efficient chain photoreductions. Dechlorinations of halocarbons (including CCl_4) have been found to be most efficient when $\bullet CO_2^-$ is the chain carrier.[10,14,16-17,18-20] Such observations have been interpretated on the basis that the formyl radical anion is a stronger reductant than α-hydroxy radicals, $E^0(\bullet CO_2^-/CO_2) = -1.8$ V.[33] Interestingly, formation of $\bullet CO_2^-$ has been reported to occur via H-atom abstraction from HCO_2^- ions by excited states of BP,[34] which proceeds with a rate constant of $k = 1 \times 10^8\ M^{-1}\ s^{-1}$.[35] Photogeneration of $\bullet CO_2^-$ in solutions containing SPEEK and HCO_2^- seemed possible if excited states of the polymeric ketone were able to abstract H-atoms from formate ions. Evidence presented below demonstrate that CCl_4 undergoes chain dechlorination upon photolysis of aqueous solutions of SPEEK, but the reductions are most efficient when HCO_2^- ions served as hydrogen atom donors instead of PVA.

Experimental

The sodium salt of SPEEK employed in the photochemical reactions was synthesized as described before via sulfonation of poly(ether etherketone), PEEK, with an average molar mass = 4.5 x 10^4 g mol^{-1} that was a gift from Victrex.[21-24] All other chemicals, including PVA (99+% hydrolyzed, average molar mass = 8.9-9.8 x 10^4 g mol^{-1}), were used as received from Fisher or Aldrich. Aqueous solutions were prepared from distilled water purified with a resin deionizer (U.S. Filter Service). Solutions containing both polyol and polyketone were prepared as outlined previously.[21-24] Unless otherwise stated, the photolyzed solutions contained 1.6 wt.% PVA and 0.7 wt.% SPEEK, which in terms of monomer units correspond to 0.36 M of polyol and 0.018 M of polyketone. The solutions also contained 0.1 M $NaClO_4$ as an inert electrolyte needed for potentiometric determinations and pH adjustements were carried out with NaOH and $HClO_4$. Alternatively, illuminations were performed on solutions containing 0.018 M SPEEK and $HCO_2H/NaCO_2H$ buffers, where sodium formate served as the inert electrolyte. Throughout this study the buffer concentration is given in terms of $[HCO_2^-] + [HCO_2H]$. Air-free systems were prepared by bubbling the solutions with Ar for 30 min under continuous stirring in a sealed photochemical reactor vessel. CCl_4 was washed three times with H_2O to eliminate the stabilizer and then degassed via three freeze-pump-thaw cycles. In a subsequent step, 1 mL of degassed CCl_4 was injected with gas-tight syringes into the sealed photoreactor containing the solutions saturated with Ar. Two liquid phases formed in these systems due to the low solubility of carbon tetrachloride in water (5.1×10^{-3} M or 30 μL CCl_4 in 60 mL of aqueous solution).[36]

After introduction of degassed CCl_4, the mixtures were stirred for at least 5 min prior to illumination, which created numerous small droplets of CCl_4 liquid distributed throughout the aqueous phase. The resulting kinetic data was independent of the length of this equilibration

period beyond 5 min. Concentrations of Cl^- were determined *in situ* under continuous irradiation and stirring using an ion selective electrode (ISE) from Orion in conjunction with a Radiometer K601 mercurous sulfate reference electrode and Radiometer instrumentation as described before.[9] Given that the reference electrode is sensitive to light, a new photoreactor with an internal volume of 64 mL was made from borosilicate glass. Presented in Figure 3-1 is a diagram of the vessel consisting of two joined vertical cylinders; the Cl^- ISE was immersed into the liquid present in the left cylindrical chamber whereas the reference electrode was immersed into the solution located in the right compartment. Perforated septa, through which tightly fitted electrodes were immersed into the solution, served as seals. Part of the left cylinder was flattened forming a vertical window (1.5 x 2.5 cm), which enabled exposure of the solution to light under continuous stirring. On the other hand, the right compartment was shielded from radiation using Al foil. The two horizontal tubes that join the cylinders ensured fast equilibration of the liquid samples present in each compartment. The ISE were calibrated in the dark prior to each experiment under conditions duplicating those of the photolysis experiments. Most experiments were performed at least twice, a maximum of 20% error for all data was noticed due to the lack of a statistical population.

Light from a PTI 1010 S system with a 150 W Xe arc lamp was filtered using a 10 cm water filter and an IR absorbing filter to remove infrared radiation. Photons with wavelengths between 320 and 385 nm (maximum transmittance at 360 nm) were selected by a Kopp GS-7-60 filter and focused on the flat, lateral window (38 mm × 51 mm) of the photoreactor. Variations in light intensity (I_o) were accomplished by inserting neutral density filters into the light path. Aberchrome 540 actinometry was used to measure I_o for each irradiation.[37] Incident light

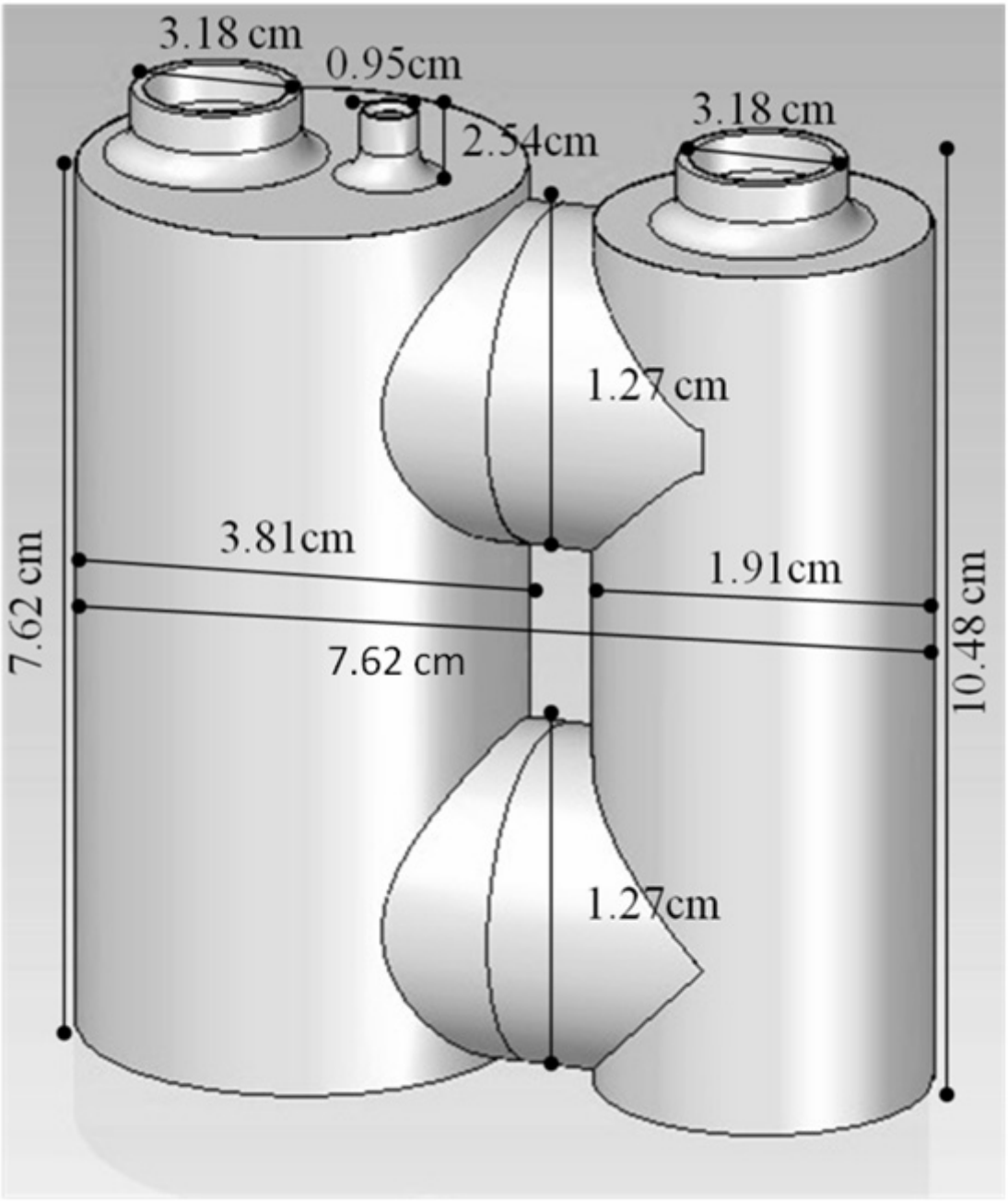

Figure 3-1. Diagram of the photoreactor employed in the illuminations.

intensities for typical reactions varied between 1-1.1 x 10^{-6} M photons s^{-1}. Identification of gaseous products was performed using a Hewlett Packard 5890 gas chromatograph connected to a Trio 2000-1133 mass spectrometer. GC-MS analysis of products from the photoreaction was performed on gas samples removed from photoreactor headspace after 24 h of photolysis. All SPEEK/PVA data is reproduced with the permission of Harris Carmichael.

Results and Discussion

All illuminations were conducted in the absence of air since O_2 is an efficient scavenger of reducing radicals including SPEEK•.[21-24] Most experiments employed the PTI system because this light source generated lower photon intensities, which favor long chain dehalogenation reactions.[18-19] Presented in Figure 3-2 is the evolution of [Cl^-] as function of illumination time for an air-free solutions at pH = 6 saturated with CCl_4 that contained 0.018 M SPEEK and 0.36 M formate buffer. Included in the Figure are the Cl^- concentrations, multiplied by 10, that resulted from photolysis of a solution at pH = 6 containing 0.36 M PVA as the H-atom donor. All photoreactions proceeded via two steps: an initial induction period lasting up to 10 min, followed by a step where Cl^- ion generation varied linearly with time. The length of the induction period was not reproducible and independent of degassing and equilibration times, pH and concentrations of reactants, but increased markedly with decreasing I_0. In most cases [Cl^-] increased slowly and non-linearly during this period but short bursts of Cl^- formation were noticed occasionally. Similar observations made during the photoreduction of CCl_3F were shown to result from scavenging of the reducing radicals by trace amounts of O_2 present in the solutions.[18] The induction period can be qualitatively understood on the basis of a mechanism that governs the reductive dechlorination of CCl_4 in the presence of O_2:[2]

$$RC\bullet OH + O_2 \rightarrow RC{=}O + HO_2\bullet/O_2^- + H^+ \quad (3\text{-}2)$$

$$RC\bullet OH + CCl_4 \rightarrow \bullet CCl_3 + H^+ + RC{=}O + Cl^- \quad (3\text{-}3)$$

$$O_2 + \bullet CCl_3 \rightarrow \bullet O_2CCl_3 \quad (3\text{-}4)$$

$$\bullet O_2CCl_3 + RHOH \rightarrow HO_2CCl_3 + RC\bullet OH \quad (3\text{-}5)$$

$$HO_2CCl_3 + H_2O \rightarrow 3Cl^- + \text{products} \quad (3\text{-}6)$$

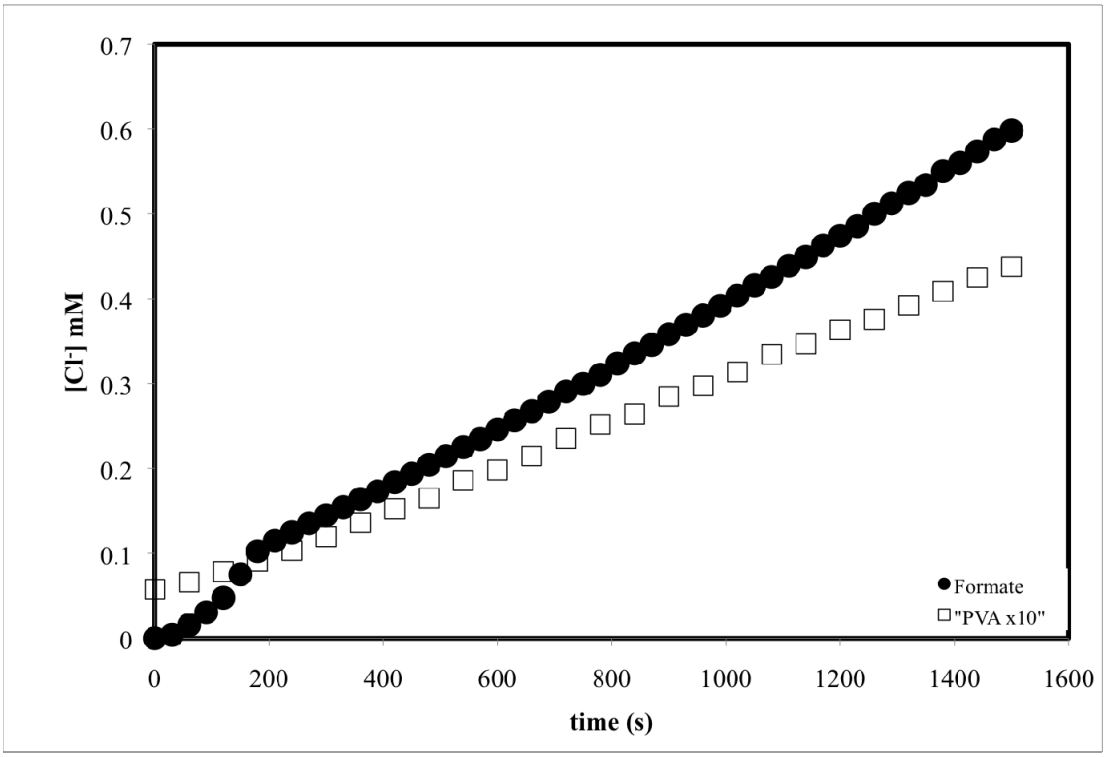

Figure 3-2 Evolution of the chloride ion concentration during photolysis of degassed solutions at pH = 6 containing excess CCl_4, 0.018 M SPEEK and 0.36 M formate buffer (●), or [PVA] = 0.36 M and 0.1 M $NaClO_4$ (□) with $I_0 = 9 \times 10^{-7}$ M (hν)/s. The Cl^- concentrations resulting from the experiment with PVA and $NaClO_4$ are multiplied by a factor of 10.

where RC•OH represents a reducing radical such as SPEEK• or the α-hydroxy radical form PVA and RHOH corresponds to the polyol. An analogous set of steps (presented later) can be envisioned in which $\bullet CO_2^-$ is the reducing radical and the corresponding electron donor is HCO_2^-.

In most cases formation of Cl^- is delayed during the induction period because O_2 scavanges RC•OH radicals via diffusion controlled step (3-2) that yields HO_2/O_2^- species,[38] which are unable to reduce carbon-halogen bonds.[39] At low $[O_2]$ some reducing radicals manage to reduce CCl_4 through step (3-3) and the resulting $\bullet CCl_3$ radicals are scavenged by O_2 in step (3-4) with $k = 2–3 \times 10^9\ M^{-1}\ s^{-1}$.[40-41] The resulting peroxy radical $\bullet O_2CCl_3$ is more reactive than $\bullet CCl_3$ toward H-atom abstraction from donor molecules, generating HO_2CCl_3 and reforming the reducing radical via step (3-5).[2] Occurrence of a reaction between $\bullet O_2CCl_3$ and PVA seems logical since the polyol is known to be a better H-atom donor than simple alcohols.[42] Halogenated hydroperoxides decay in water with complete loss of all halogen atoms via a mechanism that still remains unknown;[39] equation (3-6) represents such process in the case of HO_2CCl_3. The sequence of steps (3-3) through (3-6) explains the occasional bursts of Cl^- noticed during the induction period. Since formation of Cl^- ions was irreproducible during the induction period the kinetic data of this step were not further analyzed.

Once most of the O_2 was consumed, formation of Cl^- ions proceeded linearly with time through step (3-3). As shown in Figure 3-2, generation of Cl^- was about 11 times faster in solutions containing formate ions instead of PVA. Rates of Cl^- formation derived from the linear increase in concentration vs time were utilized to evaluate quantum yields of chloride ion formation, $Q.Y.(Cl^-)$. Such calculations were feasible because at the employed [SPEEK] most of the impinging photons were absorbed by the polyketone.[22] Considering that stirring generated a large number of CCl_4 droplets dispersed throughout the solutions which scatter light, the

quantum yields reported here must be considered lower limits. A quantum yield of 0.033 resulted for the solution containing PVA as H-atom donor whereas in the presence of formate buffer Q.Y.(Cl^-) was 0.37. Both Q.Y.(Cl^-) values are larger, particularly the second one, than the quantum yield of SPEEK• (Q.Y.(SPEEK•)) of 0.02 determined in neutral SPEEK/PVA solutions.[22] Rates of Cl^- formation larger than I_0 are suggestive that chain dechlorinations are taking place, which may result in post-irradiation effects analogous to those observed during the reduction of CCl_4 and CCl_3F.[2,18] Experiments were, therefore, conducted in which a SPEEK solution at pH = 7.3 containing formate buffer and CCl_4 were periodically exposed to light. Figure 3-3 depicts data gathered from illuminating the solution initially for 2 min followed by a dark period of the same length. At times longer than 15 min the photolysis and dark periods amounted to 4 min each. After an induction period of about 2 min, linear increases in [Cl^-] occurred during each illumination step with an average rate of 8×10^{-7} M s^{-1}. The chloride ion concentration continued to increase in the dark, but the post-irradiation reaction yielded sublinear changes in [Cl^-]. Initial rates of post-irradiation Cl^- formation were obtained from data acquired within 0.5 min after photolysis was stopped, yielding an average rate (2×10^{-7} M s^{-1}) that is 4 times lower than the value determined in the presence of light. These observations resemble those made during the radiolytic reduction of CCl_4,[1b] where Cl^- generation was faster during irradiation as compared to the ensuing post-irradiation formation.

Presented in the inset of 3- 3 are data gathered using a solution containing PVA instead of the formate buffer. Because the photoreaction rate was significantly lower under these conditions (2×10^{-8} M s^{-1}), illumination was extended for longer times to prevent any potential artifacts induced by traces of O_2. Termination of the light-exposure resulted in a very slow post-

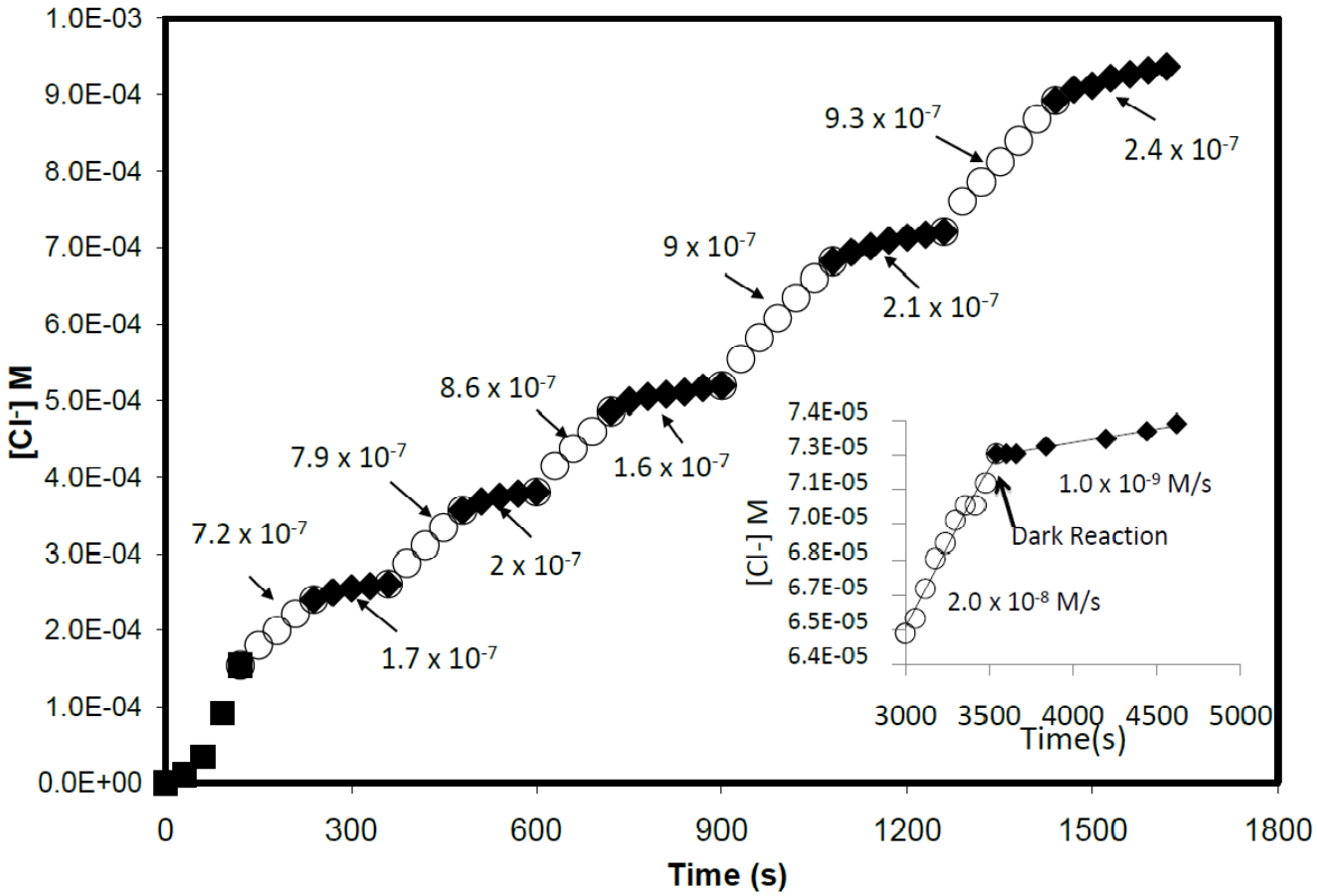

Figure 3-3. Changes in [Cl^-] during alternating illumination (○) and dark periods (◆) of a degassed solution at pH = 7.3 containing 1 mL CCl_4, 0.018 M SPEEK and 0.36 M formate buffer. The inset depicts the [Cl^-] increase during photolysis (○) and in the dark (◆) measured in a degassed solution at pH = 7.3 containing 1 mL CCl_4, 0.018 M SPEEK, 0.36 M PVA and 0.1 M $NaClO_4$. I_0 = 9 x 10^{-7} M (hν)/s in both cases; included in the plots are the rates of Cl^- ion formation.

irradiation formation of Cl^- with a rate 20 times smaller than in the presence of light. Hence, the results depicted in Figure 3-3 provide convincing evidence that the photoreduction of CCl_4 initiated by SPEEK proceeded via a chain process in systems where HCO_2^- or PVA served as H-atom donors. The chain process can be envisioned to involve reactions (3-3) and (3-7) as propagation steps,

$$\bullet CCl_3 + RHOH \rightarrow HCCl_3 + RC\bullet OH \qquad (3\text{-}7)$$

Further support for the idea that the photoreduction of CCl_4 involved a chain process was provided by an additional experiment performed with the solution that yielded the data shown in the inset of Figure 3-3. After allowing the dark reaction to proceed for about 27 min, air was admitted into the solution. As a result, $[Cl^-]$ increased linearly with a rate of 4×10^{-9} M s^{-1} in a short step lasting for only 2 min that generated about 77% of the chloride ions formed during the dark reaction without air. No further changes in $[Cl^-]$ were detected thereafter, demonstrating that the slow dark evolution in concentration illustrated in Figure 3-3 was not an artifact due to thermal drift of the ISE sensor. The faster CCl_4 dechlorination in the dark after introduction of O_2 was not unexpected since similar observations were made during the chain reductions of CCl_4 and CCl_3F.[2,18] According to the sequence of steps (3-3) and (3-7), one Cl^- ion is generated per reducing radical in the absence of air whereas the mechanism involving steps (3-3) through (3-6) yields 4 Cl^- ions per RC•OH radical. This comparison explains the fact that the post-irradiation Cl^- formation in the absence of air was 4 times slower than in the presence of O_2. Furthermore, the HO_2/O_2^- species generated via step (3-2) are not only unable to reduce CCl_4 but also terminate chains via reduction of $\bullet O_2CCl_3$.[39] This is the reason for the short Cl^- ion formation noticed after air was introduced during the dark reaction.

Illustrated in Figure 3-4 is a comparison of quantum yields of Cl^- formation as a function of pH for systems containing either formate ions or PVA as H-atom donors. Determinations of $[Cl^-]$ in solutions with pH > 8 were not possible because OH^- ions interfere with the ISE measurements. In the PVA system Q.Y.(Cl^-) reached a highest value of 0.033 at pH = 6, declining slightly when the proton ion concentration decreased. This trend is probably related to changes in the speed of SPEEK• decay noticed when second-order dimerization/ disproportionation rate constants were determined in the range $6 \leq pH \leq 8$ using the optical method described before.[21-24] As will be discussed in Chapter 4, the decay rate constant increased smoothly from 6×10^2 to 1.8×10^3 M^{-1} s^{-1} when the pH was raised from 6 to 8. A faster decay of SPEEK• means that less radicals were available to react according to step (3-3), which decreased the amount of Cl^- produced. The data presented in Figure 3-4 implies that increasing $[H^+]$ decreased Q.Y.(Cl^-) significantly. A similar trend was noticed at a higher I_0 (7×10^{-5} M(hν) s^{-1}) where lowering the pH from neutral to 5.1 decreased Q.Y.(SPEEK•) from 0.02 to 4×10^{-3}. Although direct comparisons between Q.Y.(Cl^-) and Q.Y.(SPEEK•) values obtained at very different light intensities are not meaningful, qualitative correlations between their evolutions as a function of pH seem reasonable given that SPEEK• generates Cl^-. Lower efficiencies of radical formation in acid solutions are expected since protons quench the triplet excited state of BP.[44] This effect affects negatively the efficiency of BP radicals formation. Obviously, H^+ induces a similar quenching of the triplet excited state of SPEEK, ^{3}{SPEEK}*, lowering Q.Y.(SPEEK•) and consequently decreasing Q.Y.(Cl^-).

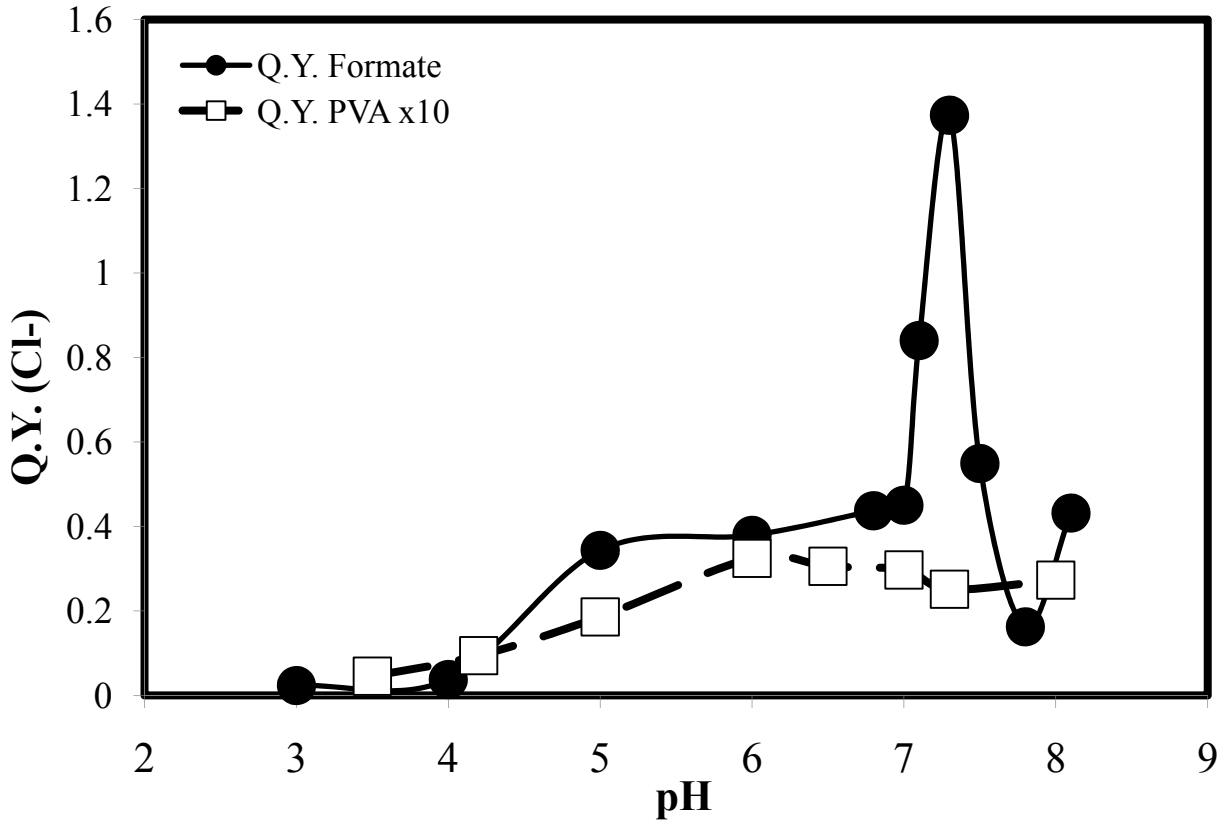

Figure 3-4. Quantum yields of Cl^- ion formation as a function of pH during photolysis of degassed solutions containing 1 mL CCl_4, 0.018 M SPEEK and 0.36 M formate buffer (●), or [PVA] = 0.36 M and 0.1 M $NaClO_4$ (□) with $I_0 = 9 \times 10^{-7}$ M (hν)/s. The quantum yields resulting from experiments with PVA and $NaClO_4$ were multiplied by a factor of 10.

An obvious difference between the two sets of data depicted in Figure 3-4 is that, in most cases, the quantum yields obtained in solutions with formate ions were between 10 to 15 times higher than the Q.Y.(Cl^-) values determined in solutions of PVA. Also, Q.Y.(Cl^-) values for formate solutions were less affected by decreases in pH, suggesting that HCO_2^- ions competed with H^+ more effectively for ^{3}{SPEEK}* than PVA. Having in mind that $pK_a = 3.7$ for formic acid, the larger decrease in Q.Y.(Cl^-) noticed at pH < 5 implies that HCO_2^- is a more effective quencher of ^{3}{SPEEK}* than HCO_2H. The most pronounced difference occurred at pH = 7.3 where Q.Y.(Cl^-) for the formate system was 55 times higher than the value obtained with the polyol as a H-atom donor. In fact, the sharp maximum of Q.Y.(Cl^-) = 1.37 depicted in Figure 3-4 at that pH for the formate system is surprising given that Q.Y.(SPEEK•) determinations at $I_0 = 7 \times 10^{-5}$ M(hν) s^{-1} showed no variations in the quantum yield at pH ≥ 7. Thus, such trend suggests that the origin of such maximum is not related to the steps that generated the reducing radicals.

The evidence presented thus far indicates that the photoreduction of CCl_4 initiated by photolysis of SPEEK took place via chain processes irrespective of the nature of the H-atom donor. Considering that the photoreaction was most efficient in formate solutions at pH = 7.3, further efforts were centered on elucidating the kinetic features of the chain process under those experimental conditions. Presented in Figure 3-5 is the dependence of Q.Y.(Cl^-) on light intensity; reproducible results were obtained only at $I_0 > 3 \times 10^{-7}$ M(hν) s^{-1} because smaller photon fluxes resulted in extremely long induction periods. Very similar quantum yields were determined at $I_0 \geq 3 \times 10^{-7}$ M(hν) s^{-1} but a drop in Q.Y.(Cl^-) was noticed at the lowest light intensity. Significant scattering of light took place in the solutions due to the presence of numerous small droplets of liquid CCl_4 that were dispersed in the aqueous phase upon stirring.

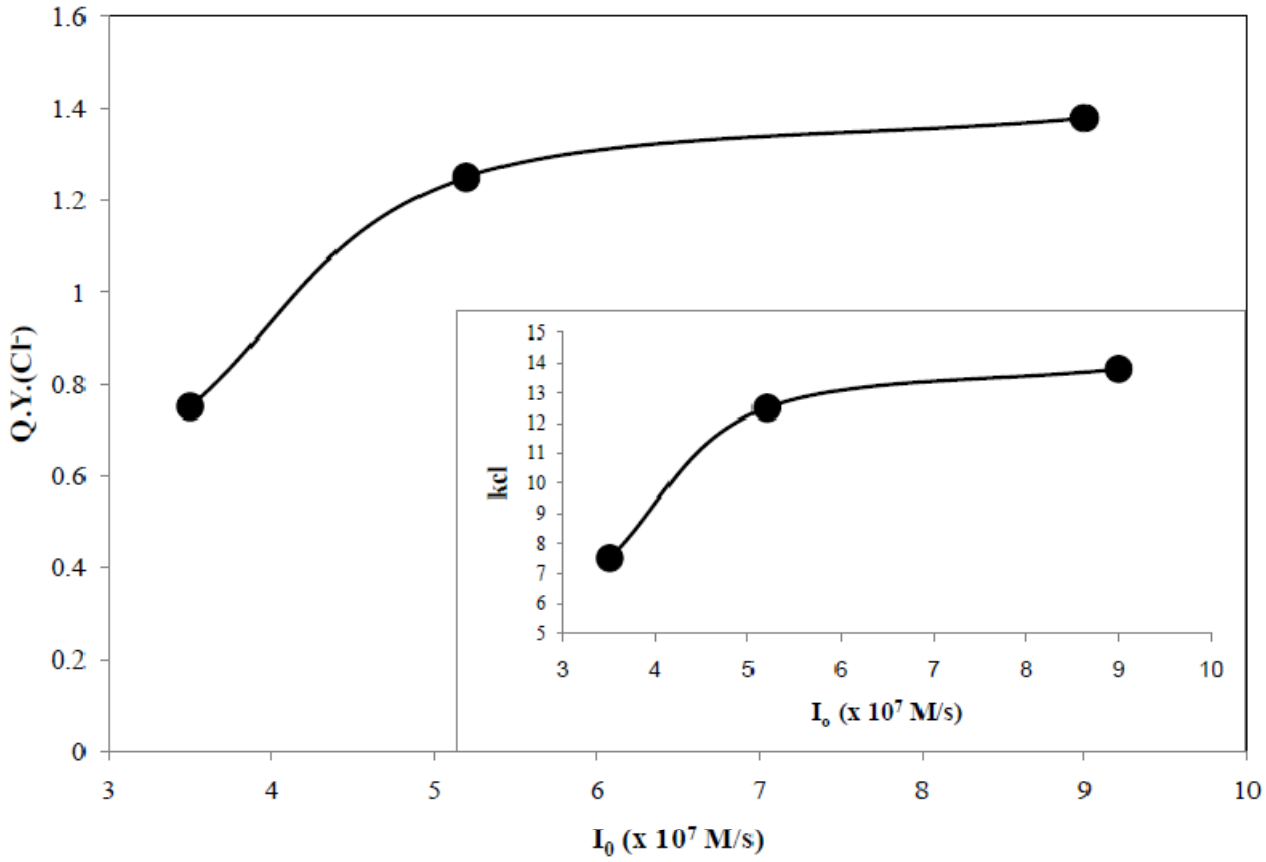

Figure 3-5. Dependence of the quantum yield of Cl^- formation on light intensity for degassed solutions at pH = 7.3 containing 1 mL CCl_4, 0.018 M SPEEK and 0.36 M formate buffer. Shown in the inset are the corresponding values of kinetic chain length as a function of the intensity of light.

Since the same stirring speed was employed in all illuminations, similar numbers of droplets were present in the solutions irrespective of any changes in reaction conditions. The decrease in efficiency observed at the lower intensities may be a consequence of losses in photon flux due to light scattering by small droplets or air bubbles in solution. Light scatters as it passes though each of the boundries.

Termination steps in free radical chain processes usually involve reactions between the chain carriers.[44] As a consequence of such second-order terminations, quantum yields of product formation scale with $(I_0)^{-0.5}$ as was found for the chain photoreduction of CCl_3F.[18] The results of Figure 3-5 show that Q.Y.(Cl^-) is nearly independent on I_0, suggesting that the termination rate law is first-order in chain carrier concentration. Interestingly, only $CHCl_3$ and CO_2 were detected in GC/MS experiments performed on irradiated solutions. Carbon dioxide is the anticipated product of the oxidation of $\bullet CO_2^-$. Typical byproducts of the free radical photoreduction of CCl_4 are CCl_3CCl_3 and CCl_2CCl_2 that result from the second-order dimerization or reduction of $\bullet CCl_3$.[21-24] The fact that none of these compounds were detected support the interpretation that radical-radical reactions are not involved in the termination process. An alternative possibility involves a reaction of $\bullet CCl_3$ with the polyketone given that trichloromethyl radicals are known to undergo addition to benzene rings.[45] Occurrence of such reaction implies a pseudofirst-order termination because of the very large [SPEEK] that is present in the solutions. At the present time the exact nature of the termination process remains unknown.

The kinetic chain length (kcl) is a useful parameter for evaluation of the efficiency of chain processes. Given that kcl = Q.Y.(Cl^-)/Q.Y.(initiating radical), and assuming that Q.Y.(initiating radical) = Q.Y.(SPEEK•), efforts were made to determine the formation quantum

efficiency of the polyketone radicals at different photon fluxes. Q.Y.(SPEEK•) was determined spectrophotometrically using the absorption signal of SPEEK• with λ_{max} = 565 nm in solutions photolyzed with $I_0 = 3\text{-}9 \times 10^{-6}$ M (hν) s^{-1} because optical detection of the radical was not possible at lower light intensities. The resulting Q.Y.(SPEEK•) value was independent of I_0 and amounted to 0.029. Utilization of this quantum yield in conjunction with the results of Figure 3-5 yielded kinetic chain link (kcl) values ranging from 31 to 43. However, optical determinations of the steady-state Q.Y.(SPEEK•) value are affected by the SPEEK• decay through a second-order radical-radical annihilation process.[21-24] Therefore, evaluations of kcl using the above value of Q.Y.(SPEEK•) may yield overestimate because this quantity is only a lower limit of the true formation quantum yield.[10] Earlier studies have shown that the quantum yield of SPEEK triplet excited states ranges between 0.04 and 0.05. Hence, the maximum value of Q.Y.(SPEEK•) amounts to 0.1 given that reaction (3-1) predicts generation of two SPEEK radicals per $^3\{SPEEK\}^*$ formed. Presented in the inset of Figure 3-5 are kcl values that resulted using the maximum quantum yield of SPEEK radicals. Kinetic chain lengths ranging from 7 to 14 were obtained, which provide convincing evidence that chain processes were involved in the photoreduction of CCl_4.

Presented in Figure 3-6 is the dependence of Q.Y.(Cl^-) on concentration of formate buffer when a constant pH of 7.3 was maintained. The Cl^- formation efficiency increased continuously until a maximum was achieved at [formate] = 0.36 M. Increases in efficiency with raising concentration of electron donor are a reflection of the competition between the spontaneous deactivation of $^3\{SPEEK\}^*$ and scavenging of the triplet state by the formate ions.

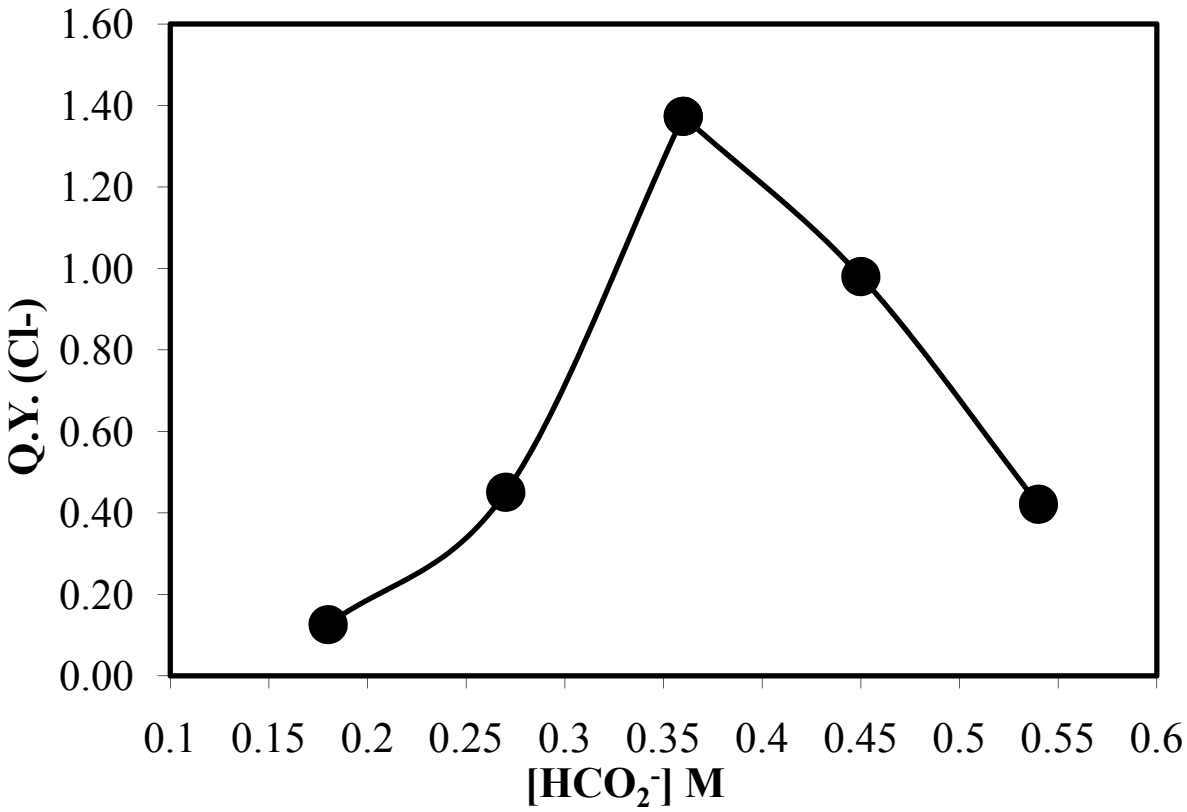

Figure 3 – 6. Quantum yield of Cl- formation for degassed solutions as a function of $[HCO_2/HCO_2^-]$ in solutions at pH = 7.3 containing 1 ml of CCl_4, 0.018 M SPEEK exposed to 9.0 x 10^{-7} M(photons)/s.

Quenching of the triplet state by HCO_2^- via H-atom transfer forms the reducing radicals and chemical quenching turns faster with increasing formate concentration. Less efficient formation of chloride ions occurred at higher buffer concentrations. This effect may be related to changes in the state of polyelectrolytes as a function of ionic strength.[46] At very high ionic strengths polyelectrolytes seem to exist in solution as individual entities whereas aggregates of the macromolecules form when the concentration of inert electrolytes decrease. If similar effects are induced by the formate ions then the obvious implication is that the photoreduction of CCl_4 occurs more efficiently when aggregates of SPEEK are present in solution than when the polyketone is present as isolated macromolecules.

Figure 3-7 depicts the variation of Q.Y.(Cl^-) with changing SPEEK concentration and shows that the formation yield increased rapidly to reach a maximum at [SPEEK] = 0.018 M. The initial increase of efficiency can be understood remembering that SPEEK is the chromophore and increasing amounts of the polyketone lead to a more effective absorption of the incident photons. Lower efficiencies of Cl^- formation were noticed at even higher [SPEEK] but such results are not surprising. The reason behind such statement is that excited states of BP are known to be quench by other benzophenone molecules with a rate constant of 1.8×10^8 M^{-1} s^{-1}.[34] Thus, occurrence of a similar phenomenon in the case of SPEEK explains the decrease in Q.Y.(Cl^-) at [SPEEK] > 0.016 M. The fact that significantly higher efficiencies of Cl^- generation in SPEEK solutions containing formate ions as H-atom donors correlates with the higher reducing power of $\bullet CO_2^-$ as compared with that of SPEEK•. Although most probably both radicals react with CCl_4 the higher photoreduction rates observed in the formate system imply that a more efficient chain process takes place when $\bullet CO_2^-$ is involved as a chain carrier. Therefore, the mechanism presented below involves mainly $\bullet CO_2^-$ and $\bullet CCl_3$ as chain carriers:

$$\{RRC{=}O\}_z + h\nu \rightarrow {}^3\{RRC{\bullet}O\}_z^* \quad (3\text{-}8)$$

$${}^3\{RRC{\bullet}O\}_z^* + HCO_2^- \rightarrow {\bullet}CO_2^- + \{RRC{\bullet}OH\}_z \quad (3\text{-}9)$$

$${\bullet}CO_2^- + \{RRC{=}O\}_z + H^+ \rightarrow \{RRC{\bullet}OH\}_z + CO_2 \quad (3\text{-}10)$$

$${\bullet}CO_2^- + CCl_4 \rightarrow {\bullet}CCl_3 + Cl^- + CO_2 \quad (3\text{-}11)$$

$$\{RRC{\bullet}OH\}_z + CCl_4 \rightarrow {\bullet}CCl_3 + Cl^- + \{RRC{=}O\}_z + H^+ \quad (3\text{-}12)$$

$${\bullet}CCl_3 + HCO_2^- \rightarrow {\bullet}CO_2^- + HCCl_3 \quad (3\text{-}13)$$

$${\bullet}CCl_3 + \{RRC{=}O\}_z \rightarrow \text{Products} \quad (3\text{-}14)$$

This mechanism explains in a qualitative fashion the main observations of the present study.

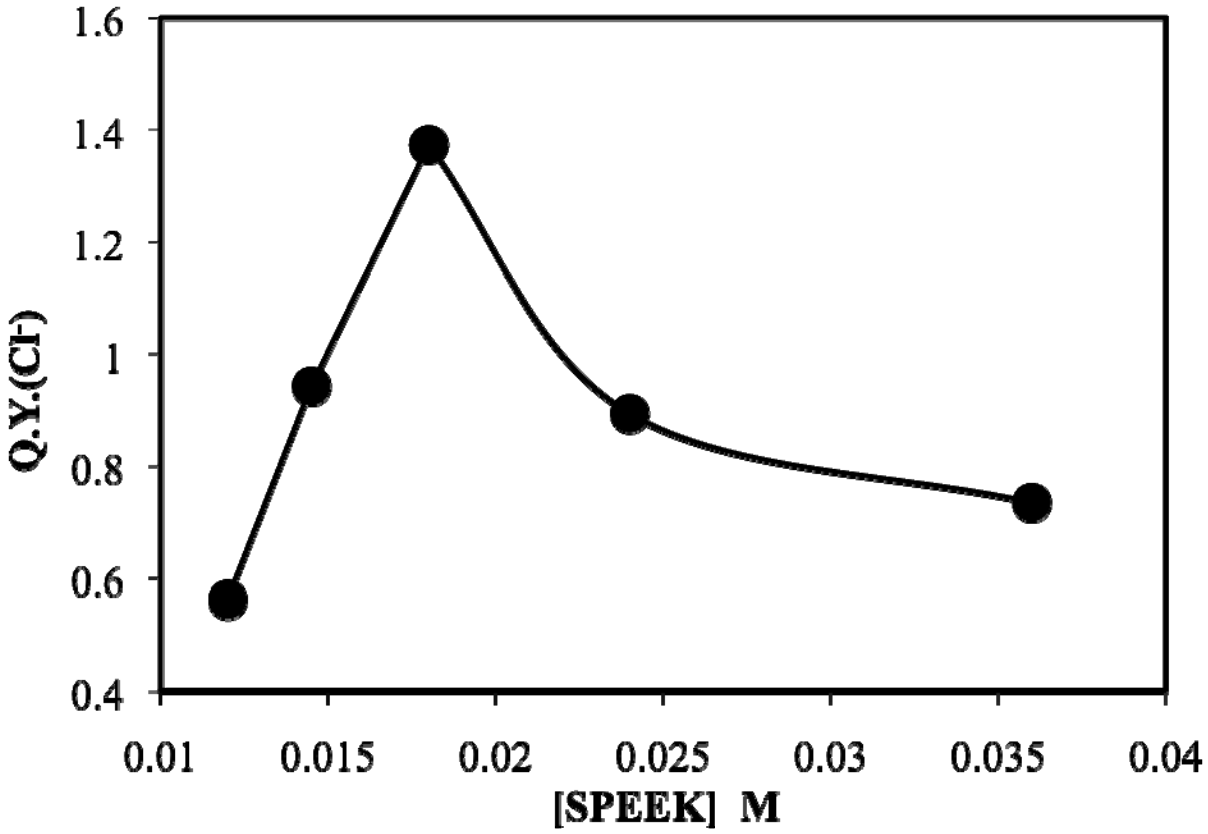

Figure 3 – 7. Dependence of quantum yield of Cl^- formation on [SPEEK] for degassed solutions at pH = 7.3 containing excess CCl_4, 0.36 M formate buffer exposed to 9.0 x 10^{-7} M(photons)/s.

Conclusion

We demonstrated the existence of a radical chain reaction involving a photoactive polymer in aqueous environment. By comparing the SPEEK/PVA to the SPEEK/formate system the general conclusion that SPEEK/formate is more efficient in dechloronation of CCl_4. The SPEEK/formate system achieved a maximum Q.Y.(Cl^-) of 1.5 at a pH of 7.3 while SPEEK/PVA system achieved a maximum of 0.033. Both systems exhibited a continued production of chloride ions during dark reaction indicating the existence of a radical chain reaction. The chain reaction mechanism presented utilizes CCl_3 radicals as a key part of the regeneration of reductive radical.

References

(1) Rusonik, I.; Cohen, H.; Meyerstein, D. *Eur. J. Inorg. Chem.* **2005**, 1227-1229.

(2) Brault, D.; Neta, P. *J. Phys. Chem.* **1983**, *87*, 3320-3327.

(3) Feldman, L.; Alfassi, Z. B. *J. Phys. Chem.* **1981**, *85*, 3060-3063.

(4) Feldman, L.; Alfassi, Z. B. *Int. J. Chem. Kin*. **1982**, *14*, 659.

(5) Radlowski, C.; Sherman, W. V. *J. Phys. Chem*. **1970**, *74*, 3043-3047.

(6) Nakagawa, S.; Shimokawa, T. *Radiat. Phys. Chem.* **2002**, *63*, 151.

(7) Singh, A.; Kremers, W.; Smalley, P.; Bennett, G. S. *Radiat. Phys. Chem.* **1985**, *25*, 11.

(8) Evans, R.; Nesyto, E.; Radlowski, C.; Sherman, W. V. *J. Phys. Chem.* **1971**, *75*, 2762-2765.

(9) Hu, C.-M.; Tu, M.-H. *J. Fluorine Chem.* **1991**, *55*, 105-107.

(10) Mönig, J.; Asmus, K.-D. *J. Chem. Soc., Perkin Trans. 2* **1984**, 2057-2063.

(11) Maldotti, M.; Andreotti, L.; Molinari, A.; Varani, G.; Cerichelli, G.; Chiarini, M. *Green Chem*. **2001**, *3*, 42-46.

(12) Betterton, E. A.; Hollan, N.; Arnold, R. G.; Gogosha, S.; McKim, K.; Liu, Z. *Environ. Sci. Technol*. **2000**, *34*, 1229-1233.

(13) Van Beek, H. C. A.; Van der Stoep, H. J. *Recl. Trav. Chim. Pays-Bas* **1978**, *97*, 279-304.

(14) Huston, P. L.; Pignatello, J. J. *Environ. Sci. Technol*. **1996**, *30*, 3457-3463.

(15) Hawari, J.; Demeter, A.; Samson, R. *Environ. Sci. Technol.* **1992**, *26*, 2022-2027.

(16) Choi, W.; Hoffmann, M. R. *Environ. Sci. Technol*. **1997**, *31*, 89-95.

(17) Choi, W.; Hoffmann, M. R. *J. Phys. Chem*. **1996**, *100*, 2161-2169.

(18) Winkelmann, K.; Calhoun, R. L.; Mills, G. *J. Phys. Chem. A* **2006**, *110*, 13827-13835.

(19) Calhoun, R. L.; Winkelmann, K.; Mills, G. *J. Phys. Chem. B* **2001**, *105*, 9739-9746.

(20) Weaver, S.; Mills, G. *J. Phys. Chem*. **1997**, *101*, 3769-3775.

(21) (a) Korchev, A. S.; Konovalova, T.; Cammarata, V.; Kispert, L.; Slaten, B. L.; Mills, G. *Langmuir* **2006**, *22*, 375-384.

(22) Korchev, A. S.; Shulyak, T. S.; Slaten, B. L.; Gale, W. F.; Mills, G. *J. Phys. Chem*. B. **2005**, *109*, 7733-7745.

(23) Korchev, A. S.; Sartin, M.; Mills, G.; Slaten, B. L.; Gale, W. F. In *Clusters and Nano-Assemblies: Physical and Biological Systems*; Jena, P.; Khanna, S. N.; Rao, B. K.; Eds, World Scientific Publishing Co.: Singapore, 2005; 371-377.

(24) Korchev, A. S.; Bozak, M. J.; Slaten, B. L.; Mills, G. *J. Am. Chem. Soc*. **2004**, *126*, 10-11.

(25) Gilbert, A.; Baggott, J. *Essentials of Molecular Photochemistry*; CRC Press: Boca Raton, 1991; Chapter 7.

(26) Canonica, S.; Hellrung, B.; Wirz, J. *J. Phys. Chem. A* **2000**, *104*, 1226-1232.

(27) Schwarz, H. A.; Dobson, R. W. *J. Phys. Chem*. **1989**, *93*, 409-414.

(28) *Intelligent Textiles for Personal Protection and Safety*; Jayaraman, S.; Kiekens, P.; Grancaric, A. M., Eds.; IOS Press: Amsterdam, Netherlands, 2005.

(29) Schreuder-Gibson, H. L.; Truong, Q.; Walker, J. E.; Owens, J. R.; Wander, J. D.; Jones Jr., W. E. *MRS Bull.* **2003**, *28*, 574-578.

(30) Gaddy, G. A.; Korchev, A. S.; McLain, J. L.; Slaten, B. L.; Steigerwalt, E. S.; Mills, G. *J. Phys. Chem. B*, **2004**, *108*, 14850-14857.

(31) Henschler, D. *Angew. Chem. Int. Ed. Engl.* **1994**, *33*, 1920-1935.

(32) Baars, D. M.; Eagles, D. B.; Emond, J. A. In *Performance of Protective Clothing*; Barker, R. L.; Coletta, G. C.; Eds, ASTM STP 900: Philadelphia, 1986, 39-50.

(33) Stanbury, D. M. *Adv. Inorg. Chem.* **1989**, *33*, 69-138.

(34) Ledger, M. B.; Porter, G. *J. Chem. Soc., Faraday Trans. 1* **1972**, *68*, 539-553.

(35) Görner, H. *Photochem. Photobiol*. **2006**, *82*, 801-808.

(36) Horvath, A. L. *Halogenated Hydrocarbons: Solubility-Miscibility with Water*; Marcel Dekker: New York, 1982; pp. 661-710.

(37) Heller, H. G.; Langan, J. R. *J. Chem Soc. Perkin Trans. 2* **1981**, 341-343.

(38) Neta, P.; Grodkowski, J.; Ross, A. B. *J. Phys. Chem. Ref. Data* **1996**, *25*, 709-1050.

(39) Fliount, R.; Makogon, O.; Asmus, K.-D. *J. Phys. Chem.* A **1997**, *101*, 3547-3553.

(40) (a) Lal, M.; Schönich, C.; Mönig, J; Asmus, K.-D. *Int. J. Radiat. Biol*. **1988**, *54*, 773.

(41) Alfassi, Z. B.; Mosseri, S.; Neta, P. *J. Phys. Chem.* **1987**, *91*, 3383-3385.

(42) Bottom, R. A.; Guthrie, J. T.; Green, P. N. *Polymer Photochem.* **1985**, *6*, 59-70.

(43) Ramseier, M.; Senn, P.; Wirz, J. *J. Phys. Chem. A* **2003**, *107*, 3305-3315.

(44) Hoyser, E. S. *Free-Radical Chain Reactions*; Wiley-Interscience: New York, 1970; Chapter 3.

(45) Sife-Eldeen, K. A. *J. Radioanal. Nucl. Chem.* **2005**, *264*, 565-570.

(46) Sedlák, M. *J. Chem. Phys.* **1996**, *105*, 10123-10133.

IV. Production and Detection of Polymeric Anion SPEEK Radicals

Introduction

Previous studies identified films from blends of poly(vinyl alcohol), PVA, and sulphonated poly(ether etherketone), SPEEK, as suitable matrices for carrying out photoreactions.[1-4] These matrices are optically transparent and form robust films that can generate reducing radicals when exposed to 300 - 400 nm photons, or direct sunlight. SPEEK contains carbonyl groups sandwiched between phenyl functions. Such combination of groups is present in benzophenone (BP) molecules ($(\phi)_2C=O$, where ϕ represents a phenyl function) which are known to undergo light-excitation followed by highly efficient intersystems crossing to (n, π^*) triplet states capable of abstracting hydrogen atoms from alcohols.[5] Photolysis of air-free solutions containing BP and alcohols results in α-hydroxy (or benzophenyl ketyl, BPK = $\bullet C(\phi)_2OH$) radicals, exhibiting a transient absorption centered at λ= 545 nm. A similar photoreaction has been proposed to occur in SPEEK/PVA films generating a long-lived polymeric BPK radical that exhibits an absorption centered at 565 nm, and an ESR spectrum very similar to that of the α-hydroxy radical from BP.[1] The proposed formation mechanism for the polymer BPK radical involves excitation of SPEEK by 350 nm photons via reaction 1,

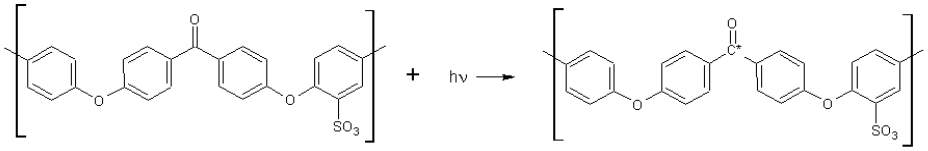

[1]

The SPEEK triplet excited state (^{3}SPEEK*) abstracts a hydrogen atom from an adjacent PVA molecule producing a SPEEK radical and a PVA α-hydroxy radical according to reaction 2,

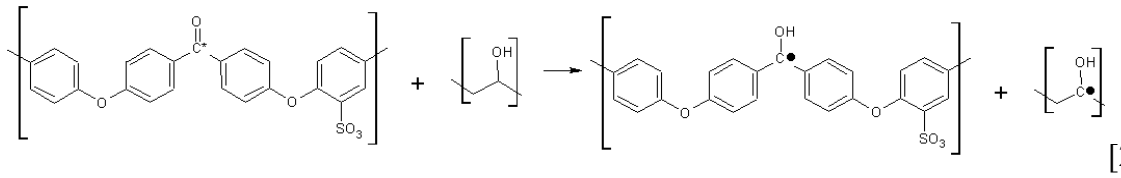

[2]

Although radicals of the polyol are easily detected in PVA films by ESR techniques, no such species were observed in analogous experiments with photolyzed SPEEK/PVA films even at 77 K.[1,6] These results suggest that the PVA radical reacts fast with another SPEEK molecule to generate a second SPEEK radical as illustrated in reaction 3,

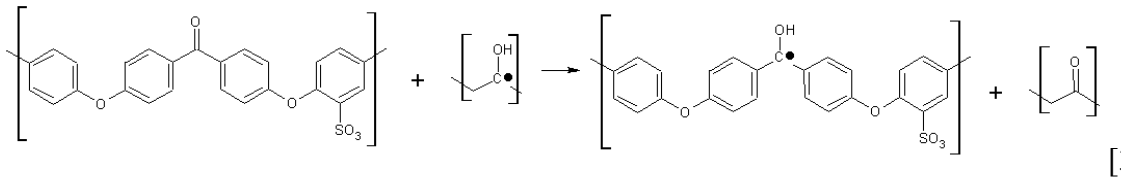

[3]

The standard reduction potential of BP to form the BPK radical is in the range of $E^0 \sim -1.3$ to -1.5 V,[6,7] whereas reduction of SPEEK to form the polymeric α-hydroxy radical has been estimated to be around $E^0 \sim -1.3$ V.[2] The large reducing power of the polymeric BPK radical suggests potential utilization of this species for the reductive degradation of chemical pollutants. As shown in the previous chapter, the polyketone radicals are able to reductively dehalogenate CCl_4, which exhibits a standard potential of $E^0(CCl_4/\bullet CCl_3,Cl^-) = -0.23$ V.[8] However, attempts to reduce $CHCl_3$ failed presumably because reduction of chloroform occurs at a potential about 1 V more negative that of CCl_4.[9]

On the other hand, α-hydroxy radicals of 2-propanol have been shown to reduce CCl_4 and also $CHCl_3$ but more slowly.[10] 2-propanol radicals exhibit a reducing power slightly higher than that of the SPEEK radicals, $E°[(CH_3)_2C=O, H^+/(CH_3)_2C\bullet OH] = -1.4$ V.[11] Hence, a logical strategy to achieve photoreduction of $CHCl_3$ initiated by SPEEK was to increase the reducing

power of the polymer radicals. Deprotonation of •C(ϕ)$_2$OH) yields •C(ϕ)$_2$O$^-$,[12] a species anticipated to be a stronger reductant since the estimated reduction potential of BP to produce the BPK anionic radical is about -2 volts.[13] Direct photogeneration of •C(ϕ)$_2$O$^-$ takes place upon photolysis of benzophenone in aqueous solutions containing amines.[14] Electron transfer from an amine molecule to triplet excited BP takes place instead of H-atom abstraction because amines act predominantly as electron donors. Support for the notion that the BPK radical anion is more active than •C(ϕ)$_2$OH) has been provided by a study showing a higher radical reactivity upon illumination of substituted BP molecules in the presence of amines.[15]

Thus, the objective of the present study was to accomplish the photogeneration of the radical anion (deprotonated) form of the α-hydroxy radical from SPEEK. The BP anionic radical has been photogenerated in solution of the ketone containing a variety of amines such as triethyl amine, butyl amine, and propyl amine.[16] Thus, combination of the SPEEK with polyamines seemed a reasonable approach for achieving the desired anionic form of the α-hydroxy radical from the polyketone. In such a system, ^{3}SPEEK* was anticipated to react via electron transfer with the polyamine. This process is illustrated by reaction 4, which results in the formation of both a SPEEK radical anion and a cationic amine radical,

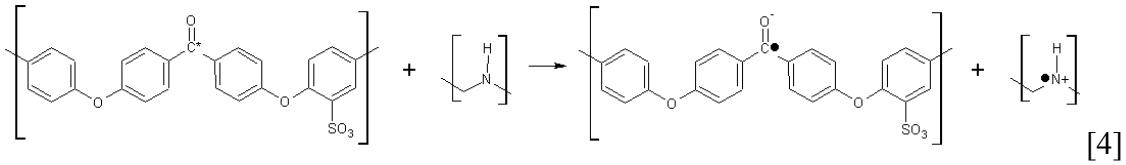

[4]

An advantage of the SPEEK/PVA system is that blends of these polymers respond to light in aqueous solution as well as when present in the form of optically transparent films.[1-4] Thus, ideal SPEEK/polyamine blends are those exhibiting similar properties. This, in turn, means that polyamine selected should lend itself to be crosslinked, be flexible and optically transparent in the solid state. Optical transparency in the visible range is a desirable property enabling detection

of absorption signals due to photogenerated radicals. For instance, $\bullet C(\phi)_2OH$) and the neutral α-hydroxy radical of SPEEK exhibit similar absorption signals centered at 545 and 565 nm, respectively.[2,12] On the other hand, $\bullet C(\phi)_2O^-$ is characterized by an absorption centered at 600 nm.[12,15,17] Consequently, an absorption maximum at around 600 nm was anticipated for the radical anion of SPEEK. Only few polymeric amines of research purity are commercially available. Potential polyamines that are good candidates are poly(vinyl amine), PVAm, poly(allyl amine), PAAm, 4, 4'-oxydianiline, ODA, and polyethyleneinamine, PEI.

Experimental

PVAm was provided by BASF Chemical and was used without further purification. PEEK samples were a gift of Vitrex Co. and served as the precursor for the formation of SPEEK. PAAm, PEI, ODA, epichlorohydrin (EPH), PVA, gluteraldyhde, dimethylformamide, methanol, diisocyanoate, HCl, NaOH and H_2SO_4 were purchased from Aldrich and were used without further purification. The structures of some of the chemicals used are presented in Figure 4-1.

Polyetherether ketone (PEEK) was received from Vitrex in sheet form. Sheets were cut into small strips and then ground into a fine powder. To prepare SPEEK, 150 grams of PEEK powder was added to 1000 ml of sulfuric acid under constant stirring. The mixture was heated to 50 ^{0}C for 24 hours and allowed to cool to room temperature, followed by stirring constantly for 30 days. Completion of the PEEK sulfonation yielded a red solution, which was slowly poured into a mixture of H_2O:HCl (5:1 volume ratio) at $T \leq 8$ ^{0}C. The generated SPEEK turned white and precipitated into string-like solids upon contacting the cold mixture. Care was taken in all further steps to maintain temperatures of $T \leq 8$ ^{0}C to hinder dissolution of SPEEK. This was accomplished by using an ice bath and occasional stirring. Once SPEEK precipitated, the solution containing solid product aged for 0.5 to 1 hour before decanting the liquid. The sulfonated polymer was then slowly exposed to a cold (8 ^{0}C or less) solution containing 0.2 M NaOH and allowing the neutralization to proceed for 0.5 to 1 h. This step was repeated until a basic solution remained. Next, SPEEK was washed with cold deionized water ($T \leq 8$ ^{0}C) via the same method as the basic wash until the pH of the resulting solution was neutral. The solid was then dried under vacuum at 120 ^{0}C and ground to a fine powder. The final powder had a tan color and was easily dissolved in water using a gentle heating and stirring.

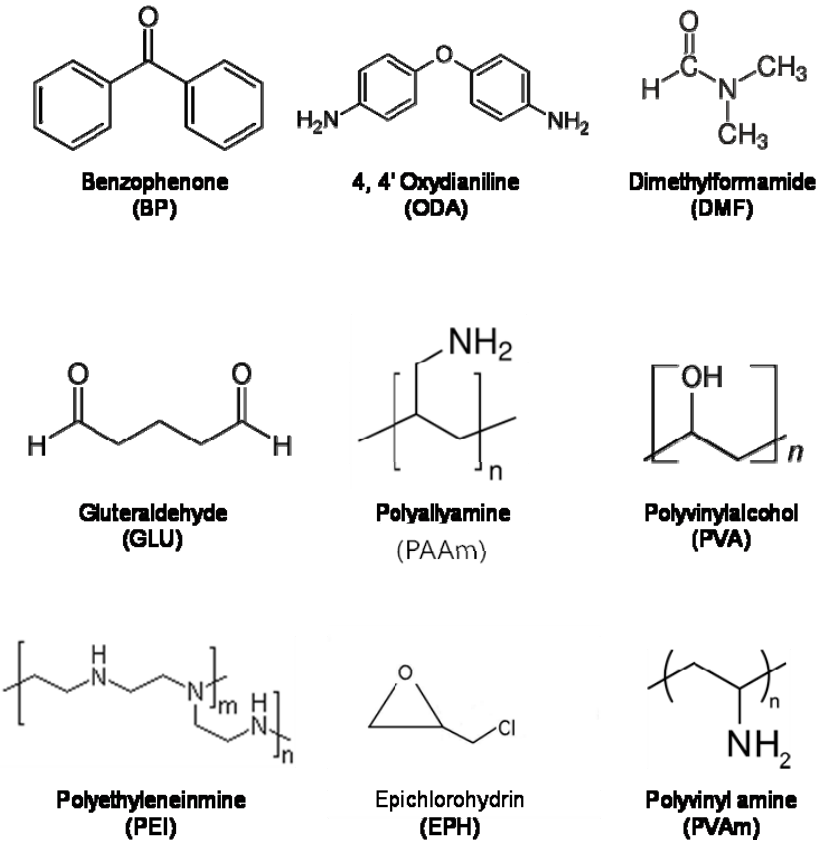

Figure 4-1 – Structures and names of chemicals used in experiments.

A Shimadzu UV-2401PC Ultraviolet-Visible Spectrophotometer was used to conduct absorption measurements. A BYK-Gardner film casting knife was employed to cast polymer films onto panes of window glass at a thickness of 50 mil. Curing of the polymer films was carried out on a GCA/Precision Scientific Conventional Forced air oven. The photochemical reactor was a Rayonet 100 circular illuminator from Southern New England Ultraviolet Company equipped with 16 RPR-3500A lamps that generated photons with $\lambda = 350 \pm 15$ nm.

X-band electron paramagnetic resonance (EPR) experiments were conducted using a Bruker ESP300E spectrometer equipped with a Varian cavity and a variable-temperature cryostat (Air Products). The microwave frequency was measured using a Hewlett-Packard 5352B frequency counter; g-tensors were calibrated for homogeneity and accuracy by comparison to a coal standard, g = 2.00285 +\- 0.00005. Simulation of the spectra employed the simulation program SIMFONIA from Bruker Instruments. The X-band EPR experiments were performed at temperatures ranging from 4 to 100 ^{0}K. Samples were excited using a 300 W Xe lamp (ILC). All EPR experiments were conducted at Argonne National Laboratory by Dr. T. Rajh.

A molar ratio of 20:1 PVA to SPEEK was determined in previous research to produce the greatest concentration of polyketone neutral radicals[1-4]. Therefore, all solutions were made having a 20:1 monomer ratio of polyamine to SPEEK. The model system consisting of BP and isopropanol in solution yielded short-lived neutral BPK radicals. In the polymer blend system PVA substituted isopropanol, whereas SPEEK served as a photosensitizer instead of BP. An interest characteristic of the polymer blends is the long lifetime of the photogenerated BPK radicals. SPEEK/polyamine blends were modeled after the triethyl amine/benzophenone system, which had been shown to yield a short-lived anionic benzylohetylketyl radical.[18] The first polymer of choice was PVAm in place of triethyl amine, and SPEEK instead of BP. An aqueous

solution of 0.018 M (monomers/L) SPEEK was prepared under heating and stirring. Once the SPEEK dissolved, the solution was allowed to cool to room temperature. A similar procedure yielded a solution containing 0.36 M (monomers/L) PVAm. Upon addition of the PVAm the solution turned white and opaque producing small insoluble fibers. These fibers were the result of an irreversible reaction between the ketone groups of SPEEK and the amine functions of PVAm. This reaction occurred instantaneously at all pH values, impeding casting of the solutions and formation of films. After washing and drying the fibers, they were exposed to 350 nm photons but all attempts to photogenerate polyketone radicals failed.

The negative results with a primary amine can be rationalized considering the high reactivity of NH_2 groups toward carbonyl functions, yielding either imine or enimine groups in an acidic environment.[18] An alternative approach was attempted that involved less reactive amines such as secondary and tertiary amines. The ODA polyamine was synthesized according to published procedures.[19] A typical synthesis consisted of combining 10 grams of EPH with 3 grams of ethanol and 1 gram of water, followed by stirring. Once a homogenous mixture was obtained, 3 grams of ODA were slowly added. The mixture was heated to 80 ^{0}C and held at the temperature for 4 hours and then allowed to cool to 60 ^{0}C. Next, 3 g of a 50% NaOH solution was added very slowly. After stirring for a short time the mixture was placed in a vacuum to remove the water. Once the mixture was water-free, 6 grams of DMF were added under stirring. Three water washes were then performed, where each cleansing step consisted of adding 5 g of H_2O allowing a few minutes of stirring and then decanting the liquid. The final product (ODA-EPH) was obtained by eliminating any residual water under vacuum.

Small quantities of films were prepared using the following method: 4 g of ODA-EPH, 2 g of PEI and 0.2 g of SPEEK were combined in 7 mL of DMF under continuous stirring. The

mixture was cast on a piece of glass inside a conventional oven and cured at 80 ^{0}C for 3 hours. Once curing was completed the films were removed from the glass using a razor blade taking care to obtain as large samples as possible. The resulting films were transparent brownish and brittle materials.

Using the same monomer ratios employed for the SPEEK/PVA system, (20:1 monomer ratios) a solution of SPEEK:poly(allyamine) in water was prepared yielding a final concentration of amine monomers equal to 0.36 M. The solution turned opaque for a few minutes but changed to transparent with a slight yellowish color. The outcome of the reaction was also found to be pH dependent, the solution would turn irreversibly opaque at pH values lower than 9 but remained transparent at higher basicities. Films were produced by casting transparent solutions onto a clean piece of glass and oven-drying at 30 ^{0}C for 3 h. Crosslinking was attempted using different chemicals such as gluteraldehyde and diisocanoynate.[20,21] Crossliker concentrations of 0.5% to 25% were used in efforts to produce transparent and insoluble films. Further attempts included addition of other chemicals that can be crosslinked including PVA and PEG.

PEI was another polyamine employed in attempts to produce transparent, insoluble and flexible blend film with SPEEK. This polyamine contains primary, secondary and tertiary amine functions. Preparation of SPEEK/PEI blends was as follows: a solution of SPEEK was made as previously stated and PEI was added yielding a final concentration (in terms on amine monomer units) of 0.36 M. Insoluble products resulted upon decreasing the pH below 9 but no precipitates formed at lower acidities. Films were prepared by taking a freshly made transparent PEI/SPEEK solution and adding 2 mL of epichlorohydrin under continuous stirring. The solution was then cast on a piece of glass using a Gardner knife and oven-dried for 3 h at 30 ^{0}C. The resulting insoluble film was cut into pieces of 2.5 by 5 cm and placed in methanol overnight in order to

remove residual ions and crosslinker, followed by removing from the alcohol and drying. Presented in Table 4-1 is a compilation of all the experiments performed with different polyamine and crosslinkers. Numerous combinations in Table 1 were unable to yield films with the desired properties, therefore, only those combinations of SPEEK/polyamines and corsslinkers that yielded the desired result will be presented and discussed in the following section. Experiments were first performed in solution in order to test if combinations yielded the desired radical species. Combinations that produced positive results were then utilized to explore the formation of films.

Table 4-1 A table of polymeric amine films and their observed properties.

Composition	Crosslinker	Mechanical Properties	Optical Properties	λ_{max}	Solubility (H_2O)
APEEK/PVA	Gluteraldehyde	Flexible	Green/Transparent	none	Insoluble
PVA/PAA/SPEEK	None	Flexible	Transparent	560 nm	Soluble
PVA/PAA/SPEEK	Gluteraldehyde	Flexible	Transparent	560 nm	Insoluble
PVA/PAA/SPEEK	Diacrylate	Flexible	Transparent	560 nm	Slighty Soluble
PVA/PAA-HCl/SPEEK	Gluteraldehyde	Flexible	Transparent	560 nm	Insoluble
PVA/PAA-HCl/SPEEK	None	Flexible	Transparent	560 nm	Soluble
PAA/SPEEK	Gluteraldehyde	Brittle	Transparent	none	Insoluble
PAA/SPEEK	Diacrylate	Flexible	Transparent	none	Insoluble
PAA/SPEEK	None	Flexible	Transparent	600 nm	Soluble
PEG/SPEEK/PAA	Gluteraldehyde	Liquid	N/A	N/A	N/A
PEG/SPEEK/PAA	Diacrylate	Flexible	White/Nontransparent	N/A	Soluble
PEG/SPEEK/PAA	None	Flexible	White/Nontransparent	N/A	Soluble
BTDA/ODA/PAA	Heat	Brittle	Yellow/Transparent	none	Insoluble
BTDA/ODA/PAA/SPEEK	Heat	Brittle	Yellow/Transparent	none	Insoluble
ODA/EPH/SPEEK/PAA	Heat	Flexible	Green/Transparent	560 nm	Insoluble
ODA/EPH/SPEEK/PEI	Heat	Flexible	Green/Transparent	600 nm	Insoluble
PVAm/SPEEK	Gluteraldehyde	Fibers	N/A	N/A	Insoluble
PVAm/SPEEK	Diacrylate	Fibers	N/A	N/A	Insoluble
PVAm/SPEEK	Epichlorohyrdin	Fibers	N/A	N/A	Insoluble
PVAm/SPEEK	None	Fibers	N/A	N/A	Insoluble
PVA/SPEEK	Gluteraldehyde	Flexible	Transparent	565 nm	Insoluble
PEI/SPEEK	Epichlorohyrdin	Flexible	Transparent	590 nm	Insoluble

Results and Discussion

4.1 SPEEK/PVA and SPEEK/Amine Systems

A previously reported system of SPEEK/PVA is able to produce polyketone radicals upon exposure to 350 nm light that exhibit a characteristic absorption with a maximum at 565 nm depicted in Figure 4-2. Tracking the changes in the absorption maximum at 565 nm revealed that the absorbing species decays via a second-order radical-radical dimerization reaction represented by reaction 5,

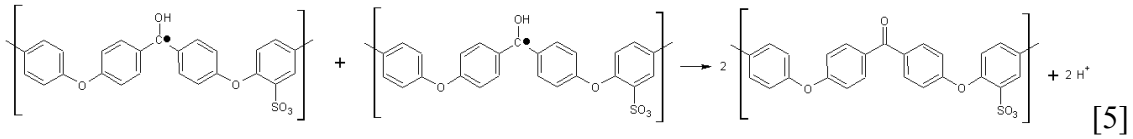

[5]

Using the changes in the absorption maximum of the neutral SPEEK radical, a second-order rate constant for the decay reaction can be calculated. Rate constants for the decay of neutral polymer radicals have been reported to be 2.9 x 10^2 M^{-1} s^{-1} in unstirred, air-free aqueous solutions and 7 x 10^2 M^{-1} s^{-1} under stirring whereas in blend films the decay rate constant was 4 x 10^{-2} M^{-1} s^{-1}.[1-2] EPR measurements confirmed that the processes detected optically corresponded to the decay of neutral α-hydroxy radicals of SPEEK.[1]

4.2 Polyamine Solutions

Achievement of transparent solutions was very important because UV-Vis spectroscopic detection of photogenerated products requires a medium of high transparency. Photogeneration of radicals also requires exposure to 350 nm photons and light penetration in the solutions/films is critical. Since SPEEK/PVAm solutions were not transparent optical determinations were not possible. The first system to produce a radical absorption at 600 nm was a blend of SPEEK and PAAm; a spectrum obtained after illumination is presented in Figure 4-2. Although the resulting

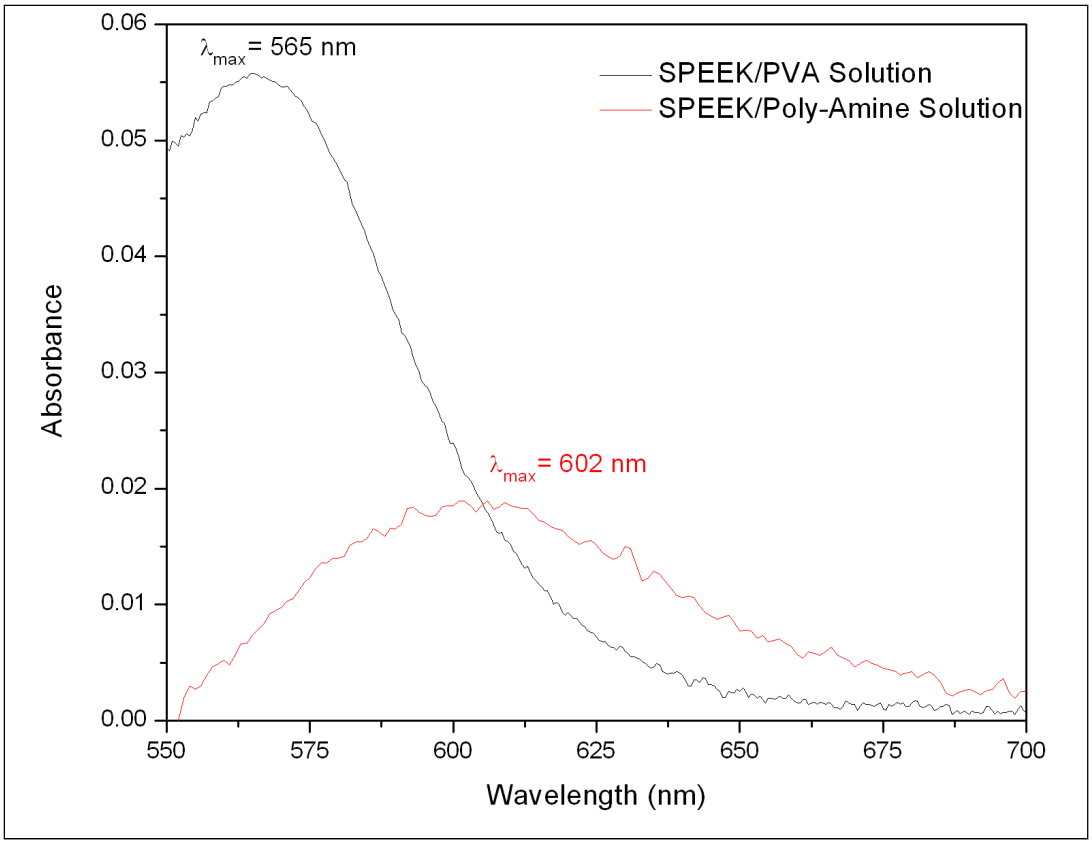

Figure 4-2 – Absorption spectrums are shown for both the neutral radical and anionic radical. Radicals were produced by exposing 3 ml of the solution to 350 nm photons for 1 minute. The SPEEK neutral radical having an absorption centered at 565 nm was generated in a degassed aqueous SPEEK/PVA solution and the anionic radical having an absorption centered at 602 nm was generated in a degassed solution of aqueous SPEEK/Polyamine.

optical signal decayed with time, the low intensity of the photogenerated absorption was unsuitable for evaluation of a decay rate constant. Decay of the signal centered at 600 nm turned the solution yellow together with formation of products exhibiting an optical signal centered at 370 nm. While pinacols (the typical products of dimerization of alcohol radicals) do not absorb light with $\lambda > 300$ nm, the new absorption may be attributed to a Light Absorbing Transient (also known as LAT) resulting from insertion of BPK radical into the aromatic ring of a phenyl group from a second polymeric radical.[1] In such a case the signal was anticipated to decay slowly with time, as was observed previously, because the LAT species are unstable products. However, the 370 nm peak remained constant for days, implying that a new functional group formed that was responsible for such absorption. While the nature of the new chromophore was not identified, a yellowish color has also been detected upon reduction of Polyaniline/PEI systems.[22]

Presented in Figure 4-3 are spectra obtained after photolysis of air-free SPEEK/PEI solutions. At pH = 12 also illumination also yielded a signal with λ_{max} at 600 nm, but as the pH was decreased to pH 10 the intensity decreased while λ_{max} blue-shifted to 585 nm. For comparison purposes, Figure 4-3 also includes the spectrum obtained after irradiation of an air-free SPEEK/PVA solution at pH = 6. An obvious conclusion is that the species detected at pH = 12 in the SPEEK/PEI solution is different from the one observed in the SPEEK/PVA system. Since the spectrum of $\bullet C(\phi)_2O^-$ is characterized by an absorbance with a maximum at around 600-620 nm, a logical conclusion is that the signal measured in the SPEEK/PEI solution at pH = 12 corresponds to the radical anion of SPEEK. As was concluded before,[2] the signal centered at 565 nm in SPEEK/PVA solutions can be assigned to the neutral SPEEK radical.

Observations made during the photolysis of BP in a 50/50 mixture of H_2O/isopropanol[23] are relevant here. In such solutions the pK_a of $\bullet C(\phi)_2OH$ was 9.2 and both

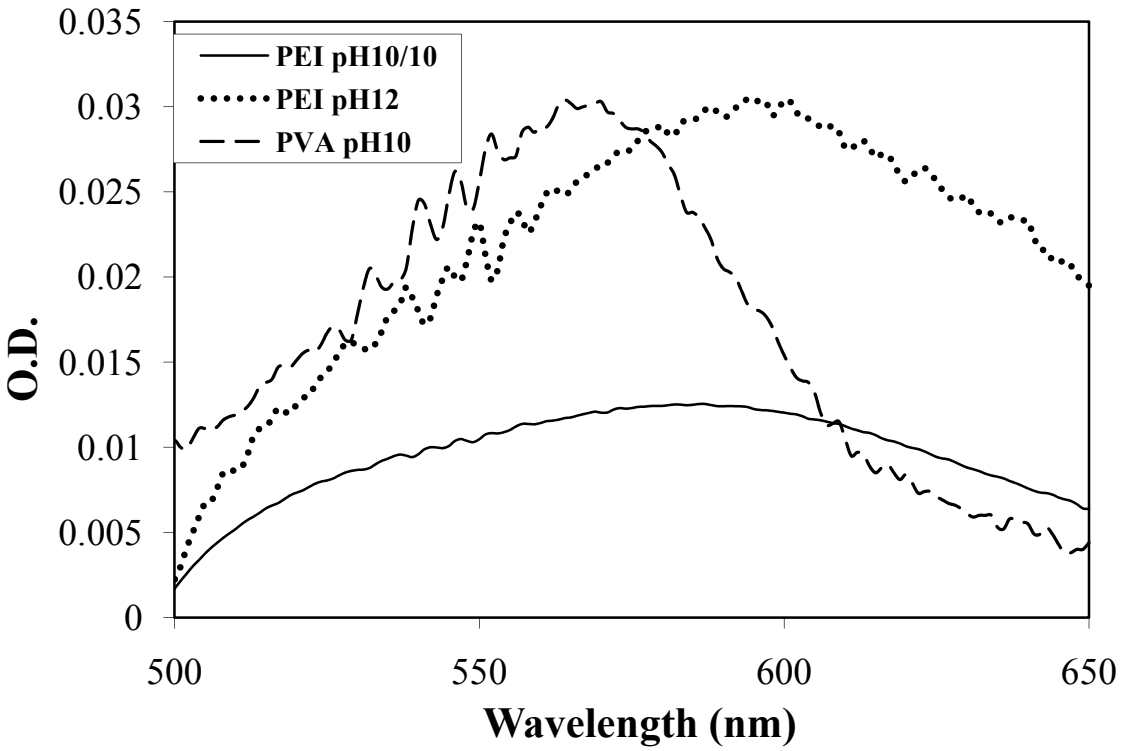

Figure 4-3 - Optical spectra after 1 min of exposure to 350 nm photons ($I_o = 8x10^{-5}$ M/s) for the amine system, SPEEK/PEI, at different pHs (pH 10 solid line, pH 12 dotted line) and the alcohol system, SPEEK/PVA (dashed line). The SPEEK/PVA shows an absorption maximum center around 565 nm while the SPEEK/PEI at pH 12 is centered around 600nm. The SPEEK/PEI at pH 10 is blue shifted to 585nm with an increase in the optical density by a factor of 10.

the neutral as well as the anionic BP radicals exhibited the same extinction coefficient of 5 x 10^3 M^{-1} cm^{-1}. Interestingly, the second-order decay rate constant was 5.9 x 10^7 M^{-1} s^{-1} when two neutral BPK radicals reacted, and amounted to 1.1 x 10^9 M^{-1} s^{-1} for the reaction between $\bullet C(\phi)_2OH$ and $\bullet C(\phi)_2O^-$. Surprisingly, the second-order rate constant for the reaction of two $\bullet C(\phi)_2O^-$ decreased with increasing alkalinity, from 1.4 x 10^8 M^{-1} s^{-1} at pH = 10 to 1.6 x 10^6 M^{-1} s^{-1} at pH = 12. Based on such observations, a logical assumption is that the neutral SPEEK radical exhibits a pK_a in the range of 9 and 10. Since both neutral and anionic radicals are present at pH = 10, the resulting spectrum is a combination of those characteristic of each radical and, as show in Figure 4-3, yielding a λ_{max} value that is located between 565 and 600 nm. Also, the reaction between the neutral and anionic SPEEK radicals can be expected to be faster than the reactions involving either two neutral or two anionic radicals. These assumptions provide a qualitative explanation for the lower absorption detected in SPEEK/PEI at pH = 10. Since the reaction between neutral and anionic SPEEK radicals predominate at this pH value, less radicals are detected after illumination.

Further experiments were performed to test the assumptions mentioned above involving spectral measurements on degassed SPEEK/PVA solutions in which the pH was systematically increased. Only modest red shifts of λ_{max} of 5-15 nm were noticed when the pH was raised from 6 to 10 but the intensity of the photogenerated optical signal decreased significantly. Also, as illustrated in Figure 4-4, the second-order rate constant for the radical decay process increased vastly upon increasing the pH. For instance, the decay rate constant varied from 570 M^{-1} s^{-1} at pH = 6 to 4 x 10^3 M^{-1} s^{-1} at pH 10. Evaluation of the decay rate constants was not possible above pH = 10 since the resulting optical signals were very weak. The failure to detect optical signals centered at 600 nm may be interpreted in terms of a fast decay of the anionic SPEEK radicals via

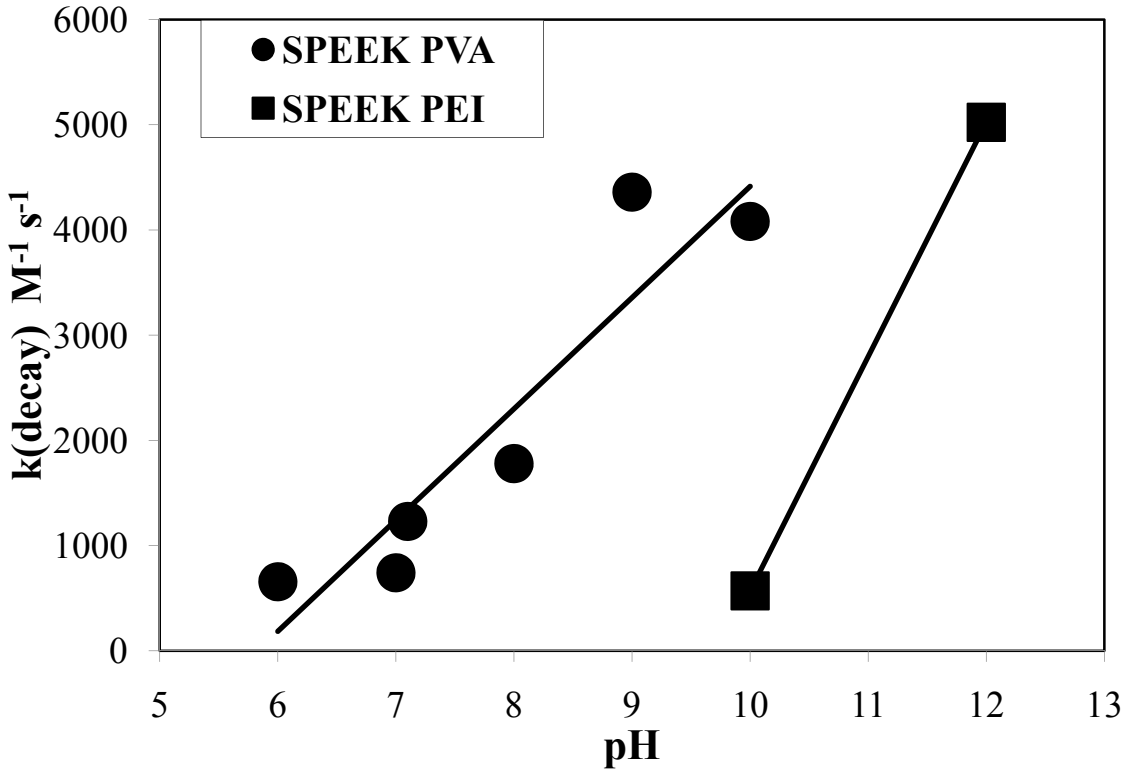

Figure 4-4 Shown is the decay rate for the radical-radical termination reaction in the SPEEK/PVA (●) and SPEEK/PEI (■) systems. As the pH decreases the decay rates decrease while the optical density increases.

reaction with neutral radicals. Such interpretation is in agreement with the pH-induced decrease in intensity of the photogenerated optical signals together with the faster radical decay processes. However, these results provide only qualitative support to the assumptions mentioned before.

Included in Figure 4-4 are values of the radical decay rate constant determined in SPEEK/PEI solutions free of air at pH values of 10 and 12. Surprisingly, a rate constant of 5.7 x 10^2 M^{-1} s^{-1} was obtained at pH = 10, which coincides with the value for SPEEK/PVA solutions at pH = 6. On the other hand, at pH = 10 the decay rate constant obtained in the SPEEK/PVA solution is 7 times larger than the value measured for the SPEEK/PEI solution. These results indicate that the anionic SPEEK radicals are somewhat stabilized by the presence of PEI in the solution. Furthermore, as shown in Figure 4-3, the optical density at 600 nm measured in the SPEEK/PEI solution at pH =12 is very similar to the one recorded at pH = 6 in an SPEEK/PVA solution. Interestingly, the radical decay rate constant determined for the SPEEK/PEI system at the high pH value (5 x 10^4 M^{-1} s^{-1}) is similar to the value obtained in the SPEEK/PVA solution at pH = 10. The faster radical rate with increasing pH noticed in SPEEK/PEI solutions is in contrast with the data obtained during photolysis of BP in H_2O/isopropanol mixtures.

4.3 Polyamine Films

The ultimate goal was to prepare thin, flexible, transparent films from aqueous precursors that enabled photogeneration of anionic radicals in the solid samples. The same characterization techniques used for solutions were employed except that a film holder replaced the holder for 1 cm optical cell. Polymer films were placed in between two thick quartz disks and were secured by means of screw clamps. The photoactivity of SPEEK/PVAm fibers was investigated initially via compressing these rather opaque materials between the two quartz disks, which yielded thin and somewhat transparent samples. After exposure to 350 nm photons the spectrum showed no

visible changes, indicating that reaction of the ketone group with the tertiary amine produced non absorbing species.

Exposure of SPEEK/EPH/ODA/PEI films to 350 nm photons yielded the spectrum shown in Figure 4-5 exhibiting an optical absorption with a maximum at 590 nm. Figure 4-6 illustrates the decay of the optical density at 590 nm. Concentrations of photogenerated radicals were estimated assuming an extinction coefficient at the wavelength of maximum absorbance equal to that of the SPEEK radical, $\varepsilon = 3.5 \times 10^3\ M^{-1}\ cm^{-1}$.[2] The inset depicts a second-order plot of the radical concentration as a function of time, yielding a rate constant of $1.7 \times 10^3\ M^{-1}\ s^{-1}$. According to the above discussion, the absorbance maximum at 590 nm is an indication that neutral and anionic radicals were simultaneously photogenerated in such films. For this reason, together with the frailty of the resulting films and the difficulty of producing consistent results led us to abandon the SPEEK/EPH/ODA/PEI system.

The first films produced from aqueous solutions that were flexible were those obtained by blending SPEEK with PAAm. Although such films were still soluble in water, they exhibited promising photochemical properties. Exposure of these films to 350 nm photons produced an absorption centered at 600 nm, the results are displayed in Figure 4-7. Attempts were made to add a chemical crosslinker to the solution that would allow for the production of insoluble films. The first cross-linker chemical utilized was gluteraldehyde and experiments were conducted that varied the degree of crosslinking by systematic altering the aldehyde concentration, temperature and concentration of the HCl catalyst. The resulting films were not transparent and, therefore, not suitable for the purposes of the present study. Similar results were obtained when diisocyanoate, was employed as a crosslinking agent. The inability to find a crosslinker able to

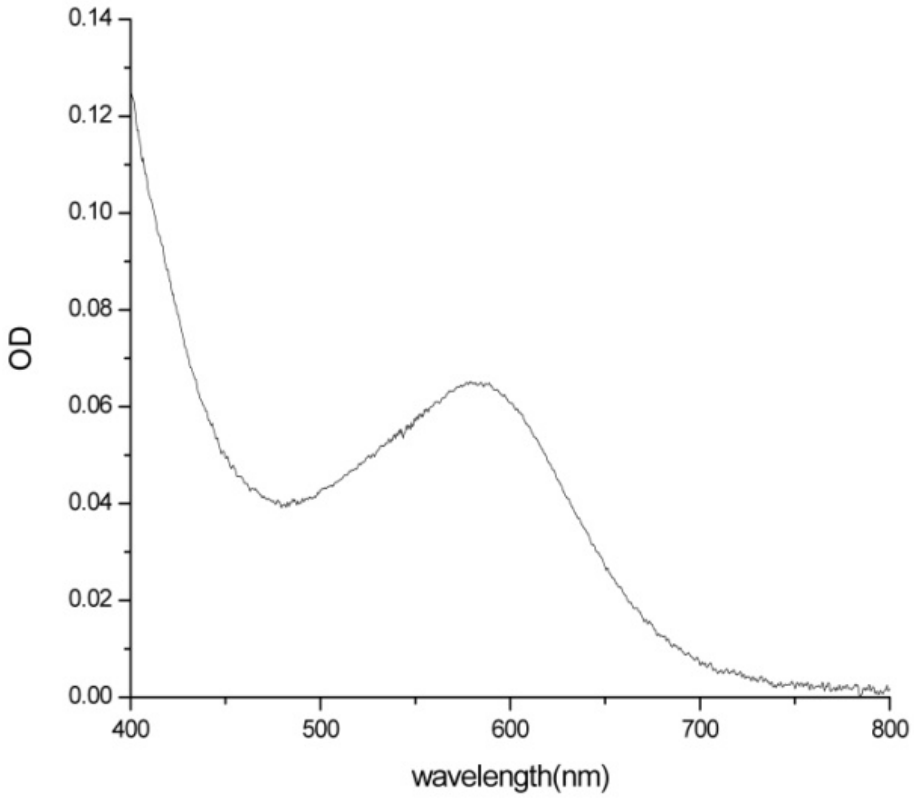

Figure 4-5 –The optical absorption after 1 minute exposure to 350 nm photons of a polymer film containing SPEEK/EPH/ODA/PEI with a maximum centered at ~600 nm.

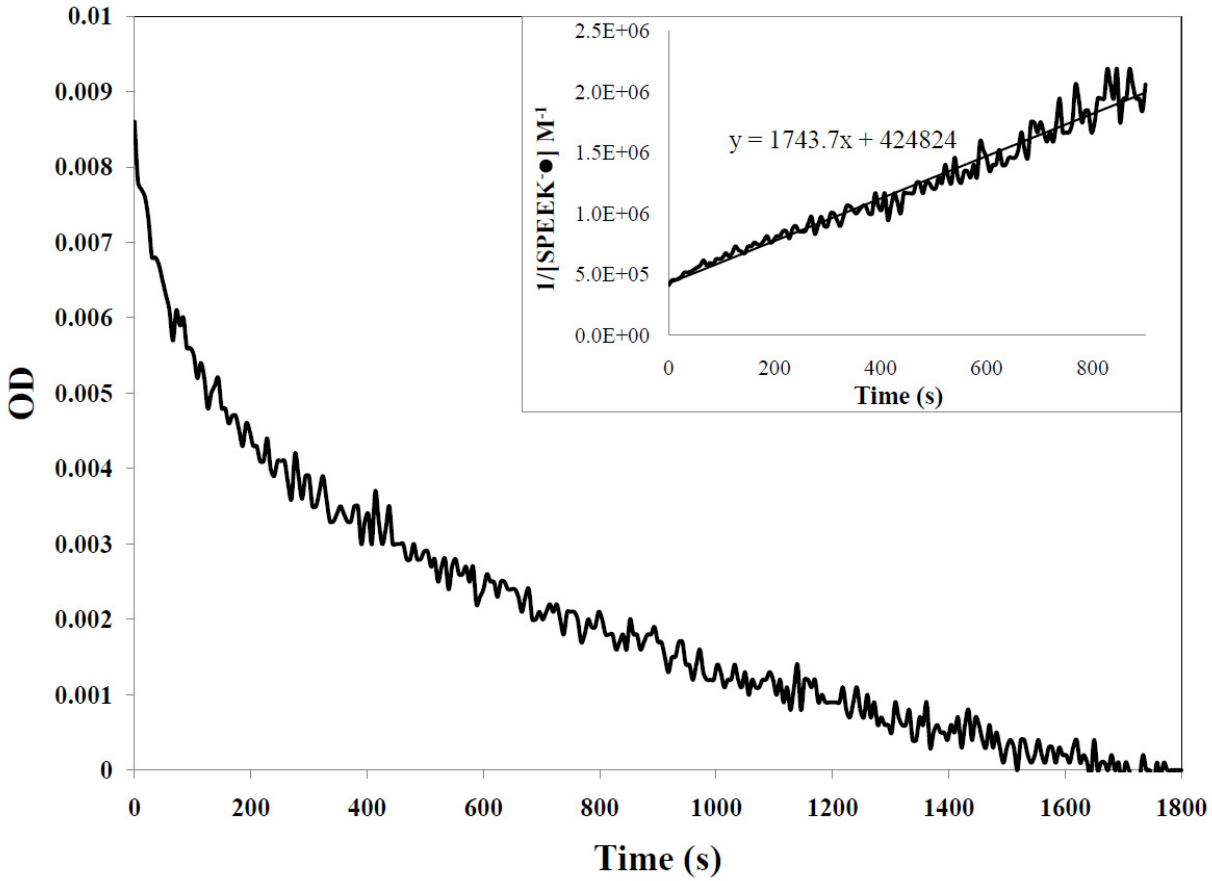

Figure 4-6 – The optical density decay at 580 nm from a radical generated in a polymer film comprised of SPEEK/EPH/ODA/PEI following a 1-minute exposure to 350 nm photons. The inset shows the data plotted as a second order decay with a linear regression giving a decay rate constant of 1743 M^{-1} s^{-1} and a $R^2 = 0.96$.

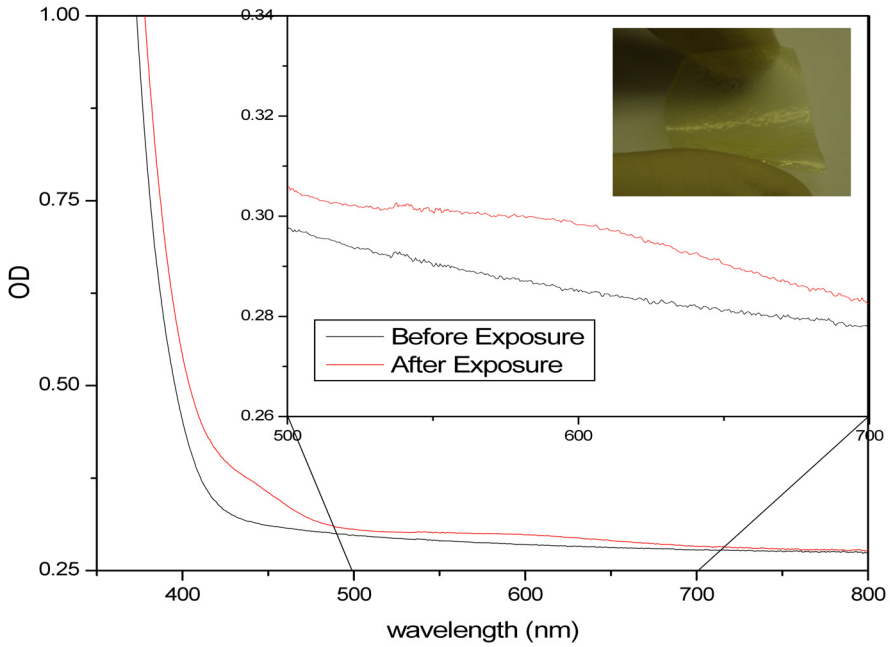

Figure 4-7 - The optical spectrum of a polymer blend comprised of SPEEK/PAA with a λ_{max} located near 600 nm after exposure to 350 nm photons ($I_o = 8x10^{-5}$) for 1 min. These polymers were flexible and transparent as shown in the inset but were still susceptible to being dissolved in water.

yield SPEEK/PAAm films with desired chemical and physical properties was the reason that no further investigations were performed with blends of these polymers.

Another polymer system that was studied consisted of blends of SPEEK and PEI that used epichlorohydrin as the corsslinking agent. Blends of SPEEK and PEI were selected given that, as illustrated in the previous section, photochemical experiments with degassed solutions showed that SPEEK radical anions are easily generated with 350 nm photons. Croslinking of EPI was successfully accomplished by means of the epoxy EPH. The ability of this compound to thermally crosslink amines has been reported in earlier studies. [17] Depicted in Scheme 4-1 is a plausible mechanism for the crosslinking process involving primary amine groups from the polymeric amine. EPH was first reacted with PEI, allowing for a halogen replacement reaction to occur. The resulting solution was mixed with an SPEEK solution and the mixture was cast onto a glass plate. Heating induced completion of the crosslinking process via epoxide ring opening and reaction with another PEI molecule. Using the techniques previously described yielded insoluble, flexible film.

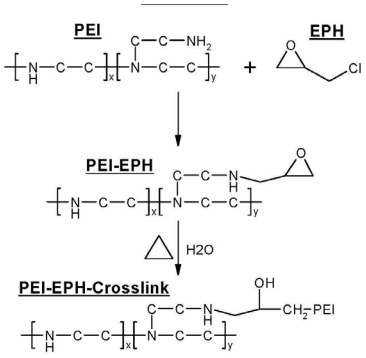

Scheme 4-1

The resulting films exhibited considerable swelling in water and they became fragile after long exposures to this liquid. Since only moderate swelling of the films occurred after immersing them in methanol, this solvent was selected as the best agent for cleansing the

crosslinked polymeric materials. Exposure of EPH/PEI/SPEEK films to 350 nm light yielded a spectrum exhibiting an absorption with a λ_{max} of 600 nm, which was identical to the spectrum shown in

Figure 4-3 obtained from SPEEK/PEI solutions. A plot of the optical signal at 600 nm versus time after photolysis was terminated is presented in Figure 4-8. As in the case of the neutral SPEEK radicals photogenerated in SPEEK/PVA films,[1] the optical signal persisted for about 30 min. These results indicate that the photogenerated SPEEK radicals anions were very long lived. A second-order plot of the radical concentration is shown in the inset of Figure 4-8, yielding a second-order decay rate constant of 9.8×10^2 $M^{-1}s^{-1}$. However, the fit yields a straight line only during the first half-life of the reaction, suggesting that the decay of the radical took place via several parallel processes.

An important question that remained unresolved pertained the long lifetime exhibited by the anionic radicals produced by illumination and films of SPEEK/PEI blends. In fact, as discussed previously, raising the pH of SPEEK/PVA solutions resulted in the formation of mixtures of neutral and anionic radicals. The data presented in Figure 4-4 indicates that the lifetime of the radicals becomes shorter when radical mixtures were photogenerated. Furthermore, SPEEK radical anions formed in SPEEK/PEI solutions at pH = 10 persisted for longer times than the species formed in SPEEK/PVA systems at the same pH. EPR measurements were performed in order to explore the properties of the radicals generated in the different blends. Presented in Figure 4-9 are EPR spectra of the paramagnetic species formed upon photolysis of SPEEK/PVA films exposed to 360 nm in the absence of air. The spectrum recorded immediately after illumination is very similar to that of the neutral BPK radical of

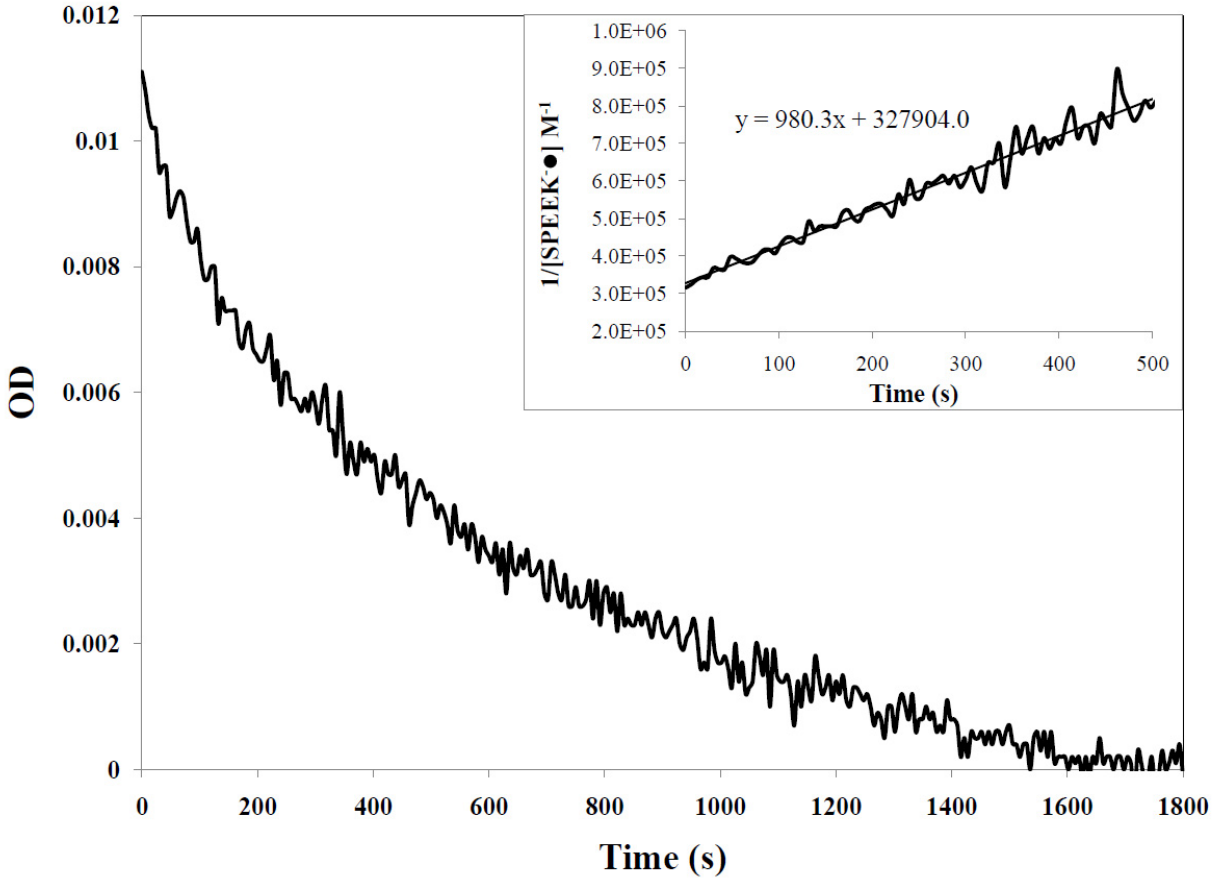

Figure 4-8 - The decay curve at 600 nm associated with the radical-radical annihilation of two amine radicals in an EPH/PEI/SPEEK film after exposure to 350nm light. The inset shows the data plotted as a 2nd order decay with linear regression fitted to the data giving a decay rate constant of 980 M^{-1} s^{-1} and a R^2 = 0.96.

benzophenone,[21] and is identical to the spectrum assigned earlier to the neutral SPEEK radical.[1] As reported in the earlier study, this species exhibits a lifetime of several hours in the absence of O_2. Included in Figure 4-9 is a simulation of the spectrum, which agrees well with previous results obtained by means of ENDOR methods.[1]

Shown in Figure 4-10 are spectra collected upon illumination of EPH/PEI/SPEEK films with 360 nm photons at room temperature and in the absence of air. Similar findings were made in experiments performed at 77 K, except that the resulting paramagnetic species were stable at the low temperature. Comparisons of these results with the spectra depicted in Figure 4-9 indicate that the signal obtained in EPH/PEI/SPEEK films is broader (line width = 14.2 G) than the one detected in SPEEK/PVA films (line width = 9.7 G). Also, the species formed in the presence of PEI decayed more slowly than the SPEEK neutral radical formed in films with PVA. Signals due to polyamine radicals were not detected, suggesting that such species reacted fast with another benzophenone group of SPEEK to form a second paramagnetic species of the polyketone. Similar observations were made in SPEEK/PVA films were the polyol radical generated, even at low temperatures, a second SPEEK radical. The photogenerated spectrum is assigned to the anionic radical of SPEEK. Also shown is a simulation of the spectrum, which was obtained considering interactions of the unpaired electron with protons from the aromatic rings of the benzophenone functions present in SPEEK, as well as interactions with a neighboring cationic N atom. Included in the Figure 4-10 are the coupling constants employed in the simulation. Unlike the case of the spectrum presented in Figure 4-9, simulations that included only electron-proton interactions failed to reproduce the features of the signal obtained in the presence of PEI. This means that about 3.5 % of the electron density is delocalized into a neighboring N^+ cation. Such interaction is anticipated to increase the stability of the

photogenerated SPEEK radical anion, which explains the kinetic data presented in Figure 4-4. The higher stability of the radical anion as compared with the neutral radical when the latter is formed at high pH values results from partial delocalization of the unpaired electron into surrounding amine cations. Further experiments are needed to test the anticipated higher reducing power of the anionic SPEEK radicals.

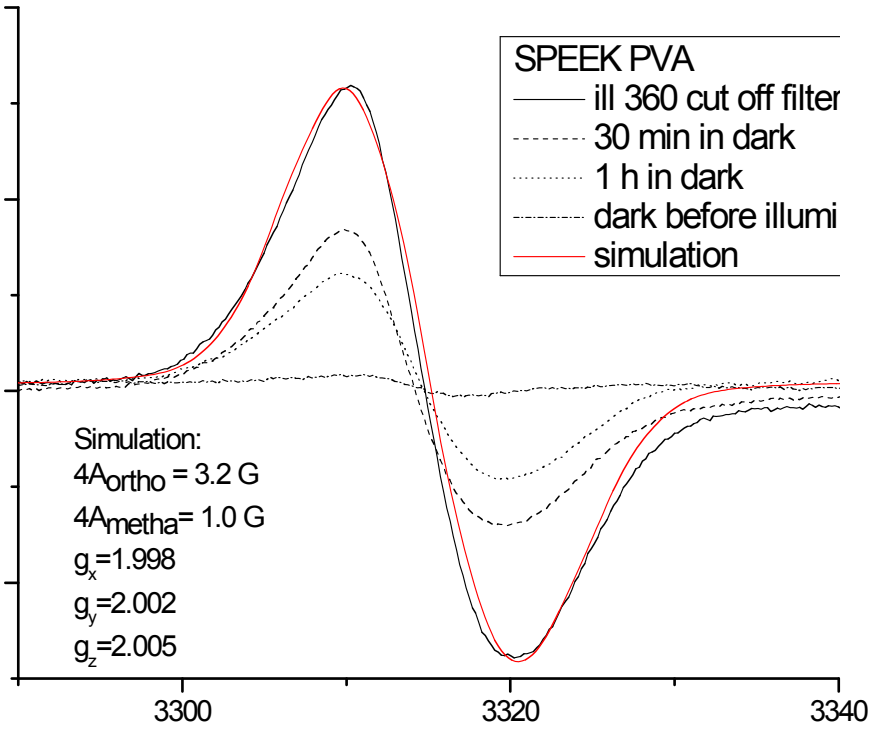

Figure 4-9 – Time-evolution of the EPR spectrum of neutral SPEEK radicals at room temperature. The paramagnetic species were produced via illumination of SPEEK/PVA films with 360 nm photons in the absence of air. Also shown is a simulation curve obtained using the included coupling constants.

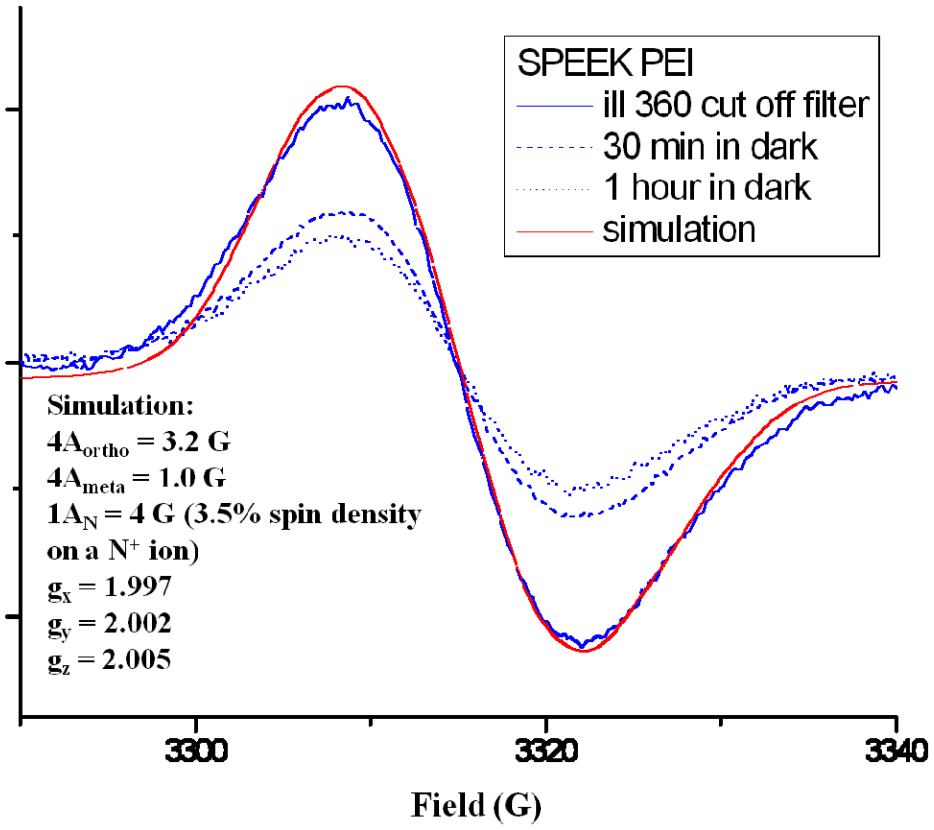

Figure 4-10 - EPR spectra recorded at room temperature after photolysis of a SPEEK/PEI/EPH film with 360 nm photons in the absence of air. Included are spectra obtained after different times in the dark following illumination, and also a simulation obtained from the listed coupling constants.

Conclusion

Generation and detection of the BPK anionic radical in flexible, transparent, insoluble films was achieved in a simple system consisting of crosslinked PEI and SPEEK. The photogenerated BPK radical anions exhibited a lifetime in the same time scale as that of the SPEEK neutral radical. Drawbacks to amine polymer films include the chelating reaction of the polyamine with any positively charged metal ions present in the polymer matrix. These polyamine films may be useful in the degradation of difficult to reduce chemical agents.

References

(1) Korchev, A. S.; Konovalova, T.; Cammarata, V.; Kispert, L.; Slaten, B. L.; Mills G. *Langmuir* **2006**, *22*, 375-384.

(2) Korchev, A. S.; Shulyak, T. S.; Slaten, B. L.; W. F. Gale, W. F.; Mills G. *J. Phys. Chem.* B **2005**, *109*, 77337745.

(3) A. S. Korchev, M. Sartin, G. Mills, B. L. Slaten and W. F. Gale *Clusters and Nano-Assemblies: Physical and Biological Systems*; Jena, P.; Khanna, S. N.; Rao, B. K., Eds: World Scientific Publishing Co.: Singapore; 2005, pp 371-377.

(4) Korchev, A. S.; Bozak, M. J.; Slaten, B. L.; Mills, G. *J. Am. Chem. Soc*. **2004**, 126, 10-11.

(5) Gilbert, A.; Baggott, J. *Essentials of Molecular Photochemistry*; CRC Press: Boca Raton, 1991; Chapter 7.

(6) Suryanarayana, D.; Kevan, L. *J. Phys. Chem.* **1982**, *86*, 3834-3836.

(7) Canonica, S.; Hellrung, B.; Wirz, J. *J. Phys. Chem. A* **2000**, *104*, 1226-1232.

(8) Stanbury, D. M. *Adv. Inorg. Chem.* **1989**, *33*, 69-138.

(9) Kolthoff, I. M.; Lee, T. S.; Stocesova, D.; Parry, E. P. *Anal. Chem.* **1950**, *22*, 521-525.

(10) Radlowski, C.; Sherman, W. V. *J. Phys. Chem*. **1970**, *74*, 3043-3047.

(11) Schwarz, H. A.; Dobson, R. W. *J. Phys. Chem.* **1989**, *93*, 409-414.

(12) Porter, G.; Wilkinson, F. *Trans. Faraday Soc.* **1961**, 1686-1691.

(13) Perone, S. P.; Birk, J. R. *Anal. Chem*. **1966**, *38*, 1589-1593.

(14) Bhattacharyyya, K.; Das, P. K. *J. Phys. Chem*. **1986**, *90*, 3987-3993.

(15) Allen, N. S.; Chen, W.; Catalina, P.; Green, P. N.; Green, A. *J. Photochem. Photobiol. A: Chem*. **1988**, *44*, 349-360.

(16) Hoshino, M.; Aral, S.; Imamura, M. *J. Phys. Chem.* **1976**, 80, 2724-2727.

(17) Minegishi, T.; Hiratsuka, H.; Tanizaki, T; Mori, Y. *Bull. Chem. Soc. Jpn.* **1984**, 57, 162-165.

(18) Feeney, R. E.; Blankenhorn, G.; Dixon, H. B. F. Carbonyl-Amine Reactions in Protein Chemistry. In *Advances in Protien Chemistry;* Anfinsen, C. B. Ed. Vol. 29 Academic Press Inc.: New York, NY, 1975; pp 136–199.

(19) Pannone, M. C.; Macosko, C. W. *J. Appl. Poly. Sci.* **1987**, 34, 2403-2409.

(20) Ergozhin, E. E.; Mukhitdinova, B. A.; Chalov, T.K.; Iskakova, R. A. *Russ. J. Appl. Chem.* **2005**, 80, 1687-1690.

(21) Reinking, N.; US Patent #2951822, 1960.

(22) Kioussis, D. R.; Smith, D.F.; Kofinas P. *J. Appl. Poly. Sci.* **2001**, 80, 2073-2083.

(23) Beckett, A.; Porter, G. *Trans. Faraday Soc.* **1963**, 2038-2050.

V. Conclusions

PVA/PAA polymer matrix was used for the reversible formation of silver nanoparticles by electrochemical methods. Cyclic volmatetric method was able to generate large irreversible particles (>100 nm) that exhibited broad optical absorption maximum centered around 450 nm. Galvanostatic methods employing a range of current densities from 155 to 310 $\mu A/cm^2$ were able to mimic the results obtained in the CV method with optical signatures centered around 450 nm and the particles were only observed at the polymer/ITO interface. Employing higher current densities ranging from 620 to 1550 $\mu A/cm^2$ were able to generate small (<15 nm) reversible particles with optical absorptions being centered less than 400 nm. Generated nanoparticles were discovered up to 3000 nm into the polymer matrix. The higher current densities allowed for the optical switching times to exceed 1 second but only for small number of cycles. Optimal settings were discovered to be at 620 where reversible optical switching was found to occur at a maximum speed of 1 second for over 30 cycles. The diffusion of silver ions was determined to be 2.0×10^{-8} cm^2/s by exhaustive electrolysis.

Polymeric radicals of PVA/SPEEK and Formate/SPEEK generated in degassed solutions containg 20:1 monomer ratios of hydrogen donors (PVA or formate) to SPEEK and saturated with CCl_4 by 350 nm photons. The generated radicals were able to dechlorinate CCl_4 resulting in ionic chlorine detected by an ion selective electrode. The rate of Cl^- generation by Formate/SPEEK was found to be an order of magnitude faster than the PVA/SPEEK system. Evidance of a chain reaction involving CCl_3 radicals and SPEEK was determined by the

quantifying the quantum yield of chloride ion formation and is believed to be a polyelectrolyte effect allowing SPEEK tertiary structure to unfold and react more readily with CCl_4. An order of magnitude larger in chloride ion rate of production was detected for formate containing solutions and determined that the difference in rates is attributed to the PVA matrix interaction producing aglomeration restricting the CCl_4 from reacting with the SPEEK radicals.

The generation of a long lived anionic SPEEK polymeric radical in aqueous solutions and polymeric films was achieved by exposing SPEEK/Polyamine systems to 350 nm photons. The production of the SPEEK anionic radical is believed to have a higher reduction potential of ~2 V compared to the 1.5 V reported for the neutral radical. The confirmation of anionic radicals was obtained spectroscopically by UV-Vis and ESR measurements. The determined rate of decay was determined to be first order with radicals in solution having a rate constant of 5.7×10^{-2} M^{-1} s^{-1} with radicals generated in films having a rate constant of 5×10^{-2} $M^{-1}s^{-1}$. The generated anionic radical are comparable to the neutral radical rate constants with solutions having a 7×10^{-2} M^{-1} s^{-1} and for films a decay rate constant of 4×10^{-2} M^{-1} s^{-1}. The stability of the anionic radical is attributed to the electron density being shared by with the amine group.